POINT–CONTACT SPECTROSCOPY IN METALS

A.G.M. JANSEN

POINT–CONTACT SPECTROSCOPY IN METALS

PROMOTOR
PROF. DR. P. WYDER

CO -REFERENT
DR. A P van GELDER

POINT–CONTACT SPECTROSCOPY IN METALS

PROEFSCHRIFT

TER VERKRIJGING VAN DE GRAAD VAN DOCTOR IN DE
WISKUNDE EN NATUURWETENSCHAPPEN
AAN DE KATHOLIEKE UNIVERSITEIT TE NIJMEGEN OP GEZAG VAN
DE RECTOR MAGNIFICUS PROF. DR. P.G.A.B. WIJDEVELD,
VOLGENS BESLUIT VAN HET COLLEGE VAN DECANEN
IN HET OPENBAAR TE VERDEDIGEN
OP DONDERDAG 24 APRIL 1980
DES NAMIDDAGS TE 2.00 UUR PRECIES

door

ALOYSIUS GERARDUS MARIA JANSEN
geboren te Breda

1980
Druk: Krips Repro Meppel

Iedereen, die op enigerlei wijze een bijdrage heeft geleverd aan het tot stand komen van dit proefschrift wil ik hiervoor hartelijk bedanken. In het bijzonder Riki Gommers en Lies Remers voor de verzorging van de lay-out, de medewerkers van de dienstverlenende afdelingen van de faculteit der wiskunde en natuurwetenschappen en niet in de laatste plaats alle medewerkers van de afdeling experimentele natuurkunde 4.

Dit onderzoek werd uitgevoerd op de afdeling experimentele natuurkunde 4 van het Research Instituut voor Materialen van de Katholieke Universiteit te Nijmegen, onder leiding van Prof. Dr. P. Wyder. Een gedeelte van dit onderzoek is gesteund door de Stichting voor Fundamenteel Onderzoek der Materie (FOM) met financiele bijdragen van de Nederlandse Organisatie voor Zuiver Wetenschappelijk Onderzoek (ZWO).

We acknowledge the permission to reprint previously published papers obtained from the publishers to The Physical Review, Science and Journal de Physique.

Voor mijn ouders

Voor Marijke

CONTENTS

It is one of the fascinating aspects of the quantum theory of solids that in a metal, the electrons can move freely over a fairly large distance, called the mean free path (up to 1 cm in pure metals at low temperatures), without a collision with, for instance, impurities or lattice vibrations (phonons). In the absence of an applied voltage over the metal, the electrons move in random directions and no net current flows in the sample. In a uniform electric field, caused by an applied voltage, the electrons are accelerated over a distance of the order of the mean free path in the direction of the field and the electrons get a preferred velocity-component, the drift velocity, which is responsible for the current through the metal. After a collision, the electron comes back in equilibrium, and then the acceleration process starts again. Using this simple mean-free-path model for the electrical conduction, one can readily show that the applied voltage over a metal sample is proportional to the electrical current. This is the well known Ohm's law. Due to the high electrical conductivity of a metal, the drift velocity is very small compared to the average random velocity of the electrons (Fermi velocity). This is why Ohm's law is such a good approximation for the relation between the current and the voltage in a metal. Increasing the voltage will certainly increase the drift velocity of the electrons, but from an experimental point of view, again due to the high electrical conductivity, deviations from Ohm's law are difficult to distinguish from ordinary heating effects.

In this thesis, we discuss interesting non- linear phenomena observed in the current-voltage characteristics of metallic constrictions (point contacts) which have a linear dimension a comparable to or smaller than the electronic mean free path ℓ ($a<\ell$). In these point contacts, it is possible to have a rather high electric field within a metal, impossible otherwise, wich gives the electrons a considerable drift velocity within the metal by simply applying a voltage over the contact. No significant heating occurs in this geometry. The observed non-linearity of the current-voltage relation in metallic point contacts can be used for a fundamental study of the interactions of the electrons in a metal. A spectral analysis of the relevant scattering mechanisms for the conduction electrons in a metal is possible. This experimental method, developed in Prof. I.K.Yanson's

laboratory in Kharkov and in our laboratory in Nijmegen is nowadays called "point-contact spectroscopy".

Starting with the advent of rotating machinery at the end of the 19th century, the problem of the understanding of electrical contacts is quite old. Today, in the technology of micro electronics, the manufacturing of metallic contacts is again important in order to attach stable metallic leads to semi-conducting devices (diodes, transistors, integrated circuits). The current densities in contacts of these small-scale devices can be as large as 10^6 A/cm^2 (a few milliampères through a contact with a linear dimension of a few microns). The point contacts under study in point-contact spectroscopy and discussed in this thesis have even larger current densities (up to 10^{11} A/cm^2) and reveal remarkable non-linear behaviour. The first pioneering experiments in this rather new field were done by Yanson[1] in Kharkov (USSR) in a study of the current-voltage characteristics of tunnel junctions (two metal films separated by an oxide layer) with a short circuit between the metal films deliberately or accidentally produced. He discovered that the contact resistance of these micro contacts at liquid helium temperatures increased remarkably in a non-linear way at applied voltages which correspond to the phonon frequencies of the bulk metal forming the junction. This observation indicates that the non-linearity is related to the coupling between the conduction electrons and the phonons. Moreover, Yanson found, as the grand result for point-contact spectroscopy, that the measured voltage derivative of the resistance gives a signal as function of the applied voltage which is proportional to the electron-phonon coupling parameter $\alpha^2F(\omega)$. $\alpha^2F(\omega)$ characterizes the energy dependent electron-phonon interaction, loosely speaking, F is the phonon density of states and α the matrix element for the electron-phonon interaction averaged over the Fermi sphere.

The applicability of this spectroscopic method has been dramatically increased by the discovery that also metallic point contacts, consisting of a sharply etched needle ("spear") pressed against a bulk surface ("anvil"), are useful for an experimental study of the phenomenum[2]. These pressure-type point contacts make it possible to use the method in a simple and convenient way for an experimental study of a large variety of samples, including single crystals in order to study anisotropy effects. In figure 1 we give an example of the current-voltage characteristics for a pressure-type point contact of copper. The increase in the resistance

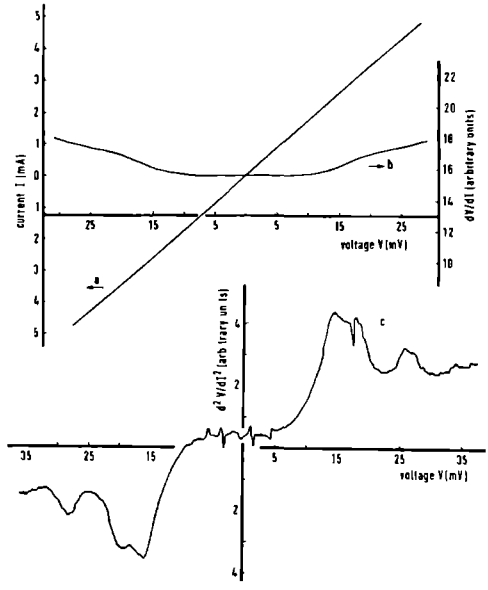

Fig. 1 Current-voltage characteristics as directly measured on a recorder of a copper point contact with a resistance R_o = 5.7 Ω at a temperature T = 1.2 K. The current I (a), the differential resistance dV/dI (b) and the second derivative d^2V/dI^2 (c) are given as a function of the applied voltage V. The structures in the d^2V/dI^2-signal around 17 and 27 mV correspond to the bulk phonon frequencies of copper.

dV/dI around 17 and 27 mV and the resulting structures in the d^2V/dI^2 signal are clearly visible. These experiments reveal in a very clear way the α^2F-spectrum for the electron-phonon interaction in copper.

The coupling between electrons and phonons plays an important role in many physical properties of metals, such as the electrical conductivity, the thermal conductivity, superconductivity etc. This makes that an experimental determination of the function α^2F is of great interest. This is of particular importance, as theoretical band structure calculations of α^2F seem to be rather difficult and not too reliable.
The point-contact method gives, as an example, detailed information about the relative strength of the coupling of the electrons with the various phonon modes (transverse and longitudinal) in a metal. For normal metals, (i.e non-superconductors), point-contact spectroscopy is, at

least until now, the only experimental method which can determine the energy dependence of the function α^2F successfully.

For an intuitive explanation of the non- linearity in the current-voltage characteristic of a point contact it is instructive to make a side step to one of the classic experiment in atomic physics: the Franck-Hertz experiment[3]. In a tube filled with a dilute gas of mercury atoms, electrons are accelerated through a potential. Increasing the potential results in an increase of the kinetic energy of the electrons. If the kinetic energy of the electrons reaches the quantum energy, which can be absorbed by a Hg atom, the conductivity of the gas chamber decreases. This process results in the periodic pattern of the conductivity of a dilute gas of mercury atoms in an applied electric field,as shown in figure 2. The Franck-Hertz experiment shows in a clear way that the emission and absorption of light is quantized, and, more important in our context, that the scattering cross section for the scattering of the electrons with Hg atoms is a measurable function of the energy. For a point contact between two metals, a simular situation holds: The electrons are accelerated in the electric field caused by the applied voltage by passing the contact area. A moderation and a slow down of the injected electrons occurs via inelastic collisions with phonons,these processes depend strongly on the energy of the electrons and give rise to a non-linear current-voltage characteristic due to the electron-phonon interaction.

In a theoretical analysis[4,5], the transport problem for the electrical current through a point contact in the limit $a<\ell$ has been solved, using the concept of "blackflow". After having suffered an inelastic collision (spontaneous emission of the phonon) the electrons which have been injected through the contact, can flow back through the constriction. This explains the increase in resistance at typical phonon energies. The theoretical analysis shows that the second derivative signal for a metallic point contact is proportional to a slight modification of the usual function α^2F. The modification has to do with the transport efficiency for the occurence of a blackflow process in the point- contact geometry.

Until now point-contact spectroscopy has been used almost exclusively to study the electron-phonon interaction. It is obviously very much worthwile to investigate the possibility if other scatterers than phonons can be probed via the same point-contact method. Recently, the interaction of electrons with magnons[6] and with paramagnetic impurities[7] has been

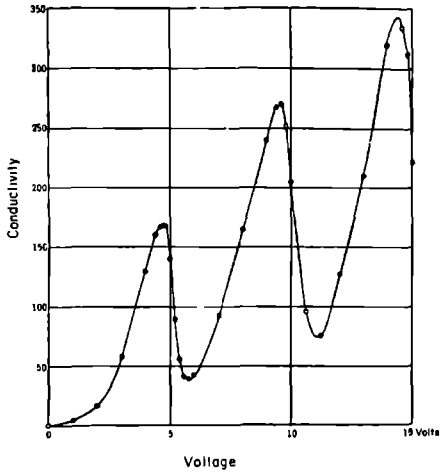

Fig. 2 The Franck-Hertz experiment from atomic physics. The conductivity dI/dV as a function of the voltage in a dilute gas of mercury atoms (After the original paper by Franck and Hertz).

detected successfully in point- contact experiments, with, respectively, ferromagnetic metals and magnetically dilute alloys (Kondo systems). These experiments give a promising future for the detection of all kinds of scattering mechanisms of the conduction electrons in a metal using point-contact spectroscopy. The only limiting condition seems to be that the electronic mean free path of the sample to be investigated in a point-contact geometry has to be comparable or larger than the dimensions of the contact.

The thesis is organized as follows. In the next chapter, a survey is given of the theoretical and experimental work done in this field with its exciting "sharp points". After this review, the following chapters treat several aspects in point-contact experiments, involving the measurement of the electron-phonon coupling in noble metals, the observation of double phonon processes, the temperature dependence of the spectroscopic method and the application of point-contact experiments to Kondo systems. All chapters are given in the form of published papers or papers to be published.

References.

1. I.K. Yanson, Zh. Eksp. Teor. Fiz. 66, 1035 (1974) {Sov. Phys. - JETP 39, 506 (1974)}.
2. A.G.M. Jansen, F.M. Mueller and P. Wyder, Proc. 2nd Rochester Conf. on Superconductivity in d- and f-band Metals, ed. D.H. Douglass (Plenum, New York, 1976).
3. J. Franck and G. Hertz, Verhand. Deut. Physik. Ges. 16, 457 (1914); ibidem p. 512.
4. I.O. Kulik, A.N. Omel'yanchuk and R.I. Shekhter, Fiz. Nizk. Temp. 3, 1543 (1977) {Sov. J. Low Temp. Phys. 3, 740 (1977)}.
5. A.P. van Gelder, Solid State Commun. 25, 1097 (1978).
6. B.I. Verkin, I.K. Yanson, I.O. Kulik, O.I. Shklyarevski, A.A. Lysykh and Yu.G. Naydyuk, Solid State Commun. 30, 215 (1979).
7. A.G.M. Jansen, A.P. van Gelder, P. Wyder and S. Strässler, to be published; see chapter VIII.

Abstract

Point contacts between normal metals at low temperatures show very interesting non-linear phenomena in the current-voltage characteristics. The observed deviations from Ohm's law in metallic constrictions can be used for an energy resolved spectral analysis of the interaction mechanisms of the conduction electrons with elementary excitations in a metal. A review is given on the theoretical and experimental work dealing with this spectroscopic method. The metallic point contacts investigated show structures in the measured second derivative d^2V/dI^2 which are in agreement with structures in the phonon density of states of the metal under study. A theoretical analysis, involving an iterative solution of the full non-linear Boltzmann equation for the transport problem of a current through a point-contact geometry, is able to show that the observed second derivative signal is proportional to Eliashbergs form of the electron-phonon interaction $\alpha^2F(\omega)$, with a slight modification due to a transport efficiency function. Non-equilibrium effects of the phonon system are discussed in relation to the observed background signal on which the α^2F-signal is thought to be superimposed. The theory can easily be extended to other scattering mechanisms than the electron-phonon interaction, and some experiments show that the interactions of conduction electrons with magnons and paramagnetic impurities can be detected using point contacts between ferromagnetic metals and between magnetically dilute alloys.

1. Introduction

The problems of electrical contacts between metals have always attracted a great deal of interest. Especially in the development of micro electronics, much effort has been put in the production of reliable contacts to these small-scale devices. For the metallic contacts, one usually expects a linear relation between the applied voltage and the current through the contact, according to Ohm's law. However, interesting non-linear behaveour can be observed in the current-voltage characteristics of metallic constrictions if the linear dimension of the contact becomes comparable to or smaller than the mean free path of the electrons in the metal. It turns out that the observed phenomenum can be used for a fundamental study of the scattering mechanisms of the conduction electrons in a metal, leading to a new experimental tool, nowadays referred to as "point-contact spectroscopy". In this paper we want to give a review on the experimental and theoretical work done in this field following the first pioneering and important publication by Yanson (1974 a).

In an experimental study of metal-insulator-metal tunnel junctions, with a short circuit in the oxide layer between the metal films, Yanson (1974 a) has found that the current-voltage characteristics of these metallic micro contacts showed a non-linear behaviour at liquid helium temperatures. To characterize the non-linearity Yanson has measured the second derivative d^2V/dI^2 of the voltage with respect to the current as a function of the voltage V. As a most remarkable result, he observed structures in the measured second-derivative signal at applied voltages corresponding to the bulk phonon frequencies of the metal forming the junction. Yanson interpreted the experimental data as a direct measurement of the electron-phonon interaction function α^2F. Roughly speaking, the Eliashberg function α^2F is the product of the phonon density of states F and the squared matrix element α for the electron-phonon interaction, averaged over the Fermi sphere. As the radius a of the investigated contacts is small compared to the mean free path ℓ of the electrons ($a < \ell$), the transport of electrons through the contact is ballistic and no longer diffuse. Within a mean free path distance, the electrons are accelerated due to the electric field caused by the applied voltage, and are injected from one metal side to the other by passing the contact (Sharvin, 1965). The accelerated electrons are brought back into equilibrium via inelastic collisions with, for

instance, phonons. In paragraph 3 of this paper, we will show in a simplified and intuitive picture that one can easily get an interpolation formula for the resistance of a contact in the intermediate regime between the limiting cases of $a >> \ell$ or $a << \ell$ and it is found that the inelastic phonon emission near the orifice yields a second derivative signal which is proportional to the Eliashberg function α^2F. Recently, theoretical work with a more fundamental approach has become available (paragraph 4). The full non-linear Boltzmann equation has been solved for the point-contact problem, introducing the concept of "backflow" (Kulik et al., 1977; van Gelder, 1978). After injection, the electrons can flow back through the orifice due to an inelastic scattering process; this process gives rise to a negative and voltage-dependent correction to the current. Hence, the non-linear current-voltage relation contains information about the inelastic collisions of the electrons. A careful analysis then shows that the measured spectrum is characterized by a slight modification of the function α^2F, involving a geometrical transport efficiency for the backflow current arising from the electron-phonon interaction. In addition, in most point-contact spectra a smooth background signal is observed, on which the α^2F-signal is thought to be superimposed. An explanation for the background signal can be given in terms of a non-equilibrium distribution of the phonon system, which gives additional corrections to the current from stimulated emission and absorption processes (van Gelder et al., 1978; van Gelder, 1980).

Experimentally, various metals have been investigated using point-contact spectroscopy for the measurement of the electron-phonon interaction (Yanson and Kulik, 1978). The method has been extended for the investigation of a large variety of samples, including single crystals, by the fact, that pressure-type point contacts, consisting of a sharply etched spear pressed against a bulk anvil, appeared to be very useful for spectroscopic investigations (Jansen et al., 1977 and 1978). In paragraph 5, the experimental techniques used for the point-contact method will be discussed. Paragraph 6 contains a survey of the experimental results of the measured electron-phonon interaction in metals using metallic point contacts. This technique provides interesting and novel results, especially for the normal metals, which have not been studied before. For instance, one gets direct experimental information concerning the relative strength of the various phonon modes (transverse or longitudinal) in the electron-phonon coupling.

The influence of the temperature will be treated in paragraph 7. An increase of the measuring temperature results in a broadening of the measured second derivative spectra. It is very interesting to compare the temperature dependence of the point-contact resistance at zero voltage with that of the bulk resistivity. Small differences in the temperature dependence for the two cases can be ascribed to differences in the transport efficiency in the bulk and in the point-contact geometry (van Gelder et al., 1980 a).

It is obvious that point-contact spectroscopy can in principle be applied to any arbitrary scatterer, not only phonons. The relevant theory will therefore be presented accordingly. In paragraph 8 experimental results will be discussed which have been performed in ferromagnets (Verkin et al., 1979) and in magnetically dilute alloys (Jansen et al., 1980 b) in order to detect other scattering mechanisms than the electron-phonon interaction. In the point-contact experiments with ferromagnets, structure is observed which can be ascribed to strong heating in the vicinity of the metallic contact. A modified temperature dependent resistivity is measured arising from electron-magnon interaction. The experiments with the Kondo systems seem to open the possibility for a direct determination of the energy-dependent scattering time for a metal containing paramagnetic impurities from the change in resistance of a point-contact.

However, a word of caution should be said about the general applicability of point-contact spectroscopy as a general tool to measure the energy dependence of the scattering length. As the technique works only if the dimensions of the point contact are small or at least comparable to the mean free path of the electrons, point-contact spectroscopy can only be applied successfully to reasonably pure metals with not too short a mean free path.

2. Methods for obtaining phonon spectra

It is rather difficult to determine theoretically the Eliashberg function α^2F, responsible for the electron-phonon interaction in metals. Therefore, it is of considerable importance to measure the phonon spectra experimentally; this can be done in several ways. Detailed phonon dispersion curves $\omega(q)$ (phonon frequency ω as function of wave number q) along the principal symmetry directions of a single crystal are obtained from

experiments with coherent inelastic neutron scattering (Dolling and Woods, 1965); these dispersion curves can then be fitted to an interatomic force model for nearest neighbor interactions (Born- von Karman analysis). By sampling over a large number of q-values, the phonon density of states $F(\omega)$ is then calculated from the dispersion curves. For materials, which absorb neutrons (i.e. ^{3}He or Cd), diffuse X-ray scattering can be used in a similar way to determine the phonon dispersion curves leading to $F(\omega)$ (Walker, 1956).

Using the superconducting tunneling mechanism in a geometry of two metal films separated by an oxide layer the electron-phonon interaction α^2F can be measured for superconducting metals (McMillan and Rowell,1969). The density of states in a superconductor is obtained experimentally from the conductivity of the tunnel junction in the superconducting state, normalized to that in the normal state. Theoretically, using the theory of strong coupling superconductors (Parks, 1969), the density of states can be found by an iterative solution of the coupled Eliashberg equations containing the function α^2F. By trial and error, it is then possible to determine α^2F by comparing the theoretically calculated density of states with the experimental results. Using the proximity effect, in a tunnel junction phonon structures have been observed in a normal metal backed by a superconductor (Chaikin and Hansma, 1976).

In tunneling experiments with superconductors put in the normal state by a magnetic field, non-linearities in the current-voltage characteristics have been observed at typical phonon energies (Rowell et al., 1969), which can be analysed in terms of an enhanced tunneling probability arising from phonon modes of the surface layer in the metal electrodes. It is interesting to note that in these tunneling experiments an increase is seen in the conductivity of the junction, where point-contact spectroscopy shows an increase in the contact resistance.

In Mossbauer experiments (Frauenfelder, 1962) a moment of the function α^2F ($\int \alpha^2F(\omega)\ \omega^n\ d\omega$ for $n = \pm 1, \pm 2$) can be measured. One should realize that the energy dependence of the electron-phonon interaction is also contained in the temperature dependence of the electrical resistivity, which could allow a determination of α^2F using a suitable analysis.

Point-contact spectroscopy seems to be an important tool to measure the function α^2F. Especially for non-superconducting metals, it is the only known method to yield detailed information on the energy dependence

of the electron-phonon interaction. As up to now phonon spectra of metals are most elaborately studied using inelastic neutron scattering ($F(\omega)$) and superconducting tunneling-spectroscopy ($\alpha^2F(\omega)$), we will compare the point-contact spectra with spectra from these experimental techniques.

3. Constriction resistance and its voltage dependence

We want to describe the voltage dependence of the electrical resistance of a metallic point contact at low temperatures which reveals the non-linearity in the current-voltage characteristics arising from inelastic scattering processes of the electrons. In this paragraph, we use a heuristic approach in order to clarify the role of the relavant parameters in point-contact experiments. In particular we discuss in detail the interactions of the electrons with the lattice vibrations, i.e. the electron-phonon interaction. In paragraph 4 a more formal solution of the non-linear Boltzmann equation for the point-contact problem will be discussed; this approach will be extended to arbitrary targets for inelastic scattering of the conduction electrons.

The interest in the understanding of electrical contacts, often called the problem of the "constriction resistance" is quite old (Holm, 1967). Already Maxwell (1904) has studied the problem of the resistance of a small metallic contact. He solved in a classical way Poisson's equation for the electrical potential energy ϕ as a function of the position $\underline{r}$

$$V^2 \phi (\underline{r}) = 0 \tag{3.1}$$

in oblate spherical coordinates. For a current flowing through a constricting circular orifice of radius a the contours of constant potential energy are given by

$$\phi(\underline{r}) = \pm \frac{eV}{2} \left[1 - \frac{2}{\pi} \arctan (1/\xi) \right], \tag{3.2}$$

where the oblate spherical coordinates may be found from the more familiar spherical coordinates r and z by solving the implicit equation $r^2/a^2 = (1 + \xi^2)(1 - z^2/\xi^2a^2)$ (figure 1). The two signs refer to the two sides of the contact. The total voltage V, applied over the contact, devided by the current through any contour of constant potential yield an expression for the contact resistance. For simplicity we choose the contour with $\xi = 0$ and $\phi(\underline{r}) = 0$, that is the orifice itself. The current I is given by

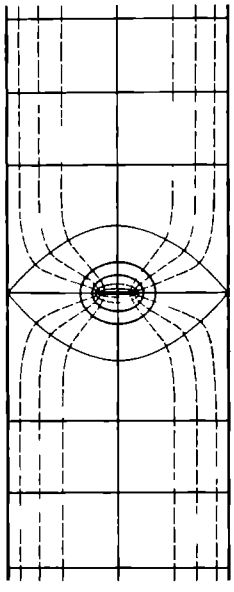

Fig. 1 Point contact in the Maxwell limit ($\ell < a$). Indicated are the electric field lines (broken curves) and the equipotential surfaces.

an integral of the current density $\underline{j}$ over the area $\underline{O}$ of the orifice

$$I = \int \underline{dO} \cdot \underline{j} = \int_0^{2\pi} d\varphi \int_0^a r\, dr\, \frac{1}{\rho e} \left(\frac{\partial \phi}{\partial z} \right)_{z=0} . \qquad (3.3)$$

Here, explicit use of Ohm's law is made in the form of $j_z = \sigma E_z = (1/\rho e)\,(\partial\phi/\partial z)$, where the conductivity of the metal is given by $\sigma = 1/\rho$. From this, one gets the Maxwellian resistance for the point contact

$$R_M = \rho/2a \qquad (3.4)$$

Maxwell's method gives the solution for the point-contact problem in the regime where Ohm's law ($\underline{j} = \sigma \underline{E}$ is valid. However, for contacts of metals where the mean free path ℓ of the electrons is much larger than the linear dimension a of the contact, this assumption does not hold any more. The problem resembles the well known Knudsen-problem in the kinetic gas theory: By pumping through a small hole in a gas container, the pressure of the gas will be lowered. However, at the moment where the path length of the gas molecules becomes comparable with the diameter of the hole, there is no longer diffuse flow and the molecules will pass the orifice ballistically. The problem was first considered by Knudsen (1934) and the different regimes are characterized by the Knudsen ratio $K = \ell/a$.

Electrical contacts in the clean limit with large Knudsen ratios

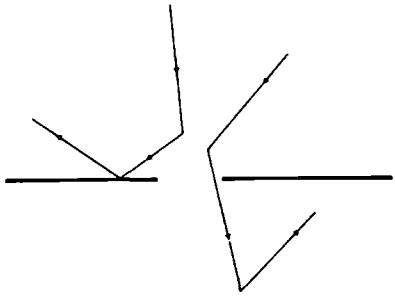

Fig.2 Point-contact in the Knudsen limit ($\ell > a$) leading to a ballistic transport of the electrons.

have a large gradient in the potential near the contact, causing the electrons to be accelerated within the metal over a short distance (figure 2). Crudely speaking, the electrons are injected with an excess energy from one metal to the other. This type of contacts with large Knudsen numbers has been discussed for the first time by Sharvin (1965). The speed increment Δv for an electron which passes the orifice is proportional to the applied voltage: $\Delta v = eV/p_F$, where p_F is the Fermi momentum. The speed increment results in a current I through the contact, given by $I = \pi a^2 n_o \Delta v = \pi a^2 (n_o e^2/p_F)V$, where n_o is the electron density. Using the Drude formula for the resistivity $\rho = p_F/n_o e^2 \ell$, one finds an expression for the resistance of a contact in the limit of high $K = \ell/a$: $R_s \simeq \rho\ell/\pi a^2$. Performing the integration over all possible angles gives a numerical factor of 4/3. The Sharvin resistance ($K = \ell/a >> 1$) of a circular contact is therefore given by

$$R_s = \frac{4\,\rho\ell}{3\,\pi a^2} \quad . \tag{3.5}$$

It should be realized that the Sharvin resistance is independent of the mean free path ℓ because $\rho \alpha 1/\ell$, as expected for ballistic transport through the contact. Using the expressions for the resistances in the Maxwell and Sharvin limit we can make an estimate of the contact radius a for i.e. a copper point contact with resistance $R = 1\ \Omega$ and residual resistivity ratio between roomtemperature and liquid helium temperature RRR=20. Using the Maxwell formula, we find $a = 4$ Å, and using the Sharvin formula $a = 120$ Å. For a reasonable pure metal we may conclude that the point contacts usually obtained in these experiments can be considered to be in the Knudsen limit ($\ell/a > 1$).

In between the limiting cases of the Maxwell resistance R_M ($K << 1$)

and the Sharvin resistance R_s ($K \gg 1$), given by equations (3.4) and (3.5), a simple interpolation formula can be found. Wexler (1966) has given a solution of the Boltzmann equation, using the variational principle for the resistance of a contact. One gets for the resistance R of the point-contact

$$R = \frac{4}{3\pi}\frac{\rho\ell}{a^2} + \Gamma(K)\,\frac{\rho}{2a} = \frac{4}{3\pi}\frac{\rho\ell}{a^2}\left(1 + \frac{3\pi}{8}\,\Gamma(K)\,\frac{a}{\ell}\right) . \qquad (3.6)$$

Here, Γ (K) is a slowly varying function of the Knudsen number K, with $\Gamma(K=0) = 1$ and $\Gamma(K = \infty) = 0.694$.

The measured current-voltage characteristic of a Cu point-contact at low temperatures is non-linear as shown in figure 3. This is clearly visible in the measured first and second derivative (dV/dI and d^2V/dI^2), also plotted in figure 3. The structure in the second derivative around 17 and 27 mV

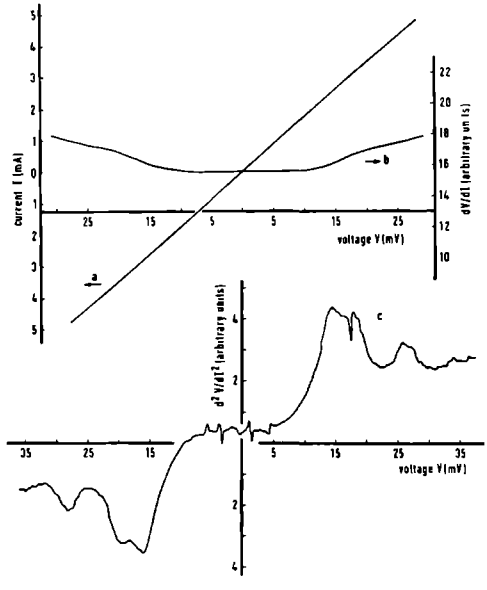

Fig. 3 Recorder output of the current-voltage characteristics of a copper point contact. The current I (a), the first derivative dV/dI (b) and the second derivative d^2V/dI^2 are given as a function of the applied voltage V. Resistance R_o = 5.7 Ω; temperature T = 1.2 K.

occurs at energies corresponding to the typical phonon frequencies of Cu; therefore the signal is directly related to the electron-phonon interaction in the metal. As the measured signal is proportional to the voltage derivative of the resistance ($d^2V/dI^2 = 1/R\ dR/dV$), the voltage or energy dependence of the contact resistance as expressed by equation (3.6) has to be considered. Usually, the electronic mean free path ℓ will be energy dependent, $\ell = \ell(\varepsilon)$. However, in equation (3.6) only the second term depends on the mean free path $\ell(\varepsilon)$ as the product $\rho\ell$ is characteristic for a given metal and is independent of the mean free path. One finds for the voltage derivative of the resistance

$$\frac{dR}{dV} = \Gamma(K)\ \frac{\rho\ell}{2a}\ \frac{d}{dV}\ \left(\frac{1}{\ell(\varepsilon=eV)}\right) . \tag{3.7}$$

The Sharvin-like term in equation (3.6) leads to no structure, but this term is essential as he allows to have an electric field within a metal.

The total scattering lengtn ℓ of the electrons is determined by the elastic scattering with the impurities (ℓ_{imp}) and the inelastic scattering with the phonons (ℓ_{ep}). Using Matthiessen's rule the total scattering length ℓ can be written as

$$\frac{1}{\ell} = \frac{1}{\ell_{imp}} + \frac{1}{\ell_{ep}} \quad . \tag{3.8}$$

Here, only the electron-phonon length ℓ_{ep} will be energy dependent and give rise to a contribution to the signal via equation (3.7). Using the well known Fermi's golden rule argument for the transition rate of an electron arising from the electron-phonon interaction, one finds for the scattering time $\tau_{ep}(\varepsilon) = \ell_{ep}(\varepsilon)/v_F$ of an electron with energy ε above the Fermi level

$$\frac{1}{\tau} = \frac{2\pi}{\hbar}\ \sum_k\ |g_q|^2\ \delta(\varepsilon_p-\varepsilon_k-\hbar\omega_q)\ (N_q+1-f_k)$$

$$+\ \delta(\varepsilon_p + \hbar\omega_q - \varepsilon_k)\ (N_q + f_k) . \tag{3.9}$$

Here, g_q is the matrix element for the electron-phonon interaction for a phonon with wave vector q and energy $\hbar\omega_q$, ε_p and ε_k the energies of electrons with momenta p and k, N_q the Bose distribution function of the phonons and f_k the Fermi distribution function of the electrons. The summation over k can be replaced by an integral

$$\Sigma_k = \frac{N_o}{2} \int d\epsilon_k \int \frac{qdq}{2k_F^2} \quad , \tag{3.10}$$

where N_o is the density of states at the Fermi level. Defining the Eliashberg function for the electron-phonon interaction as

$$\alpha^2F(\omega) = \frac{N_o}{2} \int \frac{qdq}{2k_F^2} |g_q|^2 \delta(\hbar\omega - \hbar\omega_q), \tag{3.11}$$

the scattering time can now be written as

$$\frac{1}{\tau(\epsilon)} = 2\pi \int d\omega \, \alpha^2F(\omega) [2N(\omega) + 1 + f(\epsilon+\omega) - f(\epsilon-\omega)] \, . \tag{3.12}$$

For T=0 this reduces to

$$\frac{1}{\tau(\epsilon)} = 2\pi \int_0^{\epsilon/\hbar} d\omega \, \alpha^2F(\omega) \, . \tag{3.13}$$

Therefore one finds the all important result that for low temperatures the voltage derivative of the point-contact resistance is given by

$$\frac{dR}{dV}(V) = \frac{\rho\ell}{2a} \Gamma(K) \frac{2\pi e}{\hbar v_F} \alpha^2F(eV) \, . \tag{3.14}$$

This equation allows a direct determination of α^2F by measuring the voltage derivative of the resistance of a metallic contact.

In figure 4 we have plotted the measured second derivative d^2V/dI^2 as a function of the applied voltage for a Au point contact. To compare the measured signal with the phonon spectrum, we have given in the same figure the phonon density of states $F(\omega)$ as obtained from inelastic neutron scattering experiments. As expected, there is a clear agreement in the voltage dependence of the signal with the frequencies of the transverse and longitudinal phonons. The point-contact spectrum shows a weaker coupling of the electrons with the longitudinal phonons than with the transverse phonons; this was observed for all the noble metal point contacts (Jansen et al., 1977 and 1978). Note, that the point-contact spectrum should vanish for applied voltages bigger than the Debije energy, as there are no more phonons available. However, a smooth background signal, saturating at high energies at a non-zero level, remains (short-dashed line in figure 4). Because of the spontaneous emission of phonons, the phonon system does not have to be

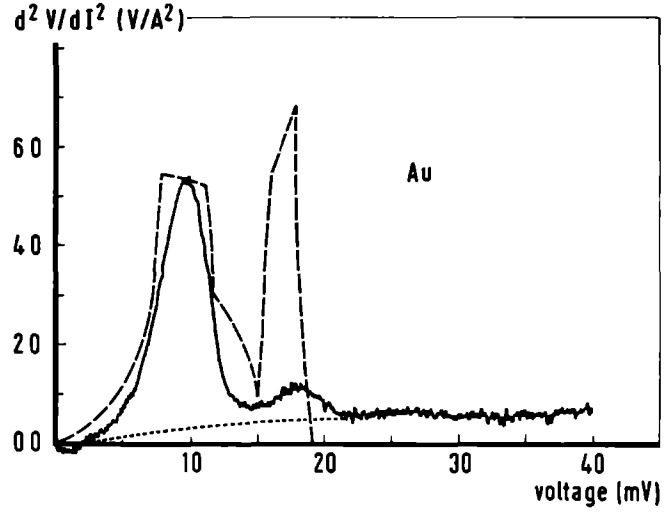

Fig. 4 Measured d^2V/dI^2 spectrum of a gold point contact. The long-dashed line gives the phonon density of states $F(\omega)$ obtained from inelastic neutron scattering (Lynn et al., 1973). The short-dashed line shows the smooth background signal.

in thermal equilibrium. If this effect is taken into account, it will be shown in the next paragraph, that these non-equilibrium phonons give rise to a background signal, which saturates above the Debije energy, in agreement with the experimental findings.

4. Solution of the Boltzmann equation

4.1 Formulation of the problem

In the previous paragraph we have discussed the observed non-linear phenomena in the current-voltage characteristics of metallic point contacts using a more phenomenological approach based on an interpolation procedure between the Maxwell and Sharvin limit. Here, we present a more fundamental discussion based on the solution of the full non-linear Boltzmann equation for the point-contact problem which has recently become available (Kulik et al., 1977; Kulik and Yanson, 1978; van Gelder, 1978 and 1980; Jansen et al., 1980 b). The solution is based on an iterative procedure. In zeroth

order, the linear relation between the current and the voltage is described for a point-contact geometry in the high Knudsen number limit, resulting in the energy-independent Sharvin resistance. In next order, energy-dependent corrections are added to the current leading to the observed non-linear behaviour of the point contacts. In our discussion, we will generalize the solution of the problem, originally proposed by Kulik et al. (1977), in such a way that the electrons can scatter with arbitrary targets, i.e. phonons, impurities, localized spins, etc. (Jansen et al., 1980 b). To avoid divergent terms in second order, van Gelder (1978 and 1980) has introduced a damping along the trajectory of the electrons. This approach gives in first order (i.e. for a contact with a large Knudsen number) the same results as without damping, while in higher orders the iterative procedure converges then apropriately.

First of all the problem has to be formulated in terms of the Boltzmann equation for the distribution function of the electrons, and the Poisson equation for the electric field, taking properly into account the boundary conditions. These equations are then solved by iteration with respect to the collision term in the Boltzmann equation, yielding solutions in zeroth and first order. Because until now point-contact spectroscopy is most successfully used for the experimental determination of the electron-phonon interaction in metals, the result will finely explicitly be applied to phonons, as the scattering targets. In context with the damping mechanism mentioned before, double collision processes will be treated as an application for higher order iterations. It is possible to discuss other interaction mechanisms which can be probed using point contacts within the same theoretical frame-work. In our analysis, we restrict ourselves mainly to a thermalized system of scatterers at a temperature $T = 0$, as most of the experiments are performed at liquid helium temperatures. The influence of the temperature, which in essence is only a thermal averaging can easily be taken into account. With respect to the electron-phonon interaction a careful analysis shows that the measured derivative d^2I/dV^2 is proportional to a new electron-phonon interaction-function α^2F_p, where the subscript p indicates the difference with respect to the usual Eliashberg function α^2F due to an efficiency factor, which depends on the angle between the momenta of the electron before and after the collision. In the last part of this paragraph the observed smooth background signal on which the α^2F-signal is thought to be superimposed will be discussed. An explanation of the back-

ground signal is given in terms of a non-equilibrium distribution of the phonons, arising from the spontaneous emission-processes in the vicinity of the contact. The analysis yields a saturating signal at high voltages. In addition, phonon-drag effects and direct electron-electron scattering can be associated with a structure at zero bias and, respectively, a signal which is linear in the applied voltage.

Formally, to solve the point-contact problem, we have to determine the current I through a point contact for an applied voltage V. The point-contact geometry is represented by an open orifice in a otherwise, non-conducting plane which separates two metallic half-spaces. The current I is given by an integral of the z-component of the current density $j_z(\underline{r})$ over the area of the orifice(conveniently placed in the z=0 plane):

$$I = \iint_{\text{orifice}} dxdy \; j_z(x,y,0) \tag{4.1}$$

with the current density per unit volume given by

$$\underline{j}(\underline{r}) = 2\, e \sum_{\underline{k}} \underline{v}_{\underline{k}}\, f_{\underline{k}}(\underline{r}) \quad . \tag{4.2}$$

$\underline{v}_{\underline{k}}$ is the band velocity of an electron with a wave vector $\underline{k}$, and $f_{\underline{k}}(\underline{r})$ the distribution function of an electron at the position $\underline{r}$. Once the function $f_{\underline{k}}(\underline{r})$ is known, the current can be calculated, and $f_{\underline{k}}(\underline{r})$ can be obtained by solving the Boltzmann equation

$$\underline{v}_{\underline{k}} \cdot \underline{\nabla}_{\underline{r}}\, f_{\underline{k}}(\underline{r}) + \frac{e}{\hbar}\, \underline{E} \cdot \underline{\nabla}_{\underline{k}}\, f_{\underline{k}}(\underline{r}) = \left.\frac{\partial f}{\partial t}\right|_{\text{coll.}} \tag{4.3}$$

with the drift terms on the left-hand side of this equation and the scattering term on the right-hand side. The electric field $\underline{E}$ in the Boltzmann equation must be obtained from Poisson's equation

$$-\Delta\, \phi(\underline{r}) = e\, \underline{\nabla} \cdot \underline{E} = -(2e/\varepsilon_o) \sum_{\underline{k}} f_{\underline{k}}(\underline{r}) \;, \tag{4.4}$$

where Δ is the Laplacian operator applied to the electrostatic potential energy $\phi(\underline{r})$ and ε_o the dielectric constant of the vacuum. As the Thomas-Fermi screening length is small (< 1 Å) for a metal, the Poisson equation reduces to the condition of charge neutrality

$$2e \sum_{\underline{k}} \left[\, f_{\underline{k}}(\underline{r}) - f_o(\varepsilon_k) \,\right] = 0 \tag{4.5}$$

inside a metal, where $f_o(\varepsilon_k) = 1/(e^{(\varepsilon_k - \mu)/k_B T} - 1)$ is the usual Fermi-Derac distribution function in equilibrium (μ is the chemical potential).

Equations (4.3) and (4.5) have to be solved with the boundary conditions

$$\phi\ (z \to \pm\infty) = \pm\ eV/2$$
$$f_{\underline{k}}\ (z \to \pm\infty) = f_o(\varepsilon_k) \quad , \tag{4.6}$$

because a voltage V is applied over the contact and the distribution has to be in equilibrium and equal to the Fermi function far from the orifice. The collision term for the gain and loss contribution to an electron state with wave vector $\underline{k}$ can be written as

$$\left.\frac{\partial f_{\underline{k}}(\underline{r})}{\partial t}\right|_{\text{coll.}} = \sum_{\underline{k}'} \left[\Gamma(\underline{k}', \underline{k}) f_{\underline{k}'}(1-f_{\underline{k}}) - \Gamma(\underline{k},\underline{k}') f_{\underline{k}}(1-f_{\underline{k}'}) \right] . \tag{4.7}$$

According to the general principles of statistical mechanics, the transition rate $\Gamma(\underline{k}',\underline{k})$ between an initial state $|\underline{k}'\ i>$ and a final state $|\underline{k}\ f>$ is given by

$$\Gamma(\underline{k}',\underline{k}) = \frac{2\pi}{\hbar} \sum_{if} P_i\ \delta(\varepsilon_f - \varepsilon_i - (\varepsilon_{k'} - \varepsilon_k)) \left| < \underline{k}\ f \left| U \right| \underline{k}'\ i > \right|^2 . \tag{4.8}$$

P_i is the probability for the system to be in the state i, and ε_i and ε_f are the initial and final energies of the target. The squared matrix-element contains the interaction U between the scattered electron and the target. Arbitrary scattering mechanisms can be chosen for the targets; the most important one is obviously the electron-phonon interaction.

Given the basic formulas for the solution of the problem, the Boltzmann equation (4.3) will be solved, using the charge neutrality condition (4.5) by an iteration with respect to the collision term taking into account the boundary conditions (i.e. an electron is specularly or diffusely reflected at the boundaries of the system). In a schematic way the successive contributions to the current from these iterations are shown in figure 5. Figure 5a gives the zeroth order field-emission current according to Sharvin's picture (1965). Figures 5b and 5c show the non-linear corrections to the Sharvin current for backflow processes, involving single and double collisions with a target respectively.

4.2 Solution in zeroth order: Sharvin current

For the solution of the Boltzmann equation it is convenient to intro-

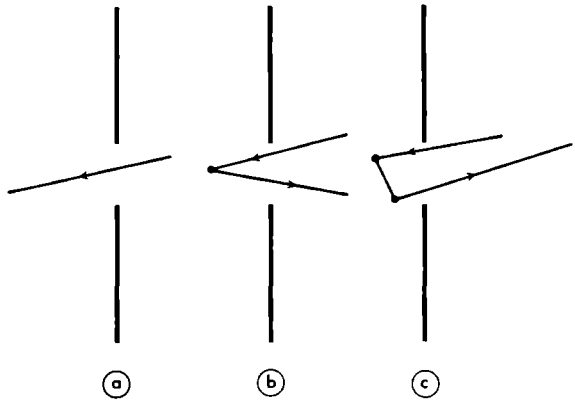

Fig. 5 Schematic view of the successive iterative contributions to the current through a point contact: zeroth order Sharvin current (a), first order single collision backflow (b) and second order double collision backflow (c).

duce a local potential $\psi_{\underline{k}}(\underline{r})$ in the expression for the distribution function $f_{\underline{k}}(\underline{r})$, defined through

$$f_{\underline{k}}(\underline{r}) = f_o\ (\varepsilon_k - \psi_{\underline{k}}(\underline{r}))\ , \tag{4.9}$$

where f_o is the Fermi function. With a first order Taylor expansion of the distribution function with respect to this local potential $\psi_{\underline{k}}(\underline{r})$ the current density in equation (4.2) becomes

$$j_z(\underline{r}) = -\ 2e \sum_{\underline{k}} v_{\underline{k}z}\ \psi_{\underline{k}}(\underline{r})\ \left(\frac{\partial f_o}{\partial \varepsilon_k}\right)\ . \tag{4.10}$$

In the limit of low temperatures this expression reduces to

$$j_z(\underline{r}) = 2e\ \langle v_{\underline{k}z}\ \psi_{\underline{k}}(\underline{r})\ \rangle_o\ , \tag{4.11}$$

where we have used the definition $\sum_{\underline{k}} \ldots . \delta(\varepsilon_k - \omega) \equiv \langle \ldots . \rangle_\omega$ for a summation over the Fermi-sphere. The distribution function on the left side of the Boltzmann equation (4.3) can also be expanded in a Taylor series, at which procedure only first order terms in the field are kept, and one gets

$$\underline{v}_{\underline{k}} \cdot \underline{\nabla}_{\underline{r}} \psi_{\underline{k}}(\underline{r}) - e\,\underline{E} \cdot \underline{v}_{\underline{k}} = - \frac{\left.\frac{\partial f_{\underline{k}}(\underline{r})}{\partial t}\right|_{coll}}{\frac{\partial f_o}{\partial \epsilon_{\underline{k}}}} \equiv - F(\underline{r},\underline{k}) \ . \qquad (4.12)$$

Using Chamber's method of trajectories, we integrate equation (4.12) along the path (variable s) of an electron. Introducing $\underline{n} = \underline{v}_{\underline{k}} / |v_{\underline{k}}|$, where $\underline{n}$ is parallel to the path s, equation (4.12) can be written as

$$\frac{\partial \psi_{\underline{k}}}{\partial s} - e\,\underline{E}.\underline{n} = - \frac{F(\underline{r},\underline{k})}{|v_{\underline{k}}|} \ . \qquad (4.13)$$

Integration from $s = -\infty$ (far from the orifice) to $s=0$ (position $\underline{r}$) yields an expression for the local potential $\psi_{\underline{k}}(\underline{r})$

$$\psi_{\underline{k}}(\underline{r}) = - [\, \phi(\underline{r}) - \phi(s = -\infty) \,] - \int_{-\infty}^{0} \frac{ds}{|v_{\underline{k}}|} F(\underline{r},\underline{k}) . \qquad (4.14)$$

The potential $\phi(s= -\infty)$ is given by the boundary condition for the starting point of the electron

$$\phi(s = -\infty) = p(\underline{r}, \underline{v}_{\underline{k}})\ eV/2 \ , \qquad (4.15)$$

where $p(\underline{r},\underline{v}_{\underline{k}}) = \pm 1$, depending on wether the starting point is at the high ($p = +1$) or low ($p = -1$) potential side of the contact. The potential $\phi(\underline{r})$ has to be found from the charge neutrality condition (4.5), which can be written as follows

$$\langle \psi_{\underline{k}}(\underline{r}) \rangle_o = 0 \ . \qquad (4.16)$$

Combining equations (4.14) and (4.16), we find for the potential energy

$$\phi(\underline{r}) = \frac{1}{\langle 1 \rangle_o} [\, \langle \phi(s = -\infty) \rangle_o - \langle G(\underline{r},\underline{k}) \rangle_o \,] \ , \qquad (4.17)$$

where $G(\underline{r},\underline{k}) = \int_{-\infty}^{0} \frac{ds}{|v_{\underline{k}}|} F(\underline{r},\underline{k})$. It should be noted that $\phi(\underline{r})$ is an even function in the velocity $\underline{v}_{\underline{k}}$ and that therefore the potential $\phi(\underline{r})$ doesn't give a contribution to the current density of equation (4.11). The electrostatic potential $\phi(\underline{r})$ determines the bottom of the conduction band, and plays no direct role in the electronic transport.

Starting with $F = G = 0$, it is possible to get an iterative solution

of the Boltzmann equation, where the collision term is used to produce the higher order iterations. In zeroth order (i.e. F = G = 0), one finds the field-emission current as discussed by Sharvin (1965). The potential energy in this zeroth order is then given by

$$\phi^{(o)}(\underline{r}) = < \phi(s = -\infty) >_o / <1>_o \ . \tag{4.18}$$

Introducing $\gamma(\underline{r})$ as the solid angle at which the orifice is seen from the position $\underline{r}$, we obtain

$$\phi^{(o)}(\underline{r}) = \pm \frac{eV}{2} \left[1 - \frac{\gamma(\underline{r})}{2\pi} \right] \tag{4.19}$$

with the + or - sign for the two sides of the contact. In particular, we have on the z-axis

$$\phi^{(o)}(x=y=o,z) = \pm \frac{eV}{2} \frac{z}{\sqrt{z^2+a^2}} \ , \tag{4.20}$$

This function has been drawn to indicate the bottom of the conduction band in figure 6. Again in zeroth order, the local potential $\psi_{\underline{k}}^{(o)}(\underline{r})$ is equal to

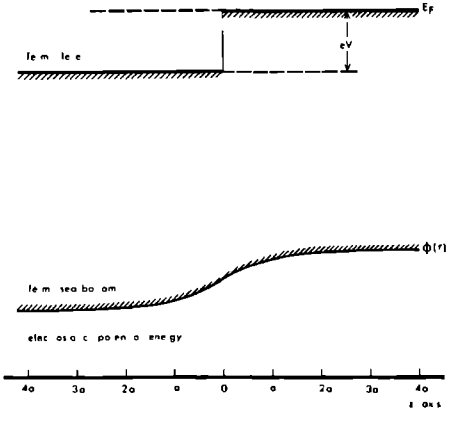

Fig. 6 The conduction band of the electrons for $T \to 0$ near a contact with radius a. The applied voltage over the contact yields the sketched Fermi levels E_F and the electrostatic potential energy $\phi(\underline{r})$ for $\underline{r}$ along the z-axis.

$$\psi_{\underline{k}}^{(o)}(\underline{r}) = -\phi^{(o)}(\underline{r}) + \phi(s = -\infty), \tag{4.21}$$

leading to a zeroth-order distribution function $f_{\underline{k}}^{(o)}(\underline{r}) = f_o(\epsilon_{\underline{k}} - \psi_{\underline{k}}^{(o)}(\underline{r}))$ for the electrons. This $f_{\underline{k}}^{(o)}(\underline{r})$ is indicated for different positions $\underline{r}$ in figure 7.

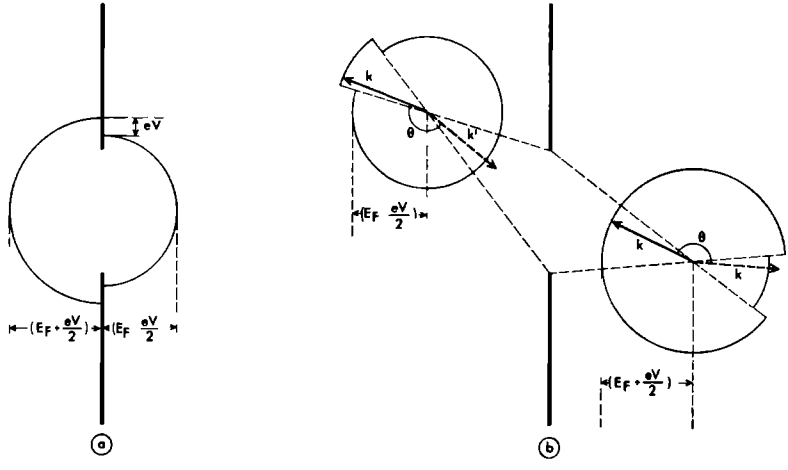

Fig. 7 The electronic distribution of the electrons in zeroth order according to the Sharvin picture at the orifice (a) and at positions near the orifice (b). The inelastic scattering processes, where the velocity directions of the electrons change from $\underline{k}$ to $\underline{k}'$, give a negative correction to the current.

Using expression, (4.21), the current through the orifice from equations (4.1) and (4.11) becomes

$$I^{(o)} = e^2 V D < |v_{\underline{k}z}| >_o , \tag{4.22}$$

where D is the area of the orifice. Evaluating expression (4.22) for a quadratic dispersion relation for the electrons yields the expression for the Sharvin resistance, already given in the previous chapter for a circular

orifice

$$R_S = R_o = V/I^{(o)} = \frac{4}{3}\frac{\rho\ell}{D} . \qquad (4.23)$$

$\rho\ell$ is a material constant and is given by $\rho\ell = mv_F/n_o e^2$ for a Drude model. R_S is energy independent and indicates an ohmic behaviour.

In the evaluation of expression (4.22) self-energy effects have been neglected. If the electronic density of states is not constant within an energy shell eV around the Fermi energy, the current $I^{(o)}$ through the point contact becomes voltage dependent (non-ohmic behaviour). Self-energy effects, arising i.e. from the electron-phonon interaction, can lead to a non-linear current-voltage characteristic for a point-contact (Omelyanchuk et al., 1977). By introducing an effective mass $m^*(\varepsilon) = m(1 + \lambda(\varepsilon))$, a quadratic dispersion relation for the energy $\varepsilon = \hbar^2k^2/2m^*(\varepsilon)$ of an electron can be defined. The renormalisation parameter $\lambda(\varepsilon)$, arising from the electron-phonon interaction, has been discussed in detail by Grimvall (1976); λ is connected with the Eliashberg function α^2F through $\lambda = \lambda(o) = 2 \int d\omega\, \alpha^2F(\omega)/\omega$.

Taking into account this type of self-energy effects, the current in zeroth order takes the form

$$I^{(o)} \sim \int dk\, k^2\, v_k \sim \int dk\, k^2 \left(\frac{d\varepsilon}{dk}\right) \sim \int_0^{eV} d\varepsilon\, \varepsilon_o , \qquad (4.24)$$

where $\varepsilon_o = \hbar^2k^2/2m$ is the electron energy without self-energy corrections. Comparing the expressions for ε and ε_o, we have $(d\varepsilon_o/d\varepsilon) = (m^*/m)_\varepsilon$. Differentiating expression (4.24) twice gives now the contribution to the second derivative signal due to a change in the electronic density of states because of the electron-phonon interaction:

$$\frac{1}{R}\frac{dR}{dV} \simeq R_o \frac{d^2I}{dV^2} = \frac{e}{E_F}\left(\frac{d\varepsilon_o}{d\varepsilon}\right)_{eV} = \frac{e}{E_F}\left(\frac{m^*}{m}\right)_{eV} . \qquad (4.25)$$

A quantitative estimate of the non-linearity according to equation (4.25) gives a value $\sim 0.2\ V^{-1}$, which is only a few percent of the usually observed non-linearity in point-contact spectroscopy due to electron-phonon scattering. Therefore, we neglect self-energy effects and assume the density of states of the electrons to be constant near the Fermi energy.

4.3 Solution in first order: backflow current

The first order corrections for the current through a point contact are negative. This is due to the fact that the injected electrons can flow back through the orifice after an inelastic scattering with a target. This collision gives rise to an energy-dependent contribution to the current. For isotropic scattering processes, the all important result is found that the change in the resistance of a point contact is proportional to the energy-dependent scattering rate of the electrons.

The first order terms of the electrostatic potential $\phi^{(1)}(\underline{r})$ and the local potential $\psi_{\underline{k}}^{(1)}(\underline{r})$ are obtained by using equations (4.4) and (4.17)

$$\psi_{\underline{k}}^{(1)}(\underline{r}) = - \phi^{(1)}(\underline{r}) - G_{\underline{k}}^{(0)}(\underline{r}) \tag{4.26}$$

$$\phi^{(1)}(\underline{r}) = - < G_{\underline{k}}^{(0)}(\underline{r}) >_o \; / \; <1>_o \; . \tag{4.27}$$

Here, in the spirit of the iterative procedure, the function $G_{\underline{k}}^{(o)}(\underline{r})$ is calculated using the zeroth order distribution function $f_{\underline{k}}^{(o)}$: $G_{\underline{k}}^{(o)}(\underline{r}) = G \{ f_o(\varepsilon_k - \psi_{\underline{k}}^{(o)}(\underline{r})) \}$. Again, as in the zeroth order case, $\phi^{(1)}(\underline{r})$ will not give a contribution to the current because the potential $\phi(\underline{r})$ is an even function of the electron velocity. It turns out that it is not necessary to calculate the electro-static potential explicitly as we could also have defined the local potential by $f_{\underline{k}}(\underline{r}) = f_o(\varepsilon_k + \phi(\underline{r}) - \psi_{\underline{k}}(\underline{r}))$, with the boundary condition $\psi_{\underline{k}}(z \pm \infty) = \pm eV/2$, in order to get the same results without an explicit expression for $\phi(\underline{r})$. Using equations (4.1) and (4.2), the correction $I^{(1)}$ (backflow current) to the total current is given by

$$I^{(1)} = 2e \iint_{\text{orifice}} dxdy \sum_{\underline{k}} \frac{v_{\underline{k}z}}{|v_k|} \times \int_{-\infty}^{0} ds \sum_{\underline{k}'} [\Gamma(\underline{k}',\underline{k}) f_{\underline{k}'}^{(o)}(1 - f_{\underline{k}}^{(o)}) - \Gamma(\underline{k},\underline{k}') f_{\underline{k}}^{(o)}(1-f_{\underline{k}'}^{(o)})] . \tag{4.28}$$

The path s is a straight trajectory parallel to $v_{\underline{k}}$ ending at the orifice (s = 0). In figure 8 we have drawn some illustrative pathes, starting at

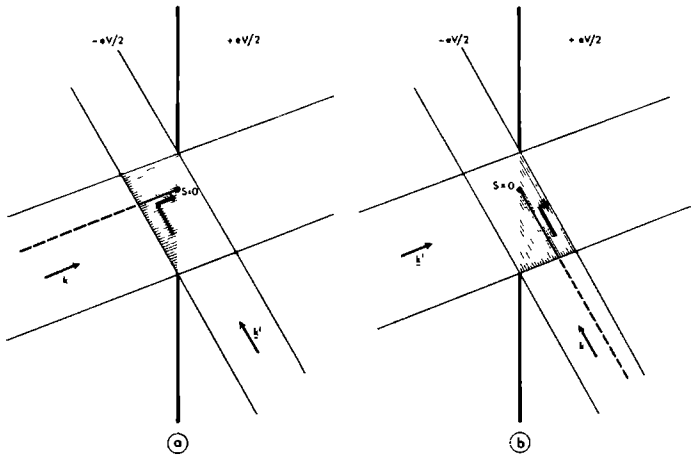

Fig. 8 Trajectories of the electrons starting far from the left (a) or right (b) side of the orifice and ending at the orifice (s=0). The pathlengthes in the shaded area of the figures contribute to the signal for inelastic scattering of the electrons from $\underline{k}'$ to $\underline{k}$.

the left side (figure 8a) and at the right side (figure 8b) of the orifice. Only the pathlengthes which lie in the shaded area of the figure can contribute to the current. For both situations, the correction to the current is negative. It is now readily shown that the spatial integrations reduce to a weightfactor $K(\underline{k},\underline{k}') = \int\int dxdy \frac{v_{kz}}{|v_k|} \int ds$ which is the common volume of two cylinders constructed with the boundary line of the orifice and whose walls are parallel to $\underline{v}_{\underline{k}}$ and $\underline{v}_{\underline{k}'}$.

In figure 9 we show the inelastic scattering of an electron in the state $\underline{k}'$ to the state $\underline{k}$ in energy space near the Fermi surface for the temperature $T \to 0$. In this low temperature limit, the summation over $\underline{k}$ and $\underline{k}'$ can be written as

$$\sum_{k}\sum_{k'} \ldots = \int_0^{eV} d\varepsilon_k \int_{\varepsilon_k}^{eV} d\varepsilon_{k'} \langle\langle \ldots \rangle_{\varepsilon_k} \rangle_{\varepsilon_{k'}} = \int_0^{eV} d\varepsilon_1 \int_0^{\varepsilon_1} d\varepsilon_2 \langle\langle \ldots \rangle_{\varepsilon_1} \rangle_{\varepsilon_2} . \tag{4.29}$$

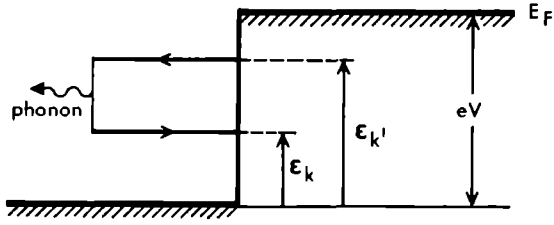

Fig. 9 Single collision backflow process in energy space, where a phonon with energy $(\varepsilon_{k'} - \varepsilon_k)$ is emitted spontaneously.

Using these results for the energy and spatial integrations, the backflow current reduces to

$$I^{(1)} = -2e \int_0^{eV} d\varepsilon_1 \int_0^{\varepsilon_1} d\varepsilon_2 \, \langle\langle \Gamma(\underline{k},\underline{k}') \; K \; (\underline{k},\underline{k}') \rangle_{\varepsilon_1} \rangle_{\varepsilon_2} . \tag{4.30}$$

The influence of the backflow current on the resistance of a point contact can now be evaluated. For small changes in the resistance (small compared with the resistance at zero voltage), the resistance change ΔR will be given by

$$\Delta R = R_o^2 \, e \, \frac{dI^{(1)}}{d(eV)} . \tag{4.31}$$

For isotropic scattering we obtain

$$\Delta R = R_o^2 \, 2e^2 \, \langle\langle K(\underline{k},\underline{k}') \rangle_o \rangle_o \int_0^{eV} d\varepsilon \; \Gamma(eV,\varepsilon) \; N(\varepsilon) . \tag{4.32}$$

Here, $N(\varepsilon) = \langle 1 \rangle_\varepsilon / \langle 1 \rangle_o$ is the normalized density of states. The relaxation time time τ for an electron with energy eV above the Fermi level is given by

$$\frac{1}{\tau}(eV) = \sum_{k'} \Gamma(\underline{k},\underline{k}') = \langle 1 \rangle_o \int_0^{eV} d\varepsilon \; \Gamma(eV,\varepsilon) \; N(\varepsilon) \tag{4.33}$$

which also defines the energy dependent relaxation rate $\Gamma(eV,\varepsilon)$. Assuming that the density of states is constant for energies $eV << E_F$ $(N(eV) = 1)$, the resistance change of a point contact at low temperatures is directly

proportional to the scattering rate

$$\Delta R = R_o^2\, 2e^2\, \frac{\langle\langle K(\underline{k},\underline{k}')\rangle_o\rangle_o}{\langle 1\rangle_o}\, \tau^{-1}(eV)\ . \qquad (4.34)$$

Using $\langle\langle K(\underline{k},\underline{k}')\rangle_o\rangle_o/\langle 1\rangle_o^2 = a^3/3$ and $\langle 1\rangle_o = m^2 v_F/\pi^2\hbar^3$, the change in the contact resistance given by expression (4.34) differs only 3.6% from the expression (3.6) for the resistance found by Wexler through an interpolation between the Maxwell and Sharvin limit. The last equation shows the grand result of point-contact spectroscopy. A direct determination of the energy-dependent scattering rate of an electron is possible from the measurement of the resistance of a point contact as a function of the applied voltage. This result can obviously be applied to arbitrary targets (equations (4.8), (4.32) and (4.34)).

4.4 Application to the electron-phonon interaction

In this section, the theory of point-contact spectroscopy will be explicitly applied to the electron-phonon interaction, starting from the general results of equations (4.28) and (4.30). A transport efficiency function is found for the electron-phonon interaction as measured in point-contact experiments, very similar to the well-known efficiency function $(1-\cos\theta)$ in the dc-resistivity of bulk metals. Here, we will limit ourself to a thermalized phonon system at a temperature T=0; the consequences of non-equilibrium effects will be treated in the next section. It is necessary to modify the solution of the point-contact problem slightly (van Gelder, 1978 and 1980) by taking into account the damping of the excited electrons in order to deal properly with multiple collision processes.

The collision term for the electron-phonon interaction in the Boltzmann equation can be written as

$$\left.\frac{\partial f_{\underline{k}}(\underline{r})}{\partial t}\right|_{coll.} = \frac{2\pi}{\hbar} \sum_{\underline{k}'} |g_{kk'}|^2 [\ \{f_{\underline{k}'}(1-f_{\underline{k}})(N_q+1) - f_{\underline{k}}(1-f_{\underline{k}'})N_q\}\ \delta(\varepsilon_{k'}-\varepsilon_k-\hbar\omega)$$

$$+ \{f_{\underline{k}'}(1-f_{\underline{k}})N_q - f_{\underline{k}}(1-f_{\underline{k}'})(N_q+1)\}\ \delta(\varepsilon_{k'}-\varepsilon_k+\hbar\omega)\ ]\ . \qquad (4.35)$$

Here, $G_{kk'}$ is the matrix element for the electron-phonon interaction, and $f_{\underline{k}}$ and N_q the Fermi-Dirac and Bose-Einstein distribution respectively, with the phonon wave number given by $q = |\underline{k} - \underline{k}'|$. Using the collision term in the expression (4.28), one gets for the backflow current in the limit T=0 (N_q=0)

$$I^{(1)} = 2e \iint_{\text{orifice}} dxdy \sum_{\underline{k}} \frac{v_{\underline{k}z}}{|v_k|} \int_{-\infty}^{0} ds \frac{2\pi}{\hbar} \sum_{\underline{k}'} |g_{kk'}|^2$$

$$\times [f_{\underline{k}'}^{(o)} (1-f_{\underline{k}}^{(o)}) \delta(\varepsilon_{k'}-\varepsilon_k-\hbar\omega) - f_{\underline{k}}^{(o)} (1-f_{\underline{k}'}^{(o)}) \delta(\varepsilon_{k'}-\varepsilon_k+\hbar\omega)] \qquad (4.36)$$

With $\sum_{\underline{k}} = \frac{N_o}{8\pi} \int d\varepsilon \int d^2n$ (where $\underline{n} = \underline{v}_{\underline{k}}/|v_k|$) the spatial integrations can be written as

$$\iint_{\text{orifice}} dxdy \frac{v_{\underline{k}'}}{|v_k|} \int_{-\infty}^{0} ds \int d^2n' = \frac{1}{4\pi} \int d\underline{r}_1 \int_{\text{orifice}} d\underline{r}_2 \frac{1}{|\underline{r}_1-\underline{r}_2|} \int d^2n' \cos^2\varphi \, \delta(|\varphi-\varphi'|-\pi) \qquad (4.37)$$

where φ and φ' are the polar angles of $\underline{k}$ and $\underline{k}'$, respectively. The coordinates $\underline{r}_1$ and $\underline{r}_2$ run over the orifice (see figure 10). Because of the change in the variables of equation (4.37), the transitions during a scattering process are no longer restricted (i.e. $v_{\underline{k}z}\, v_{\underline{k}'z} < 0$), and therefore the final result has to be multiplied by (½). For the spatial integration one gets

$$\int d\underline{r}_1 \int d\underline{r}_2 \frac{1}{|\underline{r}_1 - \underline{r}_2|} = \frac{16}{3} \pi \sigma a^3 , \qquad (4.38)$$

where πa^2 is equal to the area of the orifice, and $\sigma = 1$ if the shape is circular. Averaging over all possible crystalline directions with respect to the orifice gives the transport efficiency function η, depending on the scattering angle $\theta = \theta(\underline{n},\underline{n}')$ in such a way that $\eta(\theta) = \langle \cos^2\varphi \, \delta(|\varphi-\varphi'|-\pi) \rangle_{av}$. Realizing that $\int d^2n \int d^2n' \sim \int_{\alpha+\beta=\theta<\pi} d\alpha \int d\beta \sin\alpha \sin\beta \simeq \int_0^{\pi} d\theta \sin\theta \, (1-\theta/\mathrm{tg}\theta)$ (see figure 10), one obtains the normalized efficieny function (van Gelder, 1980)

$$\eta(\theta) = \tfrac{1}{2} \left(1 - \frac{\theta}{\mathrm{tg}\theta}\right) . \qquad (4.39)$$

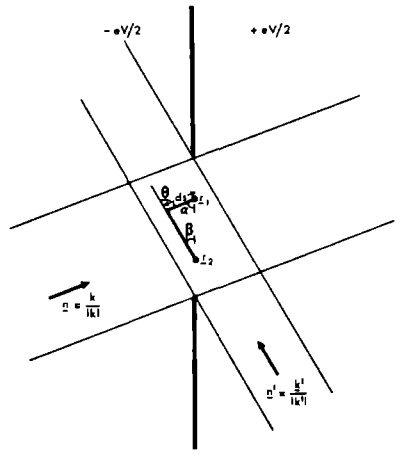

Fig. 10 Integration variables used for the evaluation of the backflow current (see text). If $\underline{n}$ and $\underline{n}'$ varie in a fixed plane, one has $\int d^2n \int d^2n' \sim \int d\alpha \int d\beta \sin\alpha \sin\beta \simeq \int_0^{\pi} d\theta \sin\theta \ (1-\theta/\mathrm{tg}\theta)$. $\alpha+\beta\ \theta<\pi$

The backflow current can now be written as

$$I^{(1)} = \frac{4}{3\pi} \frac{em^2 v_F}{\hbar^4} a^3 \int_0^{eV} d\varepsilon_1 \int_0^{\varepsilon_1} d\varepsilon_2 \ \alpha^2 F_p(\varepsilon_2) \ , \qquad (4.40)$$

where we have used $N_o = \langle 1 \rangle_o = \frac{m^2 v_F}{\pi^2 \hbar^3}$, and the expression for the electron-phonon interaction function $\alpha^2 F_p(\varepsilon)$ for the point contact situation

$$\alpha^2 F_p(\varepsilon) = \frac{N_o}{32\pi^2} \int d^2n \int d^2n' \ |g_{nn'}|^2 \ \eta(\theta(\underline{n},\underline{n}')) \ \delta(\varepsilon-\hbar\omega_{nn'}) \ . \qquad (4.41)$$

In the usual transport theory for the dc-resistivity of bulk metals, one has a similar expression for the electron-phonon interaction with the well known transport-efficiency function $(1 - \cos\theta(\underline{n},\underline{n}'))$

$$\alpha^2 F_{tr}(\varepsilon) = \frac{N_o}{32\pi^2} \int d^2n \int d^2n' \ |g_{nn'}|^2 \ (1-\cos\theta(\underline{n},\underline{n}')) \ \delta(\varepsilon-\hbar\omega_{nn'}) \ . \qquad (4.42)$$

Measurements of the second derivative d^2I/dV^2 for a metallic point contact yield a direct determination of the function $\alpha^2 F_p$

$$\frac{d^2I}{dv^2} = \left(\frac{4}{3\pi}\right) \frac{e^3 m^2 v_F}{\hbar^4} a^3 \alpha^2 F_p(eV) \quad . \tag{4.43}$$

For the logarithmic derivative of the resistance we obtain for $R \sim R_o$

$$\frac{1}{R}\frac{dR}{dV} = \frac{16}{3}\frac{e\,a}{\hbar v_F} \alpha^2 F_p(eV) \quad . \tag{4.44}$$

It is of some interest to study the qualitative difference between the behaviour of the functions α^2F (no efficiency), α^2F_{tr} efficiency $(1-\cos\theta)$ and α^2F_p (efficiency $\eta(\theta)$) at low frequencies, where the wave vector q of a phonon can be taken as proportional to the frequency ω, for normal and umklapp scattering. For the analysis, we consider a metal with a minimal separation between the spheres in a repeated zone scheme equal to the wave vector q_o. For the usual normal processes, the different parameters in the function α^2F have the following low-frequency dependence: angular integrations $\int d^2n \int d^2n' \sim \int q\,dq \sim \omega^2$, squared matrix element $|g_q|^2 \sim q \sim \omega$, and the efficiency functions $(1-\cos\theta) \sim q^2 \sim \omega^2$ and $\eta(\theta) \sim q^2 \sim \omega^2$. Therefore, in the case of normal processes no difference is expected between α^2F_{tr} and α^2F_p in the low-frequency behaviour. For umklapp scattering however, the angular integrations yield $\int d^2n \int d^2n' \sim \int (q-q_o)\, q\, dq \sim \int q^2 dq \sim \omega^3$; q_o is the minimal wave vector for the occurrence of an umklapp process. For wave vectors above the minimal value q_o, the transport efficiencies behave differently: $(1-\cos\theta) \sim$ const., and $\frac{1}{2}(1 - \theta/\mathrm{tg}\theta) \sim q^{-\frac{1}{2}} \sim \omega^{-\frac{1}{2}}$. In table I we have summarized the obtained results for the low-frequency behaviour of the functions α^2F, α^2F_{tr} and α^2F_p.

Table I: Low frequency behaviour of the electron-phonon interaction parameters α^2F, α^2F_{tr} and α^2F_p, which differ in the transport efficiency, for metals with a spherical Fermi surface.

	α^2F	α^2F_{tr}	α^2F_p
transport efficiency	-	$(1-\cos\theta)$	$\frac{1}{2}(1-\theta/\mathrm{tg}\theta)$
normal processes	ω^2	ω^4	ω^4
umklapp processes	ω^3	ω^3	$\omega^{5/2}$

In a careful analysis of the theory of the point-contact problem van Gelder (1978 and 1980) has found that the simple solutions given in the preceding section lead to divergencies if the next order approximation, i.e. multiple phonon processes (figure 5c) are considered. It is possible to overcome these divergence problems by taking into account a damping of the excited electrons along their trajectories. The zeroth order solution of the electron distribution (given in figure 7) is now exponentially damped along the path s of the electron, starting from the orifice, such that $f^{(o)} = f_o(\varepsilon_k - \psi_{\underline{k}}(\underline{r}))\ e^{-s/\ell}$, where s is the path length of the electron as measured from the orifice and ℓ the average mean free path along the trajectory. In zeroth order this damped solution gives exactly the Sharvin current, because the damping is symmetric with respect to the orifice at the (z=0)-plane. In first order a damping factor has to be added to the expression for the signal as given by equation (4.44). For point contacts with large Knudsen numbers ($K = \ell/a >> 1$), the damping can be neglected because in the calculations of the backflow current the exponential factor $e^{-s/\ell}$ is close to one ($s \sim a$). For double collision backflow processes the solution of the problem is no longer divergent, and van Gelder (1978) has found the relevant geometrical factor for the backflow current to be of the order of $a^4 \ln(a/\ell)$. The relative strength of the double-phonon signal compared to single-phonon collisions is reduced by a factor $K=\ell/a$ in the limit of large Knudsen numbers $K >> 1$. In figure 11 we have drawn the double phonon process in energy-space, resulting in a backflow current

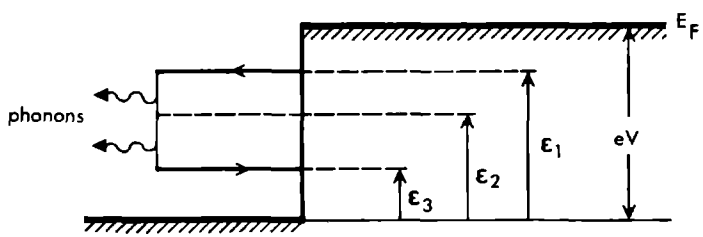

Fig. 11 Double collision backflow process in energy space, where two phonons with energy $(\varepsilon_1-\varepsilon_2)$ and $(\varepsilon_2-\varepsilon_3)$ are emitted spontaneously.

$$I^{(2)} = A \int_0^{eV} d\varepsilon_3 \int_{\varepsilon_3}^{eV} d\varepsilon_2 \int_{\varepsilon_2}^{eV} d\varepsilon_1 \, \alpha^2F(\varepsilon_1-\varepsilon_2) \, \alpha^2F(\varepsilon_2-\varepsilon_3) \qquad (4.45)$$

where $A \sim O(a^4 \ln(a/\ell))$ is the geometrical factor. For the second derivative one finds

$$\frac{d^2I^{(2)}}{dV^2} \sim \int_0^{eV} d\varepsilon \, \alpha^2F(\varepsilon) \, \alpha^2F(eV-\varepsilon) \qquad (4.46)$$

This result yields a contribution to the signal at twice the relevant phonon frequencies.

4.5 Background signal

Although no equilibrium-phonons should be present for energies above the Debije energy $\hbar\omega_D$, the measured signal of the point-contact spectrum does not reduce to zero for high applied voltages ($eV > \hbar\omega_D$). The signal which can be related to the electron-phonon interaction α^2F_p and has been discussed in the previous sections, is thought to be superimposed on a smooth background signal. The experiments show that this background signal seems to saturate at a constant level above the Debije energy. It should be noted that the multiple phonon collisions, discussed in section 4.4 (see equation 4.46), give rise to a signal for energies eV above the Debije frequency. However, it was shown theoretically and experimentally (van Gelder et al., 1978) that these processes lead to small signals and can certainly not explain the observed background entirely. Very recently (van Gelder et al., 1978 and van Gelder, 1980) a detailed explanation for the background signal was given by taking into account the non-equilibrium distribution of the phonon system. The phonon-emission processes of the injected electrons yield a non-thermalized phonon system near the orifice leading to additional backflow currents arising from stimulated emission and absorption of phonons. The problem is now to determine the non-thermalized distribution of the phonons which has to be included in the equation (4.40) leading to the signal. One finds as a result a background signal, which saturates above the Debije energy. In addition, van Gelder (1980) has also considered processes involving phonon drag effects as a possible explanation of the observed signals at low voltages, and also direct elec-

tron-electron scattering which gives a signal linear in the applied voltage.

For a determination of the phonon distribution we have to consider the transport equation for the phonons resulting from the electronic distribution given in figure 7 which allows spontaneous emission of phonons. This transport equation is obtained by equalizing the drift and collision term in the Boltzmann equation for the phonons. As usual, the collision term contains a gain and a loss term; the gain term originates from the spontaneous emission of phonons during the decay of the accelerated electrons near the contact, and the loss term describes the production of electron-hole pairs by the phonons. Giving the explicit form of the collision term, the transport equation of the phonons reads

$$\underline{c}_{\underline{q}} \cdot \frac{\partial N_{\underline{q}}(\underline{r})}{\partial \underline{r}} = \frac{\partial N_{\underline{q}}(\underline{r})}{\partial t}\bigg|_{coll.} = \frac{c_{\underline{q}}}{\varepsilon\, \ell_p(\varepsilon)} \{ \gamma(\underline{r})[1-\gamma(\underline{r})]\,(eV-\varepsilon) - \varepsilon\, N_{\underline{q}}(\underline{r}) \} \qquad (4.47)$$

Here $\underline{q}$, $\underline{c}_{\underline{q}}$ and $\varepsilon = \hbar\omega_q$ are respectively the wave vector, velocity and energy of a phonon. $\ell_p(\varepsilon)$ is the energy-dependent mean free path of a phonon, and $\gamma(\underline{r})$ the solid angle under which the orifice is seen from the point $\underline{r}$. The expression for the collision term can be understood in the following way. The phase-space restrictions with respect to the energy for the gain and loss term, are contained in the second factor between brackets on the right of equation (4.47). For an electron-hole pair creation by a phonon (loss term), the energetic phase-space is equal to the energy ε of the phonon, and the rate for these processes is proportional to $\varepsilon\, N_{\underline{q}}(\underline{r})$. For a spontaneous emission of a phonon (gain term), the production rate is proportional to the product of the phase-space $(eV - \varepsilon)$ and the geometrical factor $\gamma(\underline{r})[1 - \gamma(\underline{r})]$; the kinematic constraints are contained in the first factor on the right. The loss term is given in the relaxation time approximation by $N_{\underline{q}}(\underline{r})/\tau_p(\varepsilon) = (c_{\underline{q}}/\varepsilon\, \ell_p(\varepsilon))\, \varepsilon\, N_{\underline{q}}(\underline{r})$.

By introducing the path variable s for the trajectory of a phonon with a wave vector $\underline{q}$, the phonon transport equation can be solved and leads to the non-equilibrium phonon distribution function

$$N_{\underline{q}}(\underline{r}) = \frac{eV-\varepsilon}{\varepsilon}\, \frac{1}{\ell_p(\varepsilon)} \int_{-\infty}^{0} ds\, \gamma(s)[1-\gamma(s)]\, e^{-s/\ell_p(\varepsilon)}, \qquad (4.48)$$

where the path s starts far from the orifice ($s=-\infty$) and terminates at the position $\underline{r}$ ($s=0$) near the orifice. Assuming that we are in the Knudsen regime for the phonon mean free path ($K_p(\varepsilon) = \ell_p(\varepsilon)/a \gg 1$) we can ignore the damping term in the integral. For different directions of $\underline{q}$ the number of phonons present at the orifice ($\underline{r}=0$) can then be determined to be

$$N_{\underline{q}}(0) = \frac{eV-\varepsilon}{\varepsilon} \frac{1}{\ell_p(\varepsilon)} \begin{cases} (1/4)\ a \text{ for } \underline{q} \parallel \text{orifice} \\ (\pi/8)\ a \text{ for } \underline{q} \perp \text{orifice} \end{cases} . \qquad (4.49)$$

As an average over all $\underline{q}$-directions, we take the numerical factor to be $0.32 = 1/2(1/4+\pi/8)$ for $N(\varepsilon,eV) = \langle N_{\underline{q}}(0) \rangle_{av}$. Using this non-equilibrium distribution $N(\varepsilon,V)$, we find the contribution to the single collision backflow current by supplementing a factor $(1 + N(\varepsilon,V))$ to expression (4.40). In figure 12 we have given the various diagrams in energy space for the different collisions which have to be taken into account. Figures 12a and 12b indicate the spontaneous and stimulated emission and the stimulated absorption processes, and figures 12c and 12d give the excitation of an electron by a phonon from below to above the Fermi level. Adding up these contributions, we obtain for the single collision backflow current, with non-equilibrium phonons present

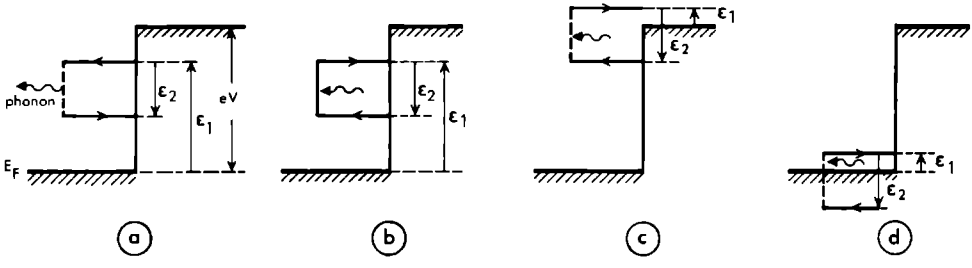

Fig. 12 Diagrams in energy space for the various contributions to the signal (including background). spontaneous and stimulated emission of a phonon (a), stimulated absorption process (b), excitation of an electron from below to above the Fermi level by a phonon (c and d).

$$I^{(1)} = -\,\text{const}\,\Big[\int_0^{eV} d\varepsilon_1 \int_0^{\varepsilon_1} d\varepsilon_2\, \alpha^2 F_p(\varepsilon_2)\{1 + 2N(\varepsilon_2,V)\} + 2\int_0^{eV} d\varepsilon_1 \int_{\varepsilon_1}^{eV} d\varepsilon_2\, \alpha^2 F_p(\varepsilon_2)\, N(\varepsilon_2,V)\Big]. \qquad (4.50)$$

Differentiating twice on gets an expression for the logarithmic voltage derivative of the resistance

$$\frac{1}{R}\frac{dR}{dV} = \frac{16}{3}\frac{e\,a}{\hbar\, v_F}\Big[\alpha^2 F_p(eV) + \int_0^{eV} d\varepsilon\, \frac{\alpha^2 F_p(\varepsilon)}{\varepsilon}\, G_1(\varepsilon) + \alpha^2 F_p(\varepsilon) G_2(\varepsilon)\Big] \qquad (4.51)$$

with $G_1(\varepsilon) = 1.28\, K_p^{-1}(\varepsilon)$ and $G_2(\varepsilon) = 0.64\, K_p^{-1}(\varepsilon)$. As it can be seen from equation (4.51), the signal $\frac{1}{R}\frac{dR}{dV}$ saturates to a constant level for applied voltages above the Debije energy. Furthermore, the ratio of the background (second and third term) to signal (first term) is of the order a in $R_o^{-\frac{1}{2}}$.

The solution of the Boltzmann equation for phonons leading to equation (4.50) holds for a random generation of phonons with no kinematic constraints, i.e. no explicit $\underline{q}$-dependence in $N_{\underline{q}}$. If kinematic constraints are taken into account the expression (4.51) for the signal formally still holds, but the functions $G_1(\varepsilon)$ and $G_2(\varepsilon)$ contain a weighted $\underline{q}$-dependence. An explicit solution of this problem is rather complicated. An excess backflow of holes would lead to a negative signal in the second-derivative spectra, which is sometimes observed experimentally around zero voltage. In addition, at low frequencies, where normal scattering prevails, the phonon generation can be peaked in the forward direction, and therefore phonon-drag effects would yield to a backflow of holes through the orifice, for higher frequencies umklapp scattering randomizes the phonon generation and phonon drag is less probable. This, too, would explain the negative signals observed in certain point contacts around zero voltage.

Direct electron-electron interaction, where the collision of two electrons creates an electron-hole, gives a contribution to the signal $\frac{1}{R}\frac{dR}{dV}$ which is linear in the applied voltage as the scattering rate for electron-electron scattering is quadratic in energy. However, if energy and momentum conservation is taken into account this contribution to the signal vanishes. Only if momentum conservation is broken up (for instance by impurities), it is possible to have random directions of the electrons, and electron-electron collisions could contribute a linear term to the signal.

5 Experimental techniques

5.1 Point-contact fabrication

Two types of point contacts have been investigated in the past, namely shorted-thin-film and pressure-type point contacts. The pioneering first point-contact experiments were performed by Yanson (1974a), using tunnel-junction geometries. Using conventional evaporation techniques, a sandwich of two films of the metal of interest, separated by an oxide layer (figure 13), is produced. Accidentally or intentionally a point contact is produced

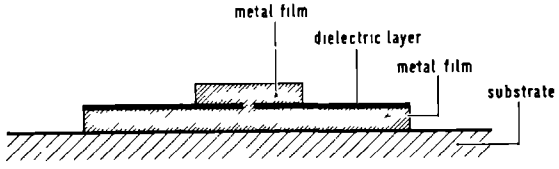

Fig. 13 Schematic view of a metal-insulator-metal tunnel junction with a short circuit between the two metal films

in the oxide layer by an electric break-down thus connecting the two metal films by a metallic short-circuit. In later experiments (Yanson and Shalov, 1976), a sharply-pointed steel needle was pressed onto the surface of the junction, providing a crack in the dielectric layer and so forming a contact.

Pressure-type contacts are much simpler to control, they have been used for the first time for point-contact spectroscopy by Jansen et al. (1976). A sharply etched metal wire ("spear") is carefully pressed against a flat metal surface ("anvil") to form the contact. The spear is fabricated by electrolytically etching a wire (50-100 μm Ø) to a tip with a curvature radius of ∿ 1 μm, as is well known from whisker technology (Dozier and Rodgers, 1964). Together with the chemically cleaned anvil the spear is then mounted in a system with a differential screw-mechanism which allows to adjust a contact while immersed in liquid helium (see figure 14). The total pitch of the differential screw is of the order of ∿ 20 μm. In order to increase mechanical stability, often a spring is bended into the wire forming the spear.

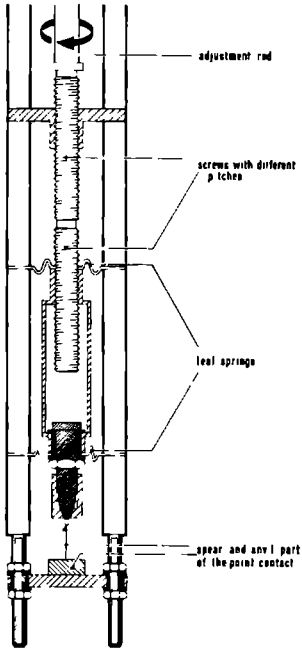

Fig. 14 Schematic view of a pressure-type point contact. By means of a differential screw mechanism the spear can be moved towards the anvil in order to adjust a contact.

Pressure-type point contacts allow the investigation of a large variety of samples, including studies of anisotropies on single crystals. It is possible to obtain stable spear-anvil contacts with resistance values up to $\sim$ 50 Ω. Thin film structures have the advantage of higher mechanical stability with usable contacts of up to $\sim$ 500 Ω. This limit is given by the fact that the contact diameter, calculated with expression (3.5), becomes comparable to the de Broglie wavelength ($\sim$ 5 Å), where a quantum-mechanical approach of the problem is necessary.

5.2 Electronics for recording derivatives

The technique for recording derivatives (dV/dI and d^2V/dI^2) in point-contact spectroscopy is the same as in experiments with superconducting tunnel junctions (McMillan and Rowell, 1969) which makes use of modulation methods. On top of the bias current, which is swept in order to vary the applied voltage, a small ac-current is superimposed. The ac-voltage over the contact is measured by phase-sensitive detection at the fundamental

frequency (1f-mode) and at twice the fundamental frequency (2f-mode) of the modulator to obtain signals which are proportional to the first and second current-derivative of the voltage. As the change in the resistance of the point contacts is usually only a few percent over the whole investigated voltage range, a bridge circuit can be used for the ac-signal to compensate the differential resistance in such a way that only changes of the resistance will be seen by the lock-in amplifiers. In figure 15 a typical block diagram is given for the bridge circuit, with current supply's and

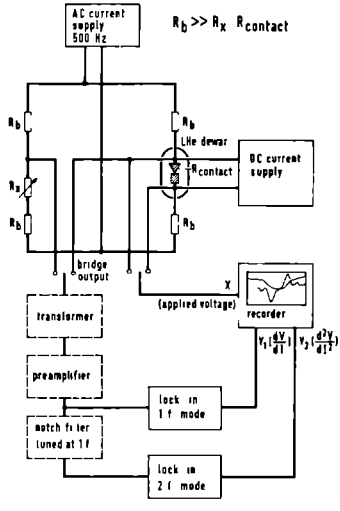

Fig. 15a Block diagram for the phase-sensitive detection of first (dV/dI) and second (d^2V/dI^2) derivatives as a function of the applied voltage for a point contact at liquid helium temperatures. In the bridge circuit the point-contact resistance $R_{contact}$ is balanced by R_x. The dashed parts in the block scheme are not essential for the measuring method.

amplifiers, as used in our laboratory (see also Adler and Jackson, 1966). By setting the resistance R_x equal to the point-contact resistance, the bridge is balanced for ac-signals. The output of the bridge goes to the two lock-in amplifiers to measure the first and second derivative simultaneously. To avoid subharmonic response at the phase-sensitive detector, a

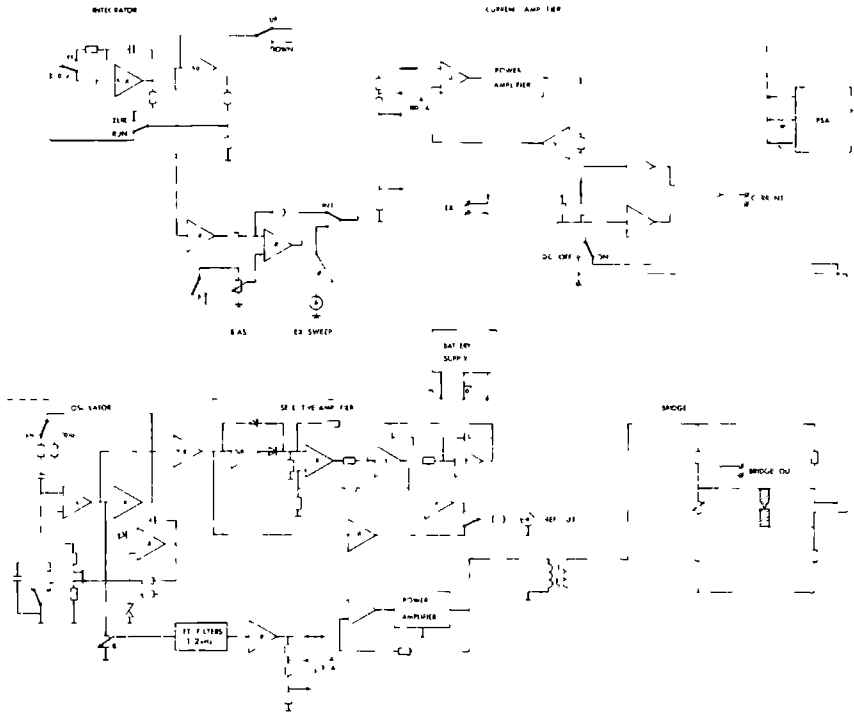

Fig. 15b Details of the main parts of the home-build electronic set-up : dc-current supply, ac-current modulator and bridge circuit. The numbers refer to commercially available operational amplifiers (Analog Devices and Texas Instruments).

notch filter is used before the 2f-mode lock-in. In addition, a transformer can give a better impedance match to the amplifiers. From the measured contact-resistance R_o and the signal V_{10} in the 1f-mode, both measured at zero bias-voltage, absolute values for the second derivative d^2V/dI^2 can be obtained from the signal V_2 in the 2f-mode:

$$\frac{d^2V}{dI^2} = \frac{4}{\sqrt{2}} V_2 \frac{R_o^2}{V_{10}^2} \quad . \tag{5.1}$$

In addition to the intrinsic line width of the spectra, the resolution in the experiment will be determined by the amplitude of the applied ac-

voltage V_{10} and the bath temperature T. For an ac-voltage with an effective value V_{10}, the instrumental linewidth is given by 1.72 V_{10} (Klein et al., 1973). As will be discussed in paragraph 7, the thermal broadening in metal-metal point-contact spectroscopy is the same as in tunneling experiments with normal-metal films where Lambe and Jaklevic (1968) have shown that the thermal linewidth is equal to 5.4 $k_B T$. Therefore, the temperature of a pumped helium bath (T = 1.5K) yields a linewidth equal to 700 μV. This value gives an indication for the modulation voltage to be used which is acceptable without averaging the relevant signal instrumentally.

6 Experimental results

In this paragraph we will discuss the experimentally obtained point-contact spectra. The first part treats the observed structure in the measured second-derivative spectra which, according to the expressions (4.43) and (4.44), can be related directly to the electron-phonon interaction function $\alpha^2 F_p$. The point-contact method has been applied to both superconducting and normal metals. Therefore, it is of considerable interest to compare $\alpha^2 F_p$, as obtained from point-contact spectroscopy while the metal is in the normal state, with $\alpha^2 F$, as obtained from superconducting tunneling spectroscopy using the Rowell-McMillan inversion scheme. Obviously, point-contact spectra of normal metals, which do not become superconductors, are particularly important as they give for the first time detailed experimental information about the energy dependent function $\alpha^2 F$ in normal metals, almost inaccessible otherwise. The experimentally determined point-contact spectra will be compared with neutron-scattering experiments, which measure the phonon density of states $F(\omega)$. If theoretical band structure calculation of $\alpha^2 F$ are available, they too can be checked against the point-contact spectra. The all important mass-enhancement parameter λ, characterizing the electron-phonon interaction for a given metal, can be extracted in a straight-forward way from the point-contact data and will be compared with values deduced from other methods or theories. In the second part of this paragraph, the experimentally observed smooth background signal will be studied in some detail. In particular, a phenomenological analysis to separate the $\alpha^2 F$-signal from this background will be given .

Figure 16 gives an example of a measured spectrum of a Pb micro-contact in the normal state as performed by Yanson (1974a) in his all important

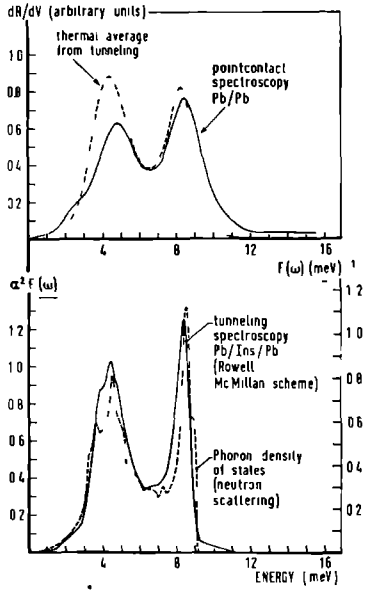

Fig. 16 Measured dR/dV point-contact spectrum of a lead micro-contact in a tunnel junction (after Yanson, 1974a). Resistance R_o = 314 Ω; temperature T = 2.0 K. The phonon density of states F(ω) (Stedman et al., 1967) and the Eliashberg function $\alpha^2F(\omega)$ (Rowell et al., 1973) are shown in the bottom part. The dashed line in the top part is the thermal average of the function $\alpha^2F(\omega)$ due to the bath temperature T = 2.0 K.

pioneering work, using the shorted-thin-film technique where the current-voltage characteristics of metallic micro-contacts in the oxide layer of a tunnel junction are studied. The usual voltage derivative of the resistance has been plotted as a function of the voltage applied over the point contact. The transverse and longitudinal phonon peaks are clearly visible at respectively 5 and 8.5 mV. In the bottom part of figure 16 we have drawn for a comparison the phonon density of states F(ω) (Stedman et al., 1967) and the Eliashberg function $\alpha^2F(\omega)$ as obtained from superconducting tunneling spectroscopy (Rowell et al., 1973). This α^2F-function has been repeated in the top part of figure 16 again, after averaging with a thermal weight function with line width 5.4 k_BT (see paragraph 7) in order to make possible a direct comparison with the point-contact spectrum. Note that above the Debije

energy a small background signal can be observed. The point-contact spectrum is very similar to the smeared Eliashberg function. Small differences are probably due to the transport efficiency function $\eta(\theta)$ in the α^2F_p-signal which is most effective at low frequencies. Using short-circuits in tunnel junctions, the electron-phonon interaction has also been measured in other superconductors, like Sn (Yanson, 1974a) and In (Yanson, 1974b) and has been compared successfully with tunneling spectroscopy.

The use of pressure-type point contacts (Jansen et al., 1976) increased the applicability of the spectroscopic method to a large variety of samples, including single crystals. In figure 17 we have shown the measured second-derivatives d^2V/dI^2 of spear-anvil contacts of the noble metals Cu, Ag and Au (Jansen et al., 1977). In the same figure are also plotted the corresponding phonon densities of states $F(\omega)$ obtained from inelastic neutron scattering (Lynn et al., 1973). Similar results for the noble metals were obtained by electric breakdown of the metal-oxide-metal geometry (Yanson and Shalov, 1976; Shalov and Yanson, 1977). All these measured curves show that for the noble metals the electrons are less strongly coupled to the longitudinal phonons than to the transverse phonons. Das (1973) has shown in a theoretical analysis that the d-band character of the noble metals is important for the electron-phonon interaction. Taking into account the hybridization of the s- and d-band electrons the matrix element for the electron-phonon interaction is calculated and it is found that the electrons are strongly coupled to the transverse phonons via umklapp scattering. As is shown by the singularity for $\theta=\pi$ in the efficiency function $\eta(\theta)$, umklapp scattering is particularly important in the point-contact spectra leading to α^2F_p. This idea was confirmed in experiments with real d-metals. In the point-contact spectra of Fe, Co and Ni (Verkin et al., 1979) it can also be seen that the transverse phonons couple stronger with the electrons than the longitudinal phonons do (see paragraph 8). In the case of Zn and Cd point contacts, consisting of film structures, however no strong energy dependence was observed in the coupling between the electrons and the phonons (Yanson, 1977).

As there exist detailed calculations for the electron-phonon interaction based on pseudo-potential theory for the alkali metals, point-contact spectra of these metals are particularly significant. Experiments of K, Na and Li have been performed at low temperatures (Jansen et al., 1980a). In figure 18 we have plotted the point-contact spectra for K and Na, and in figure 19 for

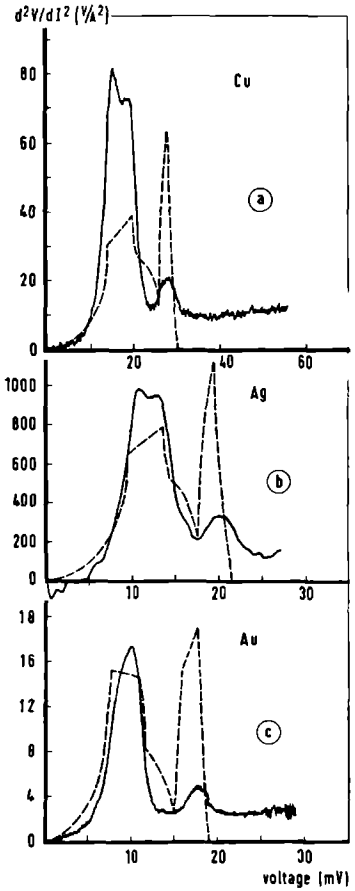

Fig. 17 Measured d^2V/dI^2 spectra of point contacts of the noble metals. Copper contact (a) with resistance R_o = 3.3 Ω and at temperature T = 1.5 K; silver contact (b) with R_o = 16.3 Ω and at T = 1.2 K; gold contact (c) with R_o = 3.3 Ω and at T = 1.2 K. The broken curves give the phonon densities of states F(ω) obtained from neutron-scattering experiments (Lynn et al., 1973).

Li. In the same figures the phonon densities of states F(ω), obtained from neutron-scattering experiments are also given. (Cowley et al., 1966; Gilat and Raubenheimer, 1968; Smith et al., 1968). The measured spectra for K and Na look very similar. As expected for metals where normal scattering is important, we observe a stronger coupling for the longitudinal phonons than

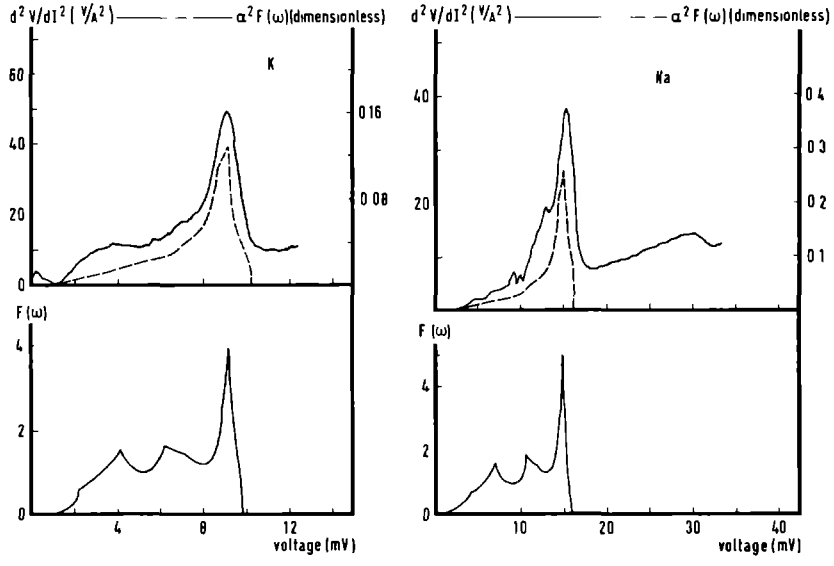

Fig. 18 Measured d^2V/dI^2 spectra for point contacts of potassium (left) and sodium (right). K point contact with resistance R_o = 2.9 Ω and at temperature T = 1.2 K; Na point contact with R_o = 1.1 Ω and at T = 1.5 K. The dashed curves are the theoretically obtained α^2F-functions (Carbotte and Dynes, 1968). The bottom figures give the phonon density of states from neutron-scattering experiments (Cowley et al., 1966; Gilat and Raubenheimer, 1968).

for the transverse ones. However, for Li it is again seen that the coupling with the transverse phonons is stronger, just as in the case of the noble metals. It has been pointed out in the literature (Danino et al., 1978) that the Li metal reveals non-alkali behaviour with much more umklapp scattering than the other alkali metals and this could explain the stronger coupling with the transverse phonons. In the figures for the alkali metals, we have also given the theoretically calculated functions $\alpha^2F(\omega)$ (Carbotte and Dynes, 1968; Hayman and Carbotte, 1971). The theory is confirmed in a remarkable way by the point-contact experiments. It should be noted that Na and Li have a martensitic phase transition (for Na at 40 K and for Li at 80 K) which could give a slight difference in the spectra measured at 1.5 K,

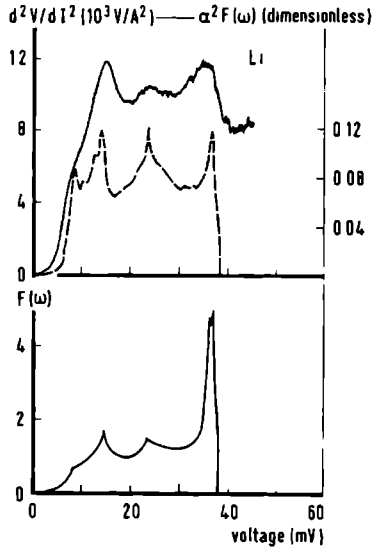

Fig. 19 Measured d^2V/dI^2 spectrum for a lithium point contact. Resistance R_o = 25.4 and temperature T = 1.5 K. The dashed curve is the theoretically obtained α^2F-function (Hayman and Carbotte, 1971). The bottom figure gives the phonon density of states from neutron-scattering experiments (Smith et al., 1968).

compared with the bcc-structure of the alkali metals above the transition temperature used for the theoretical calculations. Note the signal in the spectrum of Na in figure 18 at twice the phonon frequencies, which is due to double phonon processes as has been observed and explained for Au before (van Gelder et al., 1978). In table II we have summarized the point-contact experiments for the metals which have been investigated most extensively for the determination of the electron-phonon interaction. In principle, point-contact spectroscopy can be applied to every metal by means of a short circuit in a tunneljunction or a pressure contact in a spear-anvil geometry as long as the dimensions of the contact are comparable with the mean free path of the electrons. For instance, in our laboratory we have observed phonon structure in the point-contact spectra of Al, W, Pd, Pt and Mg.

By pressing together two different metals, the behaviour of a dissimilar point contact can be investigated. It has been shown experimentally for a Au-Cu junction (Jansen et al., 1977) that both parts of the contact give a contribution to the signal for both negative and positive voltages. As is obvious from figure 8, where it is illustrated that scattering processes at both sides of the contact contribute to the current, the additivity of the signals from the two metals is expected. An example of a sandwich junction with a Au-Mg contact is given in figure 20.

Table II The electron-phonon interaction has been studied in the following metals by means of point contacts (short-circuit in a tunnel junction or spear-anvil contact).

metal	short-circuit	pressure-type	reference
Pb,Sn	x		Yanson, 1974a
In	x		Yanson, 1974b
Cu	x		Yanson and Shalov,1976
Ag,Au	x		Shalov and Yanson,1977
Cu,Ag,Au		x	Jansen et al., 1977
Zn, Cd	x		Yanson, 1977
Fe,Co,Ni		x	Verkin et al., 1979
K,Na,Li		x	Jansen et al., 1980a

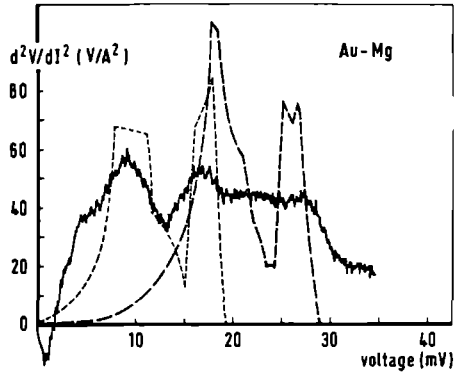

Fig. 20 Measured d^2V/dI^2 spectrum of a dissimilar point contact of a Au spear against a Mg anvil. Resistance R_o = 9.9 Ω and temperature T = 1.5 K. The phonon densities of states for Au (short-dashed curve) and for Mg (long-dashed curve) have been obtained from neutron-scattering experiments (Lynn et al., 1973; Young and Koppel, 1964).

Pressure-type point contacts allow the investigation of single crystals to look for anisotropy effects. Obviously, care has to be taken that spear and anvil have the same crystal direction at the point contact. Yanson and Batrak (1978) have measured point-contact spectra for various orientations of a Zn crystal, which due to its hexagonal structure is expected to show anisotropies. In figure 21 we show the point-contact spectra for two different directions, where both, the spear and anvil, consisted of properly aligned single crystals.

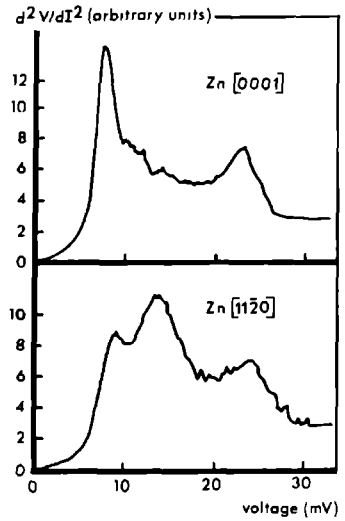

Fig. 21 Measured d^2V/dI^2 spectra for Zn point contacts along the indicated crystalline directions (after Yanson and Batrak, 1978) to show anisotropy effects in point-contact spectroscopy.

The experimental curves show that the phonon structures at 8 and 14 mV have a different strength for two perpendicular directions. This observation is in accordance with theoretical calculations of the anisotropy in the function $\alpha^2F(\omega)$ for Zn (Truant and Carbotte, 1973). As expected, for a cubic metal, such as Cu, the anisotropy effect is very small. It should be noted that the anisotropy is smeared out due to the cosine-dependence of the injected Sharvin current through the contact ($v_{kz} = |v_k| \cos\gamma$).

The preceeding discussion of the results of point-contact experiments has been mainly qualitative in a sense that only the relative energy dependence of the electron-phonon interaction has been discussed, and not its

absolute strength. However, using the expressions (4.23) and (4.44) and the measured values of the resistance R_o and the second derivative $d^2V/dI^2 = R\,(dR/dV)$ of the contact investigated, the function α^2F_p can be determined in an absolute way. It is hence possible to get directly the mass-enhancement parameter $\lambda = \int_0^\infty d\omega\, \alpha^2F(\omega)/\omega$, which renormalizes the mass of an electron for the interactions with the phonon system ($m^* = m(1 + \lambda)$), from measured point contact spectra. Van Gelder (1980) has shown that the functions α^2F, α^2F_p and α^2F_{tr} yield the same values for λ, if the squared matrix element $|g_{n',n}|^2$ in the expressions (4.41) and (4.42) can be assumed to be proportional to the phonon frequency ω. Because this sum-rule argument for the various α^2F-functions with their different transport-efficiencies, it is possible to compare the renormalization parameter λ, obtained by means of point-contact experiments with values obtained by other methods. Grimvall (1976) has given a careful literature survey of theoretically and experimentally determined values for the parameter λ. The theories involve pseudopotential calculations, and the experimental determinations make use of tunneling spectroscopy and the McMillan equation (relation between T_c and λ) for superconducting materials, or the electrical resistivity and the electronic heat capacity in the limit of high temperatures.

In order to calculate the renormalization parameter λ the α^2F_p-part in the measured spectra has to be separated from the smooth background signal. In figure 22 point-contact spectra of Au are given for several different contacts. As is clear from the figure, the background signal does not have a uniform voltage dependence for all spectra. The spectra with relatively the lowest background are practically constant above the Debije energy, and therefore are more suitable for a separation in a α^2F_p-signal and a background signal. For this type of the spectra (relatively low background) we assume that the signal $(1/R)dR/dV$ can be written as a linear combination of two functions A(V) and B(V)

$$\frac{1}{R}\frac{dR}{dV} = p\,A(V) + q\,B(V), \qquad (6.1)$$

where A(V) and B(V) represent the energy-dependent functions for respectively the α^2F_p-signal and the background signal. p and q contain the energy-independent factors according to equation (4.47) and contain the linear dimension a of the orifice in such a way that $p \propto a$ and $q \propto a^2$. According to the expression for the Sharvin resistance ($R_o \propto a^{-2}$) we have $p \propto R_o^{-\frac{1}{2}}$ and

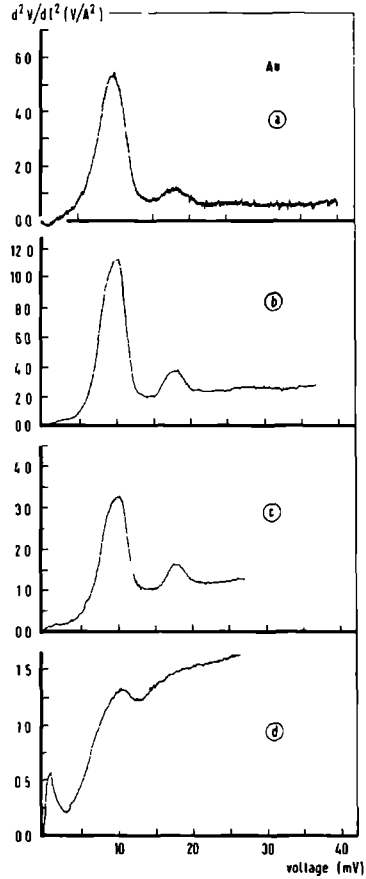

Fig. 22 Measured d^2V/dI^2 spectra for different gold point contacts (pressure type) with resistances R_o = 2.4 Ω (a), 0.7 Ω (6), 0.4 Ω (c) and 0.15 Ω (b), at a temperature T = 1.2 K.

$q \propto R_o^{-1}$. In figure 23 the measured signals at 17.5 mV (transverse phonon peak) and at 35 mV (background) are plotted for different resistances of Cu point contacts. The data are given on a double log-scale, and we expect respectively a slope of (-½) and of (-1). To be consistent, the signals at the transverse phonon peak have to be corrected for the smooth background signal; using a linear interpolation for the background between low voltages and the Debije voltage, one gets corrected signal values at 17.5 mV (shown as the open circles in figure 23). It is possible to explain deviations from the lines with slope (-½) and (-1) in figure 23 by introducing as additional parameters a transfer probability t and the number m of possible parallel contacts (van Gelder, 1978; van Gelder et al., 1978). The transfer probability

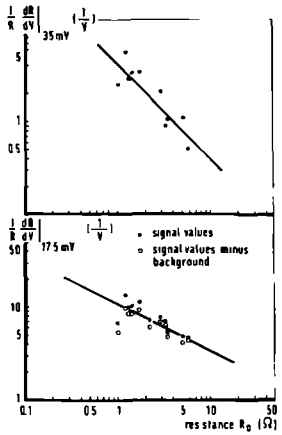

Fig. 23 Measured signal values (1/R) dR/dV for different copper point contacts at applied voltages 17.5 mV (transverse phonon peak) and 35 mV (Debije energy) as a function of the contact resistance plotted on a double log-scale. From the data at 17.5 mV the background signal has been subtracted (open circles) using a linear interpolation for the background function. According to theory, the straight lines with slope $-\frac{1}{2}$ and -1 are expected for respectively the bottom and top figure.

t accounts for oxides and impurities in the contact region which influence the amount of particle transfer through the orifice, while m allows the possibility that a point contact is formed by m parallel current paths. Here, one can assume that the parallel contacts are roughly equal in size, because for large variations in the contact sizes, only the largest contact would be important. For a transfer probability t and a number of contacts m the Sharvin current gets an extra factor tm, and the single collision backflow current a factor t^2m (a factor t for each passage). As the final result we find $p \propto R_o^{-\frac{1}{2}} t^{\frac{1}{2}} m^{-\frac{1}{2}}$ and $q \propto R_o^{-1} m^{-1}$. Therefore, due to an oxidized or dirty contact ($t < 1$) or due to multiple contacts ($m > 1$), the signal values always decrease. This confirms experimental observations, that the second-derivative signal (related to $\alpha^2 F_p$) of great many different point contacts made with one and the same material always seem to have an upper limit which

obeys the $R_o^{-1/2}$-law. The result in figure 23 shows that the spread in the data for the background signal is larger than for the α^2F_p-signal. Therefore, it may be possible that the Knudsen limit is not fully reached for the phonon mean free path. This conclusion is supported by the fact that often the background still increases above the Debije energy. Several procedures have been suggested in the literature in order to obtain the α^2F_p-signal from the measured second-derivative curve with background signal; it has been proposed ad hoc to subtract the background in the form of a hyperbolic tangent (Jansen et al., 1977), to use the measured spectrum that showed no phonon structure (Yanson, 1977) or to interpolate linearly between zero and the Debije voltage (Jansen et al., 1980a). Taking into account these considerations, and using the upper limit of the observed signal values in the point-contact spectra, the mass-enhancement parameters λ has been estimated for several normal metals. These values for t are given in table III, together with values from the literature as recommended by Grimvall (1976). The agreement is rather good. As an amusing side-step,

Table III Renormalization parameters $\lambda = \int_0^\infty d\omega\ \alpha^2F(\omega)/\omega$ obtained from point-contact experiments (λ_p) and other methods recommended by Grimvall (1976) (λ_G). The critical temperatures T_c for superconductivity of the normal metals are predicted by the McMillan equation using the λ_p-values and $\mu^*=0.10$.

metal	λ_p	λ_G	T_c(K)	reference
Cu	0.15 ± 0.02	0.14 ± 0.03	$4\ 10^{-11}$	see text
Ag	0.15	0.10 ± 0.04	$3\ 10^{-11}$	Jansen et al., 1977
Au	0.16	0.14 ± 0.05	$4\ 10^{-9}$	idem
Cd	0.13 ± 0.02	0.40 ± 0.05		Yanson, 1977
Zn	0.13 ± 0.02	0.42 ± 0.05		idem
K	0.13 ± 0.03	0.13 ± 0.03	$3\ 10^{-22}$	Jansen et al., 1980a
Na	0.10 ± 0.03	0.16 ± 0.04	-	idem
Li	0.45 ± 0.20	0.41 ± 0.15	2	idem

we have also given for the normal metals the predicted critical temperature T_c for superconductivity, obtained from the McMillan (1968)-equation

$$T_c = \frac{\theta_D}{1.45} \exp\left[\frac{-1.04(1+\lambda)}{\lambda-\mu^*-0.62\lambda\mu^*}\right], \qquad (6.2)$$

where θ_D is the Debije temperature and $\mu^* \simeq 0.10$ the Coulomb pseudo-potential. The critical temperature for Li suggests that probably the parameter λ should be smaller. Nevertheless, due to the well known comments on the McMillan equation, these predictions for T_c should not be taken too seriously.

In principle it should be possible to separate the phonon signal from the background, using the measured spectra of several contacts only and making no use of any interpolation procedure (van Gelder et al., 1980b). We will illustrate this analysis with the spectra for Cu given in figure 24. All these measured derivatives of the current-voltage characteristic have a background which is nearly constant above the Debije energy. The method makes use of the fact that the function α^2F_p is equal to zero above the Debije energy. All the spectra are first normalized such that their value at the Debije energy eV_D is equal to one. The difference between two normalized spectra will then be proportional to the function α^2F_p (see figure 25), if it is assumed that the measured signal can be considered to be built up as the sum of two unique functions for all contacts (equation (6.1)). For the 4 spectra in figure 24 we have 6 combinations yielding the function α^2F_p. Each spectrum obtained from a combination is normalized to the same value for the integral $\int dV\ \alpha^2F_p(V)$. The average of these difference functions has now been plotted in figure 25b. The error bars give the mean error of the average, and the first part of the spectrum below 5 mV is shown as a dashed line because of the uncertainty due to the structure at zero bias. From this analysis one gets for the ratio of transverse (TA) to longitudinal (LA) phonon peak a value of TA/LA = 6.8. Using the signal values for the maximum in a spectrum given in figure 23, we find $\lambda_{Cu} = 0.15 \pm 0.02$. Unfortunately, it is much more difficult to obtain in a similar way from several measured spectra the functional shape of the background signal. For this purpose, one needs the measured signal $(1/R)dR/dV$ in absolute units for a determination of the parameters t and m (van Gelder, private communication). Without going into details, the results lead to a background function which is very sensitive to small differences in the two compared spectra, and this makes it

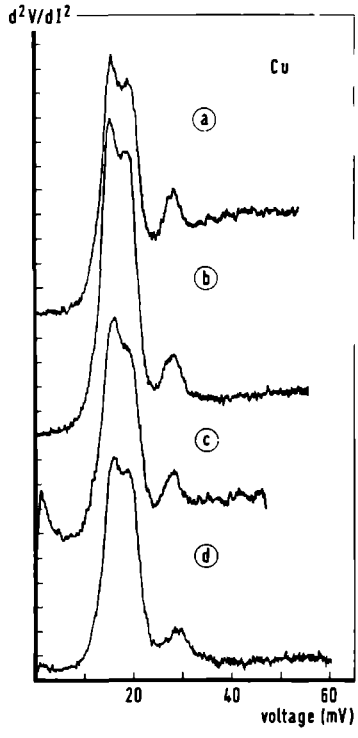

Fig. 24 Measured d^2V/dI^2 spectra for different copper point contacts at a temperature T = 1.5 K with resistances R_o = 1.3 Ω (a), 3.3 Ω (b), 5.1 Ω (c) and 5.8 Ω (d) and with signal values 1.9 VA^{-2}/div. (a), 6.3 VA^{-2}/div. (b) 13.1 VA^{-2}/div. (c) and 16.9 VA^{-2}/div. (d). The spectra are shifted in the vertical scale by 5 scale divisions respectively.

difficult to get a unique determination of the background. Small differences in the measured spectra can very easily be due to different crystalline orientations near the orifice.

In some of the experimental curves shown, the spectra often reveal a structure around zero voltage. This kind of structure has been observed on and off in the experiments in a irreproducible way and remains still unexplained. The d^2V/dI^2-signals can be negative or positive at small voltages, corresponding to a maximum or a minimum around zero voltage in the resistance of a contact. In section (4.5) the possibility of zero-bias structures (negative d^2V/dI^2-signal) due to phonon-drag effects was mentioned. It should be noted that also in the inelastic tunneling spectroscopy zero-bias structure have been observed (Wolf, 1978). Trofimenkoff et al., give an explanation of these effects in terms of "blocking". This means that the transfer of electrons at low voltages is reduced because of non-equilibrium phenomena, i.e. the available electron states are blocked due to the finite elec-

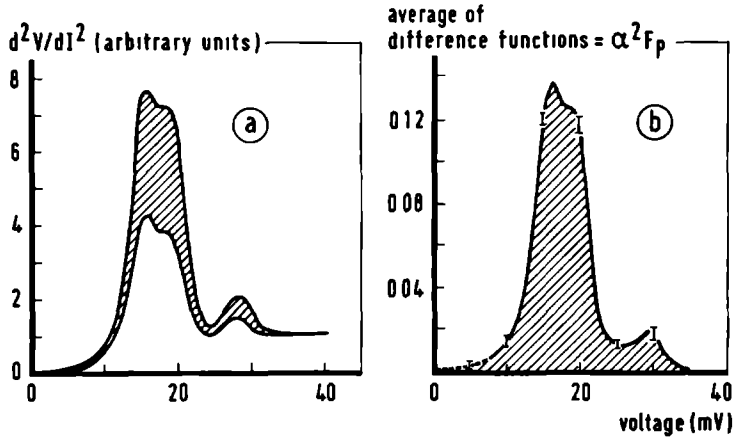

Fig. 25 A typical example to obtain the function α^2F_p from the difference of two measured spectra normalized to unity at the Debije voltage (35 mV) is given in (a). The average of the 6 difference functions α^2F_p from the 4 copper point-contact spectra plotted in figure 24 is shown in (b).

tron relaxation rates in the metal at small excitation energies. It is possible that a similar effect could give a maximum in the resistance in point-contact spectroscopy. In addition magnetic impurities are known to cause structure at low voltages in tunnel junctions. Correspondingly, one has been able to show recently with point-contact experiments (Jansen et al., 1980b), that magnetically dilute alloys give rise to a maximum in the resistance around zero voltage (see paragraph 8).

7. Temperature dependence of point-contact spectroscopy

In the theoretical analysis of the point-contact problem in paragraph 4 solutions in the low temperature limit have been considered only, as most of the experiments have been performed at liquid helium temperatures. In this paragraph, we want to describe the influence of the bath temperature on the experimental results in point-contact experiments (van Gelder et al., 1980 a). For this purpose, just as in the low temperature limit, the collision term in the Boltzmann equation has to be analysed; besides the spontaneous emission processes, the stimulated emission and absorption processes have now to be included as well. As expected, a temperature dependent broadening of the second derivative spectra is found. In experiments performed between 5 and 300 K it is shown that this broadening is very well described by the theory. In addition, the contact resistance at zero voltage shows a temperature dependence which is similar to the temperature dependence of the DC-electrical resistivity of bulk material. However, small differences between the temperature dependence of the bulk resistivity and that of the point-contact resistance are observed, and it may be possible to explain these effects as being due to the different transport efficiencies for the electron-phonon interaction in the two cases.

The formal solution of the point-contact problem has been given in paragraph 4. Obviously, at temperatures $T \neq 0$, the temperature dependent distribution functions for the phonons and the electrons have to be used explicitly in the zeroth and first order result for the current through a point-contact. In a thermalized system with no non-equilibrium phonons present, this leads to the Bose distribution $\nu(\omega)$ for the phonons and the Fermi distribution $f_o(\varepsilon)$ for the electrons. In zeroth order, the electronic distribution is again given by the Sharvin distribution as plotted in figure 7. The zeroth order distribution $f_{\underline{k}}^{(o)} = f_o(\varepsilon_k - eV)$ characterizes the electrons which come from the high voltage side of the contact, and the distribution $f_{\underline{k}}^{(o)} = f_o(\varepsilon_k)$ the electrons coming from the low voltage side. Using equations (4.1) and (4.2) the current through a circular contact with radius a is given in zeroth order by

$$I^{(o)} = \frac{3\pi a^2}{4e\rho\ell} \int_{-\infty}^{\infty} d\varepsilon \, [\, f_o(\varepsilon - eV) - f_o(\varepsilon) \,] = \frac{3\pi a^2}{4\rho\ell} V \, . \qquad (7.1)$$

The summation over $\underline{k}$ is performed over half of the Fermi sphere. As can be seen the current $I^{(o)}$ is independent of the temperature, and in first order no change in the Sharvin resistance $R_o = V/I^{(o)}$ is expected. In next order, single collision backflow processes have to be taken into account. In the iterative expression for the backflow current $I^{(1)}$ the full temperature dependent expression for the collision term has to be used (see equations (4.35) and (4.36)). Starting for the iteration again with the zeroth order distribution functions $f^{(o)}_{\underline{k}'} = f_o(\varepsilon - eV)$ and $f^{(o)}_{\underline{k}} = f_o(\varepsilon_k)$ with $\varepsilon_k = \varepsilon \pm \hbar\omega$ for the energy of the electron after a spontaneous or stimulated emission ($\varepsilon - \hbar\omega$), or a stimulated absorption ($\varepsilon + \hbar\omega$) of a phonon has taken place, the negative correction $I^{(1)}$ to the current is obtained as

$$I^{(1)} = -\frac{4\pi a^3}{e v_F \rho \ell} \int_{-\infty}^{\infty} d\varepsilon \, [\, f_o(\varepsilon - eV) - f_o(\varepsilon)\,] \times \int_{o}^{\infty} d\omega \, \alpha^2 F_p(\hbar\omega) \, [\, 1 + 2\nu(\omega) + f_o(\varepsilon + \hbar\omega) - f_o(\varepsilon - \hbar\omega)\,] \, . \qquad (7.2)$$

The factor in front at the right of the last equation is equal to the factor in expression (4.40), if the relations $\rho\ell = m v_F / n_o e^2$ and $n_o = k_F^3/3\pi^2$ are being used. Note that the correction $I^{(1)}$ to the total current I is of next order in a/ℓ_{ep}, as $I^{(1)} \sim I^{(o)} \, a/\ell_{ep}$ (see equation (3.12) for the energy dependent relaxation time $\tau(\varepsilon) = \ell_{ep}(\varepsilon)/v_F$).

We are interested in the voltage derivatives of the current. For the differential resistance at zero voltage $R_o(T) = (dI/dV)^{-1}$ $(V = 0)$ we obtain for the case where $R_o(T) - R_o << R_o$

$$R_o(T) = R_o + R_o^2 \frac{4\pi a^3}{v_F \rho \ell} \int_{o}^{\infty} d\omega \, \alpha^2 F_p(\hbar\omega) \, \frac{(\hbar\omega/2k_BT)}{\sinh^2(\hbar\omega/2k_BT)} \, . \qquad (7.3)$$

Apart from the typical difference in the transport efficiency, indicated by the subscript p in $\alpha^2 F_p(\omega)$, a similar expression is found for the temperature dependent resistivity $\rho(T)$ in bulk material (Hayman and Carbotte, 1972)

$$\rho(T) = \frac{2\pi m}{n_o e^2} \int_{o}^{\infty} d\omega \, \frac{\hbar\omega/2k_BT}{\sinh^2(\hbar\omega/2k_BT)} \, \alpha^2 F_{tr}(\hbar\omega) \, . \qquad (7.4)$$

The full expressions for the electron-phonon interaction function $\alpha^2 F_p$ and $\alpha^2 F_{tr}$, as weighted with the relevant transport efficiencies, are given by equations (4.41) and (4.42). For the second derivative of the current with respect to the voltage one finds

$$\frac{d^2I}{dV^2} = -\frac{4\pi a^3 e}{v_F \rho \ell} \int_{-\infty}^{\infty} d\omega\ \alpha^2 F_p(\hbar\omega)\ \chi\ \left(\frac{\hbar\omega - eV}{k_B T}\right) . \tag{7.5}$$

The function $\chi(z)$ has a bell-shape with half-width 5.4 $k_B T$.

$$\chi(z) = \frac{1}{k_B T}\, e^z\, \frac{(z-2)e^z + z + 2}{(e^z - 1)^3} . \tag{7.6}$$

For $T = 0$ expression (7.5) reduces to equation (4.43), and the second derivative d^2I/dV^2 is directly proportional to the function $\alpha^2 F_p$. Equation (7.5) describes the broadening of the spectrum arising from a temperature $T \neq 0$. The same function χ for the thermal broadening has been obtained in an analysis of the temperature dependence of inelastic tunneling (Lambe and Jaklevic, 1968).

In order to check the predicted broadening experimentally, the second derivative d^2V/dI^2 of a point contact has been measured as a function of temperature between helium and room temperature (van Gelder et al., 1980 a). In figure 26 we have given the measured spectra between 5 and 20 K for a Au pressure-type point contact showing the expected broadening of the spectrum. As the spectrum will be proportional to $\alpha^2 F_p$ for the lowest measuring temperature, this spectrum can be used to calculate the spectra at higher temperatures. By a convolution product with the spectrum at the lowest measuring temperature $T_o = 5$ K we determine the spectra at higher temperatures T as

$$\frac{d^2V}{dI^2}(eV)\Big|_T = \int_{-10\,k_B T}^{10\,k_B T} dE\ \frac{d^2V}{dI^2}(E)\Big|_{T_o}\ \chi\ \left(\frac{E - eV}{k_B T_{eff}}\right) . \tag{7.7}$$

In analogy to the usual quadratic addition of the line widths for the superposition of Gaussian distributions, we have taken an effective temperature $T_{eff} = \sqrt{T^2 - T_o^2}$ instead of T in formula (7.7), as we investigate the spectral averaging due to the temperature difference between T_o and T. The dashed lines in figure 26 give the calculated spectra using equation

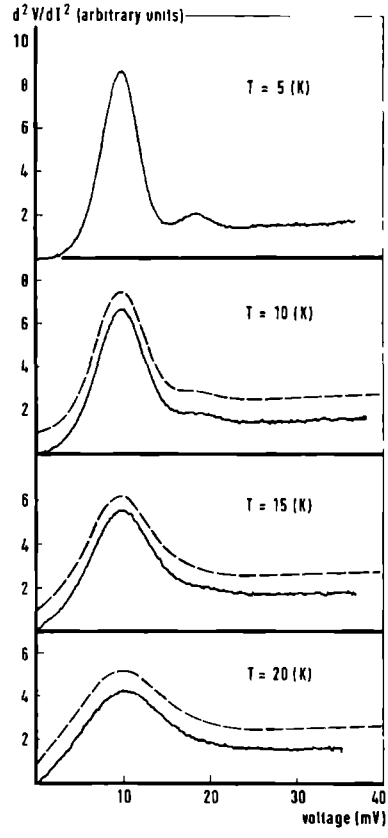

Fig. 26 Measured d^2V/dI^2 spectra at a temperature between 5 and 20 K for a Au point contact with resistance R_o = 5.1 Ω. The dashed lines (vertically shifted by one scale division) give the calculated thermal average using the measured spectrum at 5 K.

(7.7) leading to an almost perfect agreement with the experiments. Due to the use of different kind of materials in the sample holder for the pressure-type point contact, thermal expansion caused instabilities in the Au point contact upon increasing the temperature. To overcome this problem we have investigated Cu point contacts in a sample holder which was practically totally fabricated from copper. Figure 27 shows a point-contact spectrum between 5 and 270 K. Also for this temperature range the thermal broadening fits the theory.

Equations (7.3) and (7.4) show a great similarity between the temperature dependence of the bulk material resistance and that of the point-

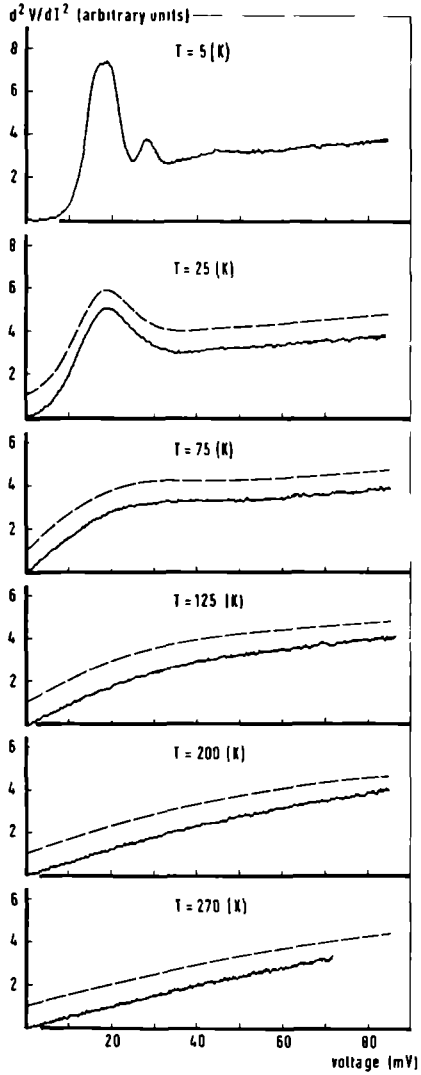

Fig. 27 Measured d^2V/dI^2 spectra at a temperature between 5 and 270 K for a Cu point contact with resistance R_o = 1.7 Ω at 5 K. The dashed lines (vertically shifted one scale division) give the calculated thermal average using the measured spectrum at 5 K.

contact resistance, apart from the typical differences in the transport efficiencies. In order to look into this problem experimentally, the point-contact resistance at zero voltage has been measured for copper as a func-

tion of the temperature. In figure 28 we have given a measured contact resistance between 5 and 300 K. In the same figure, also the resistance of a bulk piece of copper wire is shown, using the same material of which the spear-part of the point contact was fabricated. To compare the measured resistances for the two cases, we have plotted them in such a way that they fall together at low temperatures and have the same slope in the limit of high temperatures. The temperature-dependent behaviour for bulk material and a point contact looks similar, however there seems to be a characteristic difference in the two experiments. This difference can tentatively be explained in terms of the different transport efficiencies in the functions α^2F_p and α^2F_{tr}. This can be analysed in terms of a function $\Delta(T) = T - [R_o(T)-R_o]/[dR/dT]$ (see figure 28) which corresponds to the difference in the measured resistance and the straight line through $R_o(T=0)$ and parallel to the resistance in the high temperature limit. We now look for

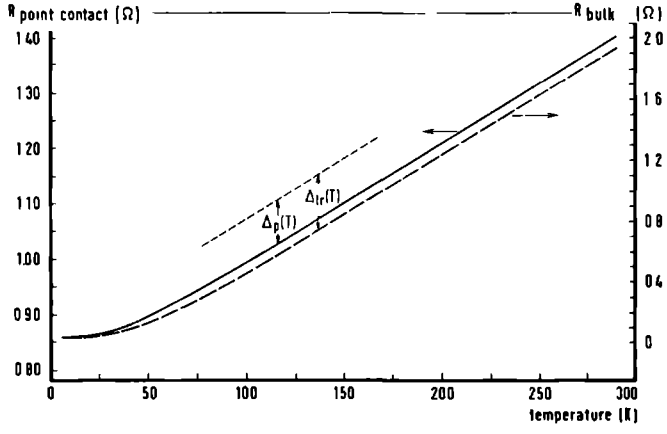

Fig. 28 Resistance at zero voltage of a Cu point contact as a function of the temperature. The dashed line is the measured resistance of bulk material (spear part of the Cu point contact). The values $\Delta_p(T)$ and $\Delta_{tr}(T)$ indicate the difference between the measured resistance values and the straight line through R(T=0), parallel to the high temperature slope of the resistance.

the difference $\delta\{\Delta(T)\} = \Delta_p(T) - \Delta_{tr}(T)$, where $\Delta_p(T)$ is related to the point-contact case and $\Delta_{tr}(T)$ to the bulk material. It follows from the

experiments that this difference $\delta\{\Delta(T)\}$ is negative. By an evaluation of the functions $\Delta_p(T)$ and $\Delta_{tr}(T)$, using the definition and equations (7.3) and (7.4), we find

$$\Delta(T) \simeq \frac{\hbar}{k_B} \frac{0.1 \int_0^\infty d\omega\ \alpha^2F(\omega)}{2 \int_0^\infty d\omega\ \frac{\alpha^2F(\omega)}{\omega}}, \qquad (7.8)$$

which holds for temperatures T roughly of the order $T > 0.3\ \theta_D$. Here, we used $\alpha^2F_p(\omega)$ for a determination of $\Delta_p(T)$ and $\alpha^2F_{tr}(\omega)$ for $\Delta_{tr}(T)$. Using the sum-rule in the normalizations $\int d\omega\ \alpha^2F_p(\omega)/\omega = \int d\omega\ \alpha^2F_{tr}(\omega)/\omega$, we conclude from the experimental found fact $\delta\{\Delta(T)\} < 0$ that the function $\alpha^2F_p(\omega)$ is shifted towards lower frequencies as compared with the function $\alpha^2F_{tr}(\omega)$; this agrees with the ω-dependence of α^2F_p and α^2F_{tr} at low frequencies. In table I of section (4.4) we have shown that for spherical Fermi surfaces umklapp scattering yields an extra factor $\omega^{-\frac{1}{2}}$ for the function α^2F_p as compared with α^2F_{tr}. As umklapp scattering is important for a noble metal like Cu, a stronger signal in the point-contact spectrum is expected at low frequencies.

It is clear that further studies are necessary to support these conclusions. For instance, the results in table I are derived for a spherical Fermi surface, and this does not hold in the case of copper. Therefore, it should be interesting to determine in detail the power law of the temperature dependence of the point-contact resistance at low temperatures, in order to investigate the scattering processes in the point-contact geometry as compared with the bulk material.

8. Detection of other scattering mechanisms than the electron-phonon interaction

Most of the experiments in the field of the point-contact spectroscopy carried out until now deal with the measurements of the electron-phonon interaction in a metal. It is obviously of great interest whether the point-contact method can be applied to study the interaction of the electrons with other elementary excitations in the metal than phonons. The grand result of the solution of the transport problem for the resistance of a point contact is summarized by equation (4.34) which states the all

important simple fact that the change in the contact resistance as a function of the voltage is proportional to the inverse of the energy-dependent scattering time of an electron. The solution is valid under the condition that the inelastic mean free path $\ell(\varepsilon) = v_F \tau(\varepsilon)$ is large compared to the linear dimension a of the contact, for this type of junction it is possible to have an electric field within a metal which accelerates the electrons according to the Sharvin picture (field-emission). In principle, every interaction-process of the conduction electrons in a metal can now be studied with point contacts in the clean limit ($\ell/a >> 1$). In this paragraph we will discuss some recent experiments, which have been performed to investigate the scattering of electrons in a ferromagnet (electron-magnon interaction) and in a magnetically dilute alloy (Kondo-effect). In point-contact experiments on ferromagnetic metals (Verkin et al., 1979), strong anomalies have been observed at voltages which can be correlated with the critical Curie temperature of a ferromagnet. In experiments on Kondo samples (Jansen et al., 1980 b) zero bias structures have been observed which can be analysed in terms of a direct determination of the relaxation time for the exchange coupling of the conduction electrons with magnetic impurities.

For the study of the electron-magnon scattering Verkin et al. (1979) have investigated point contacts of the ferromagnetic metals Fe, Co and Ni. In the measured second derivative spectra the usual structure was observed at applied voltages which were in agreement with the phonon frequencies. As an example, we show the spectrum for a Ni point contact in figure 29. The observed longitudinal phonon peak is less intense as compared with the transverse phonon peak. Besides Fe, Co and Ni, the noble metals also revealt this behaviour. This supports the idea of a strong coupling of the d-electrons with the transverse phonons via umklapp scattering in these metals (see paragraph 6). At higher voltages ($\sim$ 190 mV for Ni), i.e. at energies, which are of the order of the Curie temperature T_C (T_C = 627 K and $k_B T_C$ = 54 meV for Ni), a new type of singularity has been observed (see figure 29). This new phenomenon has been explained by Verkin et al. (1979) by considering the strong power dissipation occuring at higher voltages which causes local heating of the metal in or near the contact region As the scattering of the electrons in a metal increases at higher temperatures, the mean free path of the electrons gets much smaller and the behaviour of the metallic contacts goes over from the

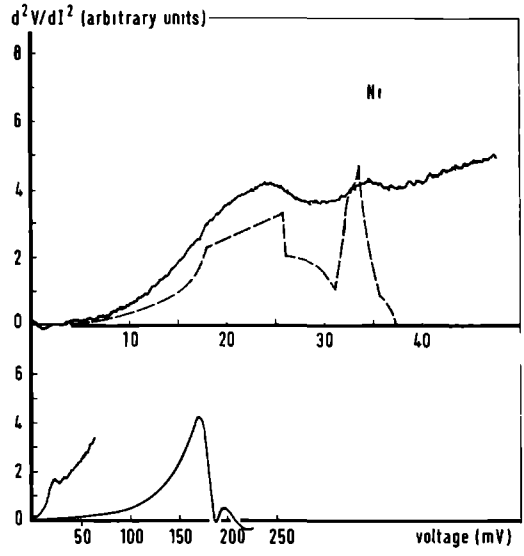

Fig. 29 Measured d^2V/dI^2 spectra for point contacts of Ni at a temperature T = 1.5 K. Top figure: resistance R_o = 6.5 Ω; bottom figure. R_o = 2.9 Ω. The dashed line gives the phonon density of states obtained from inelastic neutron-scattering experiments (Birgeneau et al., 1964). In the bottom figure the singularity around 190 mV is shown together with the expanded signal at low voltages (phonon structure).

Knudsen regime ($\ell > a$) into the Maxwell limit ($\ell < a$). For reasonably general point-contact geometries of a surounding temperature T_b, the maximum temperature T_m at the orifice due to Joule heating is given in the Maxwell limit by (Holm, 1967)·

$$T_m^2 = T_b^2 + \frac{V^2}{4L} . \qquad (8.1)$$

This simple relation has been deduced by assuming that the electronic heat conductivity K and the electrical resistivity ρ are related by the Wiedemann-Franz law Kρ = TL (L is the Lorentz number). For $T_b \to 0$, the maximum temperature T_m is proportional to the applied voltage V, and equation (8.1) gives numerically for the second term $(3.2\ V)^2$ if V is measured in millivolts. The fact that considerable heating in the vicinity

of the metallic contact takes place is supported by the occurrence of an irreversible lowering of the point-contact resistance at high voltages ($\sim$ 200 mV) which is probably due to the disappearance of strain hardening in the metal of the pressure-type point contact at a certain temperature, called the softening temperature T_{soft} (for Ni, T_{soft} = 520 K). For voltages where $T_m \sim T_c$, the resistance of the contact ($R = \rho/2a$) changes abruptly due to the increase of the electron-magnon resistivity at the Curie temperature. Assuming that the change in temperature spreads out spherically in the vicinity of the contact, the experimental results can be simulated using a step-like model for the temperature dependence of the magnon resistivity (Verkin et al., 1979). This model predicts a singularity at the voltage $V_c = 3.6\ T_c$ which is in agreement with the experiment. As a conclusion, one is tempted to say that in these point-contact experiments only the temperature dependence of the bulk resistivity, arising from electron-magnon scattering, is determined. Here, the point-contact method is not used in the sense of a tool to measure the energy dependence of the scattering time for the electron-magnon interaction.

In an other series of point-contact experiments, where Mo has been pressed against the magnetically ordering metals $GdCu_2Si_2$ and Tb (Leppin and Wohlleben, 1978), structure has been observed and ascribed to electron-magnon scattering. As the $GdCu_2Si_2$ sample is certainly not pure, the contacts are probably again in the Maxwell limit and local heating effects can explain the observed increase in the resistance, just as in the case of Fe, Co and Ni as investigated by Verkin et al. (1979), but now, due to the anti-ferromagnetic ordering in $GdCu_2Si_2$, at much lower temperatures (T_c = 12 K). In the Tb experiments, sharp maxima in the measured resistance signal have been ascribed to electron-magnon scattering, because as the energies where the peaks occur compare reasonably well with the structures in magnon density of states as obtained from inelastic neutron-scattering experiments. However, it is not clearly understood why a maximum is observed in the resistance instead of in the voltage derivative of the resistance.

Very recently experiments have been performed on point contacts, made from magnetically dilute alloys, in order to study the exchange scattering of the electrons with magnetic impurities in the metal (Jansen et al., 1980 b). The experiments were done with Au and Cu host samples with small concentrations (< 1 at.%) of respectively Mn and Fe. The point-contact

spectra revealt an interesting structure, which corresponds to a maximum in the resistance at V = 0. An explanation of the observed phenomenon can be given by considering the scattering time for the interaction of the electrons with magnetic impurities (see formula (4.34)). In figure 30 we have given the measured differential resistance as a function of the applied voltage for a AuMn junction. In the same figure we have also plotted the second derivative d^2V/dI^2, which clearly shows the phonon structure,

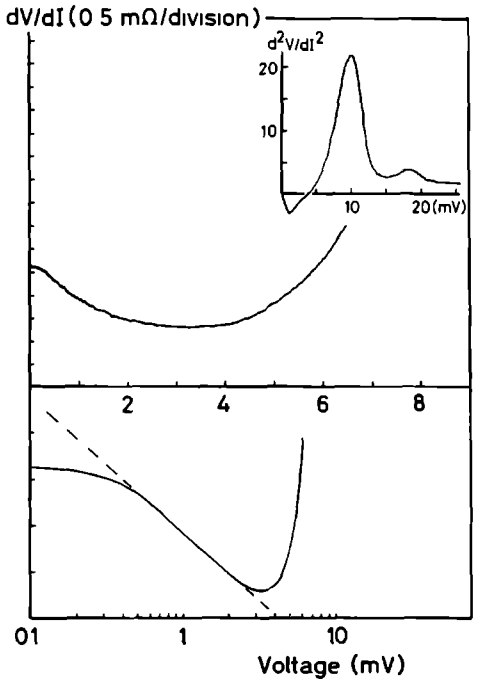

Fig. 30 Measured differential resistance dV/dI for a point contact of the magnetically dilute alloy Au-0.03 at.% Mn as a function of the applied voltage (linear and logarithmic scale). Resistance R_o = 2.1 Ω; temperature T = 1.5 K. The dashed line in the bottom figure gives the logarithmic slope of the resistance. In the insert, the second derivative signal reveals the phonon structure of Au.

indicating that we are indeed dealing with point-contact spectroscopy with a backflow current. Heating effects can be neglected as we are still in the Knudsen regime for the investigated point contacts, according to the

observed electron-phonon structure seen in the signal. Note the characteristic difference between tunneling and point-contact spectroscopy: In tunneling experiments performed on metal-insulator-metal films, structures as a function of the applied voltage have been observed, indicating a minimum in the resistance which is due to the coupling between electrons and magnetic impurities in the oxide layer (Wyatt, 1964). This in drastic contrast with the maximum in the resistance as observed in the point-contact experiments.

For a detailed analysis and understanding of most of the phenomena due to the exchange interaction in Kondo systems (i.e. bulk resistivity, specific heat, susceptibility, etc.) a determination of the energy dependence of the scattering rate is important. Theoretically, the scattering time of an electron with energy eV above the Fermi level has been evaluated for a Kondo system in several ways (Suhl, 1973). The energy-dependent scattering time $\tau(eV)$ as given by Hamann (1967) reduces i.e. in the limit $eV >> k_B T$ to

$$\frac{1}{\tau}(eV) = \frac{c}{\pi N_o}\left\{1 - \ln\left(\frac{eV}{k_B T_K}\right)\left[\ln^2\left(\frac{eV}{k_B T_K}\right) + S(S+1)\pi^2\right]^{-\frac{1}{2}}\right\} \qquad (8.2)$$

where T_K is the characteristic Kondo temperature of the dilute alloy and c the concentration of magnetic impurities with spin S. From the Hamann formula for the scattering rate, the temperature dependence for the bulk resistivity can be obtained, which is formally similar to the voltage dependence of $\tau^{-1}(eV)$ in equation (8.2). It is therefore reasonable to compare the point-contact data as a function of voltage qualitatively with bulk resistivity measurements as a function of temperature. Note that from a theoretical point of view, it is a coincidence due to the nature of the specific logarithmic terms in the expression for the scattering time that the temperature dependence of the resistivity and the energy dependence of the inverse of the scattering time behave similar.

The Kondo temperature for a AuMn-system is very low ($T_K \sim 10^{-13}$ K). Using $|\ln T_K| >> 1$, equation (8.2) can then be simplified to $\tau^{-1}(eV) \propto \{1 - 2\ln(eV)/\ln(k_B T_K)\}$. In figure 30 we have also plotted the measured point-contact resistance as a function of the voltage in a logarithmic scale. It can be seen that over a limited range around 1 mV a logV-behaviour is observed. For higher voltages, the resistance increases due to the electron-phonon interaction, and at low voltages ordering effects

and temperature smearing play a role in the rounding off of the resistance maximum. Similar ordering effects have been observed for concentrations $\gtrsim$ 0.02 at.% Mn in Au in bulk resistivity experiments (Loram et al., 1971). In figure 31 point-contact experiments for different Mn concentrations in the Au samples are shown. Upon increasing the Mn concentration, firstly a broadening of the resistance maximum at V = 0 occurs, and then the maximum splits up in two maxima. Qualitatively the same behaviour has been observed in bulk resistivity experiments as a function of the temperature (Loram et al., 1971). The experiments with more concentrated samples can

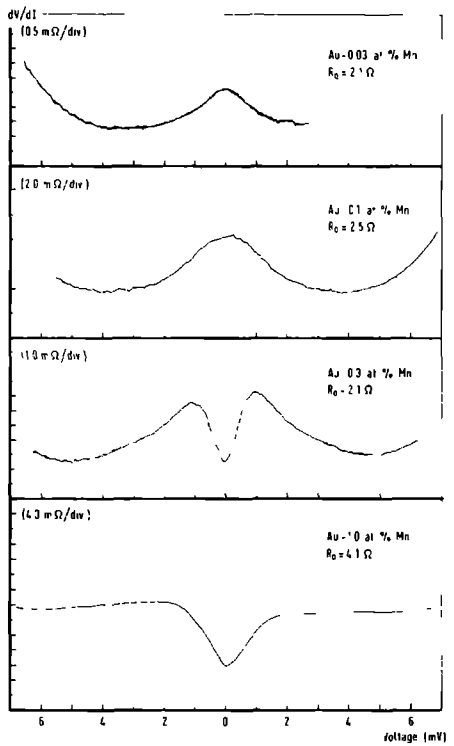

Fig. 31 Measured differential resistance dV/dI for Au point contacts with different concentrations of Mn.

be described by ordering, or equivalently, internal magnetic fields. This is clearly demonstrated in figure 32, where the resistance of a AuMn point contact is given as function of voltage in magnetic fields up to 30 kG. Also in CuFe dilute alloys maxima in the resistance at V = 0 have been

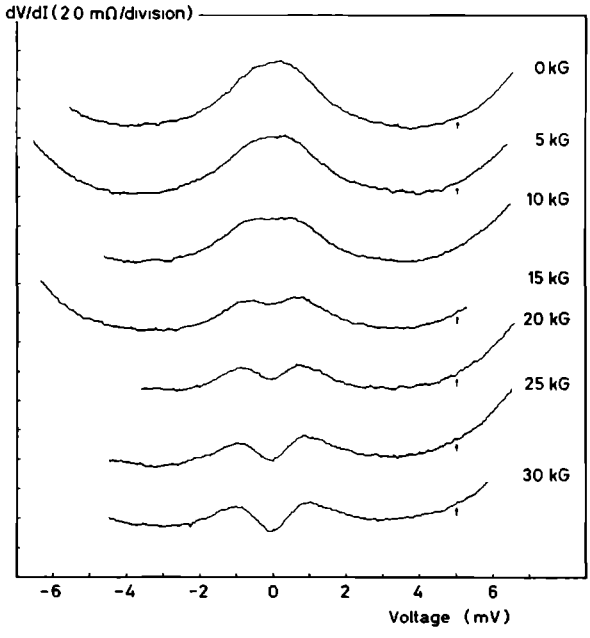

Fig. 32 Measured differential resistance dV/dI for a point contact of Au-0.1 at.% Mn in an applied magnetic field (perpendicular to the contact area). Resistance R_o = 2.5 Ω, temperature T = 1.5 K. The curves are shifted with respect to the reference point indicated by (↑).

observed (Jansen et al., 1980 b). For the CuFe case, the temperature of the helium bath used for the experiments lies below the Kondo temperature (∿ 30 K). Therefore, for very small voltages, the unitarity limit giving the maximum in the cross-section for the electronic scattering might be reached. A first indication gives the experimental result with a flat part in the resistance below 0.5 mV (∿ 20% of the Kondo energy $k_B T_K$ = 2.6 mV). However, the bath temperature should be lowered even more to give clear evidence for an observation of the unitarity limit.

These first experimental results on ferromagnetic metals and on Kondo samples show convincingly that point-contact spectroscopy is a most promising and interesting tool for investigating the scattering mechanism of the conduction electrons in metals. Although this new spectroscopy has

been applied most successfully until now mainly for the study of the electron-phonon interaction, it is quite clear that the method will be equally useful for other interaction mechanisms as well. However, one has always to keep in mind that in order to bring the conduction electrons out of equilibrium within a distance of the order of the mean free path, it is essential that the samples to be studied with point-contact spectroscopy have to have an energy dependent mean free path of the electrons which is at least of the order of the spatial dimensions of the contact.

References

Adler J.G. and Jackson J.E. 1966, Rev. Sci. Instr. 37, 1049.

Birgeneau R.J., Gordes J., Dolling G. and Woods A.D.B. 1964, Phys. Rev. 136A, 1359.

Carbotte J.P. and Dynes R.C. 1968, Phys. Rev. 172, 476.

Chaikin P.M. and Hansma P.K. 1976, Phys. Rev. Lett. 36, 1552.

Cowley R.A., Woods A.D.B. and Dolling G. 1966, Phys. Rev. 150, 487.

Danino M., Kaveh M. and Wiser N. 1978, J. Phys. (Paris) 39, C6-1046.

Das S.G. 1973, Phys. Rev. B 7, 2238.

Dolling G. and Woods A.D.B. 1965, Thermal Neutron Scattering, ed. P.A. Egelstaff (New York: Academic Press Inc.).

Dozier J.W. and Rodgers J.D. 1964, IEEE Trans. Microwave Theory Tech. 12, 360.

Frauenfelder H. 1962, The Mössbauer Effect (New York: W.A. Bergamin Inc.).

van Gelder A.P. 1978, Solid State Commun. 25, 1097.

——— 1980, to be published.

van Gelder A.P., Jansen A.G.M., Strassler S. and Wyder P. 1978, J. Phys. (Paris) 39, C6-602.

van Gelder A.P., Jansen A.G.M. and Wyder P. 1980 a, to be published.

——— 1980 b, to be published.

Gilat G. and Raubenheimer L.J. 1966, Phys. Rev. 144, 390.

Grimvall G. 1976, Phys. Scr. 14, 63.

Hamann D.R. 1967, Phys. Rev. 158, 570.

Haymann B. and Carbotte J.P. 1971, J. Phys. F: Metal Phys. 1, 828.

——— 1972, J. Phys. F: Metal Phys. 2, 915.

Holm R. 1967, Electric Contacts (Berlin: Springer Verlag).

Jansen A.G.M., Mueller F.M. and Wyder P 1976, Proc. 2nd Rochester Conf. on Superconductivity in d- and f-band Metals, ed. D.H. Douglass (New York: Plenum).

——— 1977, Phys. Rev. B 16, 1325.

——— 1978, Science 199, 1037.

Jansen A.G.M., van den Bosch J.H., van Kempen H., Ribot, J.H.J.M., Smeets P.H.H. and Wyder P. 1980 a, J. Phys. F: Metal Phys. 10, 265.

Jansen A.G.M., van Gelder A.P., Wyder P. and Strässler S. 1980 b, to be published.

Klein J., Léger A., Belin M. and Défourneau D. 1973, Phys. Rev. B 7, 2336.

Knudsen M. 1934, Kinetic Theory of Gases (London: Methuen).

Kulik I.O., Omel'yanchuk A.N. and Shekhter R.I. 1977, Fiz. Nizk. Temp. 3, 1543 (Sov. J. Low Temp. Phys. 3, 740).

Kulik I.O., Shekhter R.I. and Omel'yanchuk A.N. 1977, Solid State Commun. 23, 301.

Kulik I.O. and Yanson I.K. 1978, Fiz. Nizk. Temp. 4, 1267 (Sov. J. Low Temp. Phys. 4, 596).

Lambe J. and Jaklevic R.C. 1968, Phys. Rev. 165, 821.

Leppin H.P. and Wohlleben D.K. 1978, J. Less Common Metals 62, 303.

Loram J.W., Whall T.E. and Ford P.J. 1971, Phys. Rev. B 3, 953.

Lynn J.W., Smith H.G. and Nicklow R.M. 1973, Phys. Rev. B 8, 3493.

Maxwell J.C. 1904, A. Treatise on Electricity and Magnetism (Oxford: Clarendon).

McMillan W.L. 1968, Phys. Rev. 167, 331.

McMillan W.L. and Rowell J.M. 1969, Superconductivity vol. 1, ed. R.D. Parks (New York: Marcel Dekker Inc.).

Omel'yanchuk A.N., Kulik I.O. and Shekhter R.I. 1977, Pis'ma Zh. Eksp. Teor. Fiz. 25, 465 (JETP Lett. 25, 437).

Parks R.D. 1969, ed. Superconductivity (New York: Marcel Dekker Inc.).

Rowell J.M., McMillan W.L. and Dynes R.C. 1973, A Tabulation of the Electron-Phonor Interaction in Superconducting Metals and Alloys, part I, Bell Tel. Labs., Murray Hill, USA (unpublished).

Rowell J.M., McMillan W.L. and Feldman W.L. 1969, Phys. Rev. 180, 658.

Shalov Yu.N. and Yanson I.K. 1977, Fiz. Nizk. Temp. 3, 99 (Sov. J. Low Temp. Phys. 3, 48).

Sharvin Yu.V. 1965, Zh. Eksp. Teor. Fiz. 48, 984 (Sov. Phys. - JETP 21, 655).

Smith H.G., Dolling G., Nicklow R.M., Vijayaraghavan P.R. and Wilkinson M.K. 1968, Neutron Inelastic Scattering, Proc. Symp., Copenhagen vol. I, p. 149 (Vienna: IAEA).

Stedman R., Almqvist L. and Nilsson G. 1967, Phys. Rev. 162, 549.

Suhl H. 1973, ed. Magnetism vol. V (New York: Academic Press).

Trofimenkoff P.N., Kreuzer H.J., Wattemaniuk W.J. and Adler J.G. 1972, Phys. Rev. Lett. 29, 597.

Truant P.T. and Carbotte J.P. 1973, Can J. Phys. 51, 922.

Verkin B.I., Yanson I.K., Kulik I.O., Shklyarevski O.I., Lysykh A.A. and Naydyuk Yu.G. 1979, Solid State Commun. 30, 215.

Walker C.B. 1956, Phys. Rev. 103, 547.

Wexler G. 1966, Proc. Phys. Soc. London 89, 927.

Wolf E.L. 1978, Inelastic Tunneling Spectroscopy, ed. T. Wolfram (Berlin: Springer).

Wyatt A.F.G. 1964, Phys. Rev. Lett. 13, 40.

Yanson I.K. 1974 a, Zh. Eksp. Teor. Fiz. 66, 1035 (Sov. Phys. - JETP 39, 506).

—— 1974 b, Fiz. Tverd. Tela 16, 3595 (Sov. Phys. Solid State 16, 2337).

—— 1977, Fiz. Nizk. Temp. 3, 1516 (Sov. J. Low Temp. Phys. 3, 726).

Yanson I.K. and Batrak A.G. 1978, Pis'ma Zh. Eksp. Teor. Fiz. 27, 212 (JETP Lett. 27, 197).

Yanson I.K. and Kulik I.O. 1978, J. Phys. (Paris) 39, C6-1564.

Yanson I.K. and Shalov Yu.N. 1976, Zh. Eksp. Teor. Fiz. 71, 286 (Sov. Phys. - JETP 44, 148).

Young J.A. and Koppel J.U. 1964, Phys. Rev. 134, A1476.

PHYSICAL REVIEW B VOLUME 16, NUMBER 4 15 AUGUST 1977

Direct measurement of electron-phonon coupling $\alpha^2F(\omega)$ using point contacts: Noble metals

A G M Jansen, F M Mueller, and P Wyder
Physics Laboratory and Research Institute for Materials University of Nijmegen, Toernooiveld, Nijmegen The Netherlands
(Received 30 December 1976)

A new technique of forming tiny point contacts between normal metals is described By measuring the voltage derivative of the resistance of such contacts at 1 2 K, structure is found which is consistent with bulk-phonon densities of states Similar results were reported recently by Yanson using a shorted film technique When interpreted, the observed structures yield electron-phonon coupling parameters in close agreement with literature values

The measurement of the electron-phonon interaction has attracted considerable interest.[1-3] Recently Chaikin and Hansma have estimated the electron-phonon coupling parameter λ in Al and Cu using proximity-effect tunneling,[4] and Hoyt and Mota have estimated λ's for Cu, Ag, and Au using concentration-squared extrapolations based on the McMillian equation and the superconducting critical temperature of α-phase noble-metal–rich alloys.[5] In this paper we report measurements of the voltage derivative of the resistance of junctions formed by tiny contacts between two noble metals, which show deviations from Ohm's law.[6] Structures are seen which coincide well with bulk phonon spectra, and when interpreted yield λ's close to those expected[1-5] for noble metals. Some of our results have been presented qualitatively at the Rochester meeting.[3]

We were stimulated to try our experiments by the work of Yanson.[7,8] He used shorted junctions formed from normal metallic films separated by an insulator. The measured junctions were in the normal state, either because of the Dewar temperature or because of the application of an external magnetic field. His Cu results are in excellent agreement with those presented here. It occurred to us that if we could form tiny *metallic* bridges from sharp points, the resulting junctions would, in the normal state, be Sharvin junctions,[9] and perhaps be simpler to form and control than those formed from shorted films. The major potential disadvantages of such junctions, compared with those formed from films involved questions of mechanical stability.

We formed a sharp tip ($\sim\frac{1}{2}$ μm) on a thin wire ("spear") through an electrolytic etching technique. This was mounted rigidly on a subassembly with a larger wire ("anvil"), cooled to 1.2 K and carefully pressed into the anvil. The separation was first crudely adjusted using mechanical differential screws and then finely adjusted, using a piezoelectric substage. We estimate that the anvil-spear separation could be controlled this way to better than 10^{-6} cm. An individual point contact was made and broken many times until a stable and reproducible value of resistance was achieved. Using the piezoelectric lever arrangement, the resistance of noble-metal point contacts ranged from 2.5 to 60 Ω. Once formed, the point contacts had stable resistances for 3–4 h. The first and second derivative ($\partial V/\partial I$ and $\partial^2 V/\partial I^2$) were recorded using conventional ac modulation, phase-sensitive detection, and lock-in techniques, similar to those used in superconducting tunneling-spectroscopy The modulation voltage was small, typically 300 μV The resistance $R(V) = \partial V/\partial I$ was smooth as a function of voltage, but not constant. For applied voltages greater than about 30 mV, the resistance of all such junctions increased linearly with voltage; below 30 mV, the behavior was roughly parabolic. Thus the resistance of the junctions was distinctly non-Ohmic in both regimes, but metallic in the sense that it was a monotonically increasing function of voltage. For a clear discussion on this point we refer to Rowell *et al.*[2]

The voltage dependence of various $(\partial R/\partial V)$ $[\equiv(\partial^2 V/\partial I^2)/(\partial V/\partial I)]$ fell into three distinct types: Those presented here in Fig. 1 ("normal"); those which had a large second derivative peak at less than 5-mV bias ("anomalous"), those which showed structure similar to that in Fig. 1, but with a rapid oscillatory modulation of order 1 mV ("multiple-junction"). Similar effects were seen by Yanson and Shalov[8] in their film experiments. In our experiments the three types divided roughly as 70%, 25%, and 5% of the formed junctions, respectively. In Figs. 1(a)–1(c) typical results are given for $\partial R/\partial V$ of Cu, Ag, and Au as a function of voltage for "normal" junctions. In all cases $R(V)$ was nearly a symmetric function of V and $\partial R/\partial V$ an antisymmetric function of V. Two pieces of structure are seen at voltages less than 30 mV, above this value $\partial R/\partial V$ is constant. In the same figure literature values are given for the phonon density of states $F(\omega)$ for Cu,[10] Ag,[11] and Au,[12] obtained from neutron scattering experiments. The

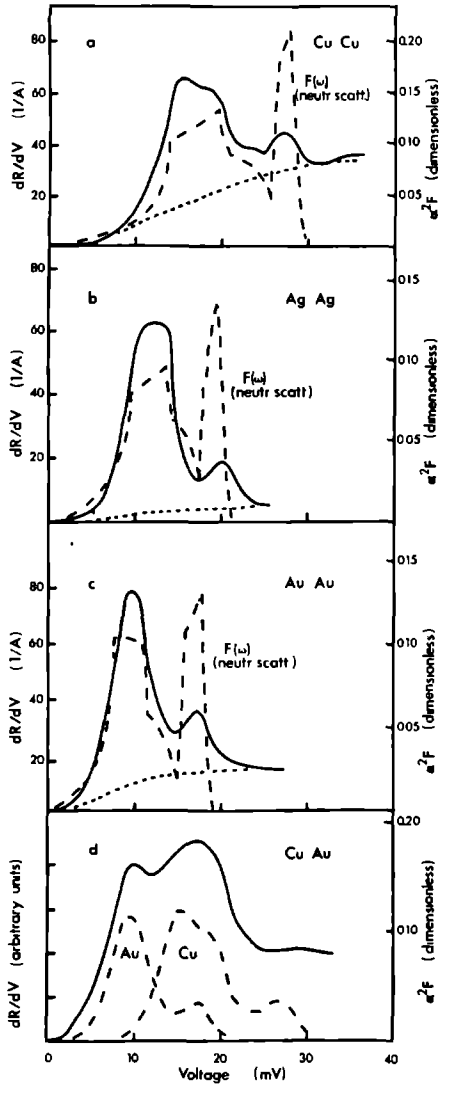

FIG 1 Measured voltage derivative of the resistance of point contacts as a function of applied voltage of (a) Cu-Cu, (b) Ag-Ag, (c) Au-Au, and (d) Cu-Au, plotted as the solid lines (left-hand scale) The right-hand scale is derived through Eqs (2) and (3) In (a), (b), and (c) the background functions are shown as short-dashed curves, and phonon density of states from Ref 12 as long-dashed curves The dotted line in (b) shows the small measured anomaly at zero bias In (d) is plotted as long-dashed curves the difference between the measured solid curve and the background function for Au and Cu, respectively

coincidence of the low voltage peak of our results with the transverse phonon peak is excellent The higher peak coincides well with the longitudinal peak, with a small disagreement in the case of Ag. We believe, therefore, that bulk phonons play a significant role.

The resistivity ratio (RR) of our samples given in Table I is low and the resistance at zero voltage Ω_0 is high compared with previous experiments on metallic contacts.[7] Estimating the contact radius a_M from $a_M = \rho/2\Omega_0$ (ρ is the resistivity of the metal, Maxwell[13] derived this formula using Ohm's law) and the data of Table I we find values smaller than 0 2 A. These are far smaller than our estimates of the residual impurity scattering length l_{imp}. Thus the flow of electrons through the contact orifice would have additional impedance due to the Knudsen[14] effect. Wexler[15] has given a detailed treatment of the resistance in the case where the orifice size a is small compared with the scattering length l. He gives

$$R_{int} = \Gamma(K)/2\sigma a + 4K/3\pi\sigma a\,, \qquad (1)$$

where Γ is a slowly varying function of the Knudsen number $K = l/a$ which takes the value 1 at zero and $\frac{9}{128}\pi^2$ at high K and $\sigma = 1/\rho$ the conductivity of the bulk material. The first term in this formula is dominant for small K and similar to the resistive formula of Maxwell [13] The second term dominates for high K and is similar to the formula of Sharvin.[9] The regime of high K is of interest here and the radii given in Table I are found from $a^2 = 4\rho l/3\pi\Omega_0$. These radii are much larger than our Maxwellian estimates, but the condition $K \gg 1$ is still fulfilled. We assume that only the scattering length l depends on the voltage V (or energy eV). Thus since ρl is independent of l and Γ a slowly varying function of K, the derivative $\partial R/\partial V$ is given by

$$\frac{\partial R}{\partial V} = \frac{\Gamma \rho l}{2a}\,\frac{\partial}{\partial V}\,\frac{1}{l(eV)} \qquad (2)$$

and the total scattering length by $1/l = 1/l_{imp} + 1/l_{ep}$, where

$$\frac{1}{l_{ep}} = \frac{1}{v_F \tau(eV)} = \frac{2\pi}{\iota_F h}\int_0^\infty d\omega\, \alpha^2F(\omega)[2N_0(\omega) + 1 - f_0(eV-\omega) + f_0(eV+\omega)] \qquad (3)$$

is the energy-dependent phonon-emission length at energy eV, and α^2F the frequency-dependent electron-phonon coupling constant Thus at low temperatures we obtain directly α^2F, given as the right-hand scales of Fig 1. In the theories of electron-phonon coupling reviewed by Zavaritskii and Grimvall,[1] $1/l_{ep}$ becomes constant at high en-

TABLE I. Experimental parameters for the four point contacts plotted in Fig. 1. Ω_0 is the junction resistance at zero voltage, l_{imp} the 1.2-K resistive scattering length, l_{ep} the 30-meV electron–phonon emission length, a the orifice radius, and K the Knudsen ratio l/a. λ_P is twice the integral of the derived α^2F/ω.

	RR	Ω_0 (Ω)	ρl (10^{-11} Ω cm^2)	l_{ep} (10^{-4} cm)	l_{imp} (10^{-4} cm)	a (10^{-8} cm)	K	λ_G	λ_M	λ_P
Cu-Cu	71	5.7	0.71	0.89	3.25	72.7	96	0.14 ± 0.03	0.16	0.14
Ag-Ag	43	16.3	0.91	1.01	3.26	54.9	140	0.10 ± 0.04	0.16	0.15
Au-Au	23	32.0	1.04	1.16	1.25	37.1	162	0.14 ± 0.05	0.21	0.16
Cu-Au	35	2.5	0.88	...	2.51	122.2	...	...	...	...

ergy, i.e., $(\partial/\partial eV)(1/l_{ei}) \to 0$. We see that our results contain a phonon-emission effect, and another smooth ("background") effect. We have approximated the second effect through the dashed functions presented in Fig. 1, given by

$$B(V) = C \tanh^2(1.5\, eV/k\theta_D), \qquad (4)$$

where C is a constant fitted at 30 mV. To compare with other experiments, we integrate to find the λ_P's, λ_G is taken from Grimvall[1] and λ_M from Hoyt and Mota,[5] given in Table I. On the basis of the close coincidence of the structure of Fig. 1 with phonon structures, and the agreement with literature values of λ, we conclude that the voltage derivative of the resistance of small point contacts provides a simple and convenient method to measure $\alpha^2F(\omega)$ in normal metals. The same conclusion was reached by Yanson in his experiments using evaporated films.

We will briefly give some other experimental results and conclusions.

(i) Figure 1(d) tests the possibility of dissimilar junctions—here with a "spear" of Cu and "anvil" of Au. The results suggest that the effect is additive—as was given by Wexler,[15] Eq. (69).

(ii) Using anvils of single crystals, preliminary experiments seem to show that the results do *not* depend on the exposed crystalline face. The form of the variational function of Wexler suggests that the half width at half maximum of the electrons which pass the orifice is 45°. This is 82% of 54.7°, the angle between [100] and [111].

(iii) Plotting all our experimental data, the amplitude of the first peak scales as Ω_0 to the 0.36 ± 0.13 power, this is consistent with the analysis above (0.5 power). The size of the residuals suggest that the internal consistency of the data is of the order of 20%.

(iv) Yanson has defined γ, the ratio of the "background" to the first peak height.[8] γ shows a dependence as Ω_0 to the power −0.54 for Yanson's Cu data and −0.53 for ours. Thus B does *not* depend on Ω_0.

(v) B depends on the residual resistance ratios RR of the anvils as the power −0.52.

(vi) The ratio of the α^2F's of Fig. 1 to the related $F(\omega)$'s shows that α^2 is strongly ω or energy dependent. Transverse phonons couple to the electron gas about four times more effectively than longitudinal phonons in noble metals. This is consistent with the results and conclusions of a theory of Das, who first suggested[16] in a quantitative way, that d electrons were important and strongly umklapp coupled to transverse phonons in noble metals. It is likely that the same is true in transition metals—or "transition-metal compounds."

ACKNOWLEDGMENT

We wish to thank H. W. H. M. Jongbloets for help in setting up the experiments and A. P. van Gelder for helpful theoretical discussions. This work was performed as part of the research program of the Stichting voor Fundamenteel Onderzoek der Materie (FOM) with financial support from the Nederlandse Organisatie voor Zuiver Wetenschappelijk Onderzoek (ZWO).

[1] N. V. Zavaritskii, Usp. Fiz. Nauk 108, 241 (1972) [Sov. Phys.-Usp. 15, 608 (1973)]. G. Grimvall, Phys. Scr. 14, 63 (1976).

[2] J. M. Rowell, W. L. McMillan, and W. L. Feldman [Phys. Rev. 180, 658 (1969)] and J. G. Adler [Phys. Lett. A 29, 675 (1969)] first observed normal metal phonons in tunnel junctions.

[3] *Second Rochester Conference on d- and f-band Superconductors*, edited by D. H. Douglass (Plenum, New York, 1976), and references therein.

[4] P. M. Chaikin and P. K. Hansma, Phys. Rev. Lett. 36, 1552 (1976).

[5] R. F. Hoyt and A. C. Mota, Solid State Commun. 18, 139 (1976).

[6] I. Stone, Phys. Rev. 6, 1 (1898), P. W. Bridgman, *ibid.* 9, 269 (1917); R. Holm, *Electric Contacts* (Springer-Verlag, Berlin, 1967).

[7] I. K. Yanson, Zh. Eksp. Teor. Fiz. 66, 1035 (1974).

[Sov Phys -JETP 39, 506 (1970)]
[8]I K Yanson and Yu N Shalov, Zh Eksp Teor Fiz 71, 286 (1976) [Sov Phys -JETP 44, 148 (1976)]
[9]A Sharvin junction is a metallic junction in the extreme Knudsen regime ($l/a > 1$) Yu V Sharvin, Zh Eksp Teor Fiz 48 984 (1965) [Sov Phys -JETP 21, 655 (1965)]
[10]R M Nicklow, G Gilat, H G Smith, L J Raubenheimer, and M K Wilkinson, Phys Rev 164, 922 (1967)
[11]W A Kamitakahara and B M Brockhouse, Phys Lett A 29, 639 (1969)
[12]J W Lynn, H G Smith and R M Nicklow, Phys Rev B 8, 3493 (1973)
[13]J C Maxwell, *A Treatise on Electricity and Magnetism*, 1891 (Dover New York, 1954)
[14]M Knudsen, *Kinetic Theory of Gases* (Methuen, London, 1934)
[15]G Wexler, Proc Phys Soc Lond 89, 927 (1966)
[16]S G Das, Phys Rev B 7, 2238 (1973)

Reprint Series
10 March 1978, Volume 199, pp 1037-1040

SCIENCE

Normal Metallic Point Contacts

The (nonohmic) resistance of tiny metal contacts shows new structure at metal phonon energies.

A G M Jansen, F M Mueller, P Wyder

Summary The measured voltage derivative of the nonlinear resistance of tiny point contacts can be separated into a phonon-emission effect (α^2F) and an analytic functional form (background effect) The α^2F's show structure coincident with bulk phonon densities of states Values of the integral of $2\,\alpha^2F/\omega$ are closely related to literature values The background effect is related to the impurity concentration of the materials

With the widespread use of miniaturized semiconducting devices (diodes transistors, and integrated circuit chips), new problems arose in attaching stable metallic leads Although the currents that flowed through the metallic leads were small—typically of the order of a few milliamperes—the contacts were so small that the resulting current densities were enormous—as large as 10^6 amperes per square centimeter Such high current densities were well above anything encountered in the laboratory or in technology before In such a regime, new phenomena, which in the ordinary world are very tiny, become important All metallic crystals contain impurities, vacancies, or dislocations In a strong current density (or equivalently, a strong electric field), these defects force electrons to stream around them and hence exert forces on them, they move or diffuse, driven by the electron "wind" This process is now called electromigration (*1*) When such diffusion takes place in constant strong fields for a long time, the defects migrate and become trapped—for example, at the metal-semiconductor interface Mechanically, contacts with piled-up vacancies and impurities become weaker and weaker—and eventually break These technical problems are now well understood, but the solution has involved a wide variety of disciplines

Background: Large Contacts

The general problem of understanding electrical contacts is quite old it first arose with the advent of rotating electrical machinery in the early 1890's The classical solution in the ohmic regime was given by Maxwell (*2*) by solving Poisson's equation for the electrical potential V as function of coordinate $\vec{r}$

$$\nabla^2 V(\vec{r}) = 0 \qquad (1)$$

in oblate spherical coordinates Contours of constant potential of current flowing through a constricting circular orifice of radius a are given by

$$V(\vec{r}) = \pm V_0[1 - \frac{2}{\pi} \arctan(1/\xi)] \qquad (2)$$

where the oblate spherical coordinate ξ may be found from the more familiar spherical polar coordinates r and z by solving the implicit equation $r^2/a^2 = (1 + \xi^2)(1 - z^2/\xi^2 a^2)$ The two signs refer to the two sides of the circular orifice the geometry has cylindrical symmetry The resistance of such a contact may be found by dividing the total voltage drop (here $2V_0$) by the total current flowing through any contour of constant voltage For simplicity, we choose the contour $V(\vec{r}) = 0$, that is, the orifice itself ($\xi = 0$) The current I is given (in cylindrical coordinates) by an integral of the current density $\vec{J}$ over the area $\vec{O}$ of the orifice

$$I = \int d\vec{O} \cdot \vec{J}$$

$$= \int_0^{2\pi} d\varphi \int_0^a r dr\, \sigma \left(\frac{\partial V}{\partial z}\right)_{z=0} \qquad (3)$$

where σ is the conductivity and $\partial V/\partial z$ is the z component of the electric field $\vec{E}$ The Maxwellian resistance (*2*) of the contact is then given by

$$R_M = \frac{\rho}{2a} \qquad (4)$$

where ρ is the resistivity ($\equiv 1/\sigma$) Equation 4 has been verified (*3*) to an accuracy of about 1 percent for a wide variety of "practical" contacts There are also many exceptions (*3*)

New Phenomena in Small Contacts

In this article we focus on some interesting exceptions that have been examined (*4*, *5*) at Nijmegen In these experiments the contact radii are made so small (~ 40 angstroms) that the current densities are orders of magnitude (10^{10} to 10^{11} amp/cm^2) larger than those previously considered We were stimulated to try such experiments by the work of Yanson (*6*), who used a technique that depends on puncturing two metallic films, separated by a thin (100 Å) insulating layer, with a burst of voltage coupled through a high resistor It oc-

A G M Jansen is a graduate student and F M Mueller and P Wyder are professors of physics at the Physics Laboratory University of Nijmegen Nijmegen Netherlands All three are connected with the Stichting voor Fundamenteel Onderzoek der Materie (Foundation for Fundamental Research on Matter) This article is an English translation of an article written for the *Nederlands Tijdschrift voor Natuurkunde*

0036-8075/78/0310-1037$01 00/0

curred to us that if we could form such tiny metallic bridges from sharp points the resulting junctions might be simpler to form and control than those formed from shorted films The major potential disadvantages of point contacts involved questions of mechanical stability

Experimental technique We formed a sharp tip (of radius ~ ½ micrometer) on a thin wire (spear) by an electrolytic etching technique (7) This was mounted rigidly on a subassembly with a larger wire (anvil) cooled to 1 2°K and the spear anvil separation was carefully adjusted On the basis of the results discussed below we believe that within the etched tip of the spear there are microscopic regions which on this scale are large conical mountains rising 100 to 200 A above the average plane of the tip Usually one of these is dominant actually touches first and forms the metallic resistive junction we measure The separation is first crudely adjusted by means of differential screws and then finely adjusted by using a piezoelectric substage We can control the separation to better than 10 $^{-8}$ cm by means of the *piezoelectric lever arrangement*

The experimental apparatus is shown in Fig 1 The resistance of the point contacts formed in noble metals at a low temperature (1 2°K) is quite high—about 10 ohms If we estimate the radius a_M of such a contact from the Maxwell equation (Eq 4) we find the tiny value of about 0 2 A This is far smaller than both the classical resistive scattering length l (about 10^4 A) and the quantum mechanical de Broglie wavelength λ (about 5 A) Moreover the measured contact resistance is distinctly nonlinear or nonohmic

Nonlinear contacts In Fig 2 we show the voltage dependence of the current and the first and second derivatives of a nonlinear I V characteristic curve for a point contact of copper whose resistance was 5 7 ohms at a voltage near zero [The measuring technique involved phase sensitive detection of first and second harmonics similar to that used in tunnel junction spectroscopy of superconductors (*8*)] Figure 2 is a direct photograph of the output of an x y plotter The (dynamical) resistance (curve b) is nearly an exactly symmetric function of voltage the nonlinear second derivative (curve c) nearly an antisymmetric function The broad peaks in curve c at ± 15 and ± 27 millivolts are reproducible from sample to sample and contact to contact The small structure near zero bias and the narrow dip at +17 mV are electrical noise The tiny ripple seen at > 30 mV is the intrinsic mechanical and electrical noise in the experiment New phenomena have arisen because of the small size high current density and high electric field of the point contacts

Scattering Length versus Radius

Let us consider the classical scattering length question first The problem of the flow of classical electrons of large scattering length l through a small orifice resembles a problem in gas kinetic theory (9) As the pressure in a gas vessel is lowered for example by pumping through a small hole into a vacuum the mean free path l between collisions increases Eventually the path length will be larger than the orifice radius a One then no longer has diffusive flow and the gas molecules penetrate the orifice ballistically This problem was first considered by Knudsen (*10*) in 1909 and is now called the Knudsen effect The different regimes are characterized by the Knudsen ratio $K = l/a$

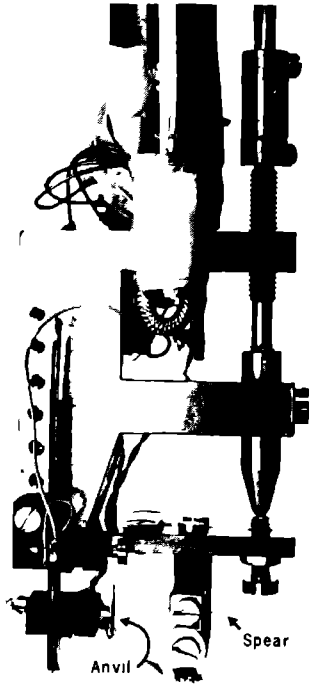

Fig 1 Experimental apparatus The spear on the right is moved into the anvil on the left by means of differential screws and a piezoelectric lever arrangement The separation can be controlled to better than 10 $^{-8}$ cm

In the case of electrical contacts the major effect (in the regime of high Knudsen ratios) is to cause a steep voltage gradient or high effective electric field to develop in the contact region Crudely then in this regime the contact serves as a device to inject electrons of high kinetic energy from one metal into another but with a carefully controlled excess kinetic energy or velocity This excess velocity is given by $\Delta v = \pm eV/p_f$ where the sign depends on whether the particles passing through the orifice are holes or electrons e is the electric charge V is the voltage drop across the contact and p_f is the Fermi momentum The excess current I is proportional to the current density times the area or $ne\Delta v\pi a^2$ where n is the particle density Calculating the resistance as V/I we find $R = p_f/ne^2\pi a^2$ In the Drude theory of the electron gas the quantity p_f/ne^2 is equal to ρl the resistivity times the effective scattering length In the high K regime the resistance of an electrical contact has been estimated by Sharvin (*11*) as

$$R_S = \frac{\rho K}{4a} = \frac{K}{2} R_M = \frac{\rho l}{4a^2} \qquad (5)$$

(Note that in this form the resistance is quadratically dependent on the inverse of a) In our experiments the Knudsen resistance is larger than the Maxwell resistance by the factor $K/2$ or about 100 Using the Sharvin formula we find the (larger) estimate for a of about 40 A

Quantum effects Thus a is much larger than the de Broglie wavelength so that direct quantum mechanical Fresnel (edge of the hole) interference phenomena (*12* p 161) would be weak and would be visible only if a large voltage (about 600 mV) were impressed on the contact However if two or more of the mountains on the etched tip were of roughly equal height but spaced far apart then it would be possible to see the quantum mechanical analog of Young (double slit) interference (*12* p 114) If the two mountains were spaced 600 A apart then by the Heisenberg relation an extra momentum p of about 10^{-22} gram centimeter per second would be needed or an excess energy of about 0 5 mV for free electrons to see interference

In a few of our formed contacts we see exactly the same emission phenomena as will be discussed below but with a 60 percent (height) modulation at a frequency of about 0 75 mV We interpret these as quantum interference effects due to multiple junctions Such effects were also seen in the experiments of Yanson (*6*)

Interpolation Formula

Between the two regimes—low K (Maxwell) and high K (Sharvin)—one needs an interpolation formula which systematically treats the problem and yields these extreme limits. Wexler (*13*) has given such a formula based on a variational solution to the nonlocal Boltzmann equation. He transformed the problem of electron flow through an orifice into the problem of an emitting disk. The transformation is similar to that used by Babinet in treating the analogous problem of the equivalence of screens and holes in geometric optics (*12* p. 147). Wexler's interpolation formula is

$$R_{\text{int}} = \frac{I(K)}{2\sigma a} + \frac{4K}{3\pi\sigma a} \qquad (6)$$

where $I(K)$ is a slowly varying function of K and takes the value 1 for $K = 0$ and $9\pi^2/128$ for large K. The first term is like the Maxwell resistance, the second like the Sharvin resistance. In our experiments we take the partial derivative of the contact resistance with respect to voltage V. We assume that the orifice radius is independent of voltage and the scattering length is dependent on voltage (or energy, eV). The combination K/σ in the Sharvin-like term is independent of voltage since l/σ is independent of the scattering length. Thus only the first term enters the partial derivative

$$\frac{dR}{dV} = \frac{I(K)l}{2\sigma a}\frac{\partial}{\partial V}\left(\frac{1}{l(eV)}\right) \qquad (7)$$

(Note that the structureless second term in Eq. 6 serves as a series ballast resistor to establish the voltage drop on the contact. The first term is the active one.) The total scattering length l is given by

$$\frac{1}{l} = \frac{1}{l_{\text{imp}}} + \frac{1}{l_{\text{ep}}} \qquad (8)$$

where l_{imp} is the scattering length due to impurities and where l_{ep} the electron-phonon emission length is given by

$$\frac{1}{l_{\text{ep}}} = \frac{1}{v_F\tau(eV)} = \frac{2\pi}{v_F\hbar}\int_0^{\infty} d\omega\alpha^2F(\omega) \times [2N_0(\omega) + 1 - f_t(\omega - eV) + f_0(\omega + eV)] \qquad (9)$$

where v_F is the Fermi velocity, $\alpha^2F(\omega)$ the electron-phonon coupling, $1/\tau(eV)$ the energy-dependent emission rate and $\hbar$ Planck's constant over 2π. Equation 9 is the condensed-matter analog of Fermi's second golden rule. The matrix element squared is α^2, the coupling constant and $F(\omega)$ is the phonon density of states. The thermal Bose (N_0) and Fermi (f_0) factors enter because in condensed matter one needs to thermodynamically average over the system. At low temperatures as in our experiments the Bose factor vanishes and the Fermi factors are nearly step functions. Taking the voltage derivative these become Dirac delta functions centered at $\omega = \pm eV$. In the low-temperature limit only the one at $\omega = eV$ contributes.

Table I. Experimental parameters for the point contacts of Fig. 3. Symbols: R_0, resistance of the point contact at zero voltage; $k\theta$, Debye energy; a, radius of the contact determined from $R = (4/3\pi)(\rho l/a^2)$; K, Knudsen number; λ_t, electron-phonon parameter recommended by Grimvall (*15*); λ_M, electron-phonon parameter determined by Host and Mota (*16*); and λ_f, electron-phonon parameter determined by the point-contact technique.

Material	R_0 (ohm)	$k\theta$ (meV)	a (10^{-6} cm)	K	λ_t	λ_M	λ_f
Cu-Cu	5.7	29.2	72.7	96	0.14 ± 0.03	0.16	0.14
Ag-Ag	16	19.1	54.9	140	0.10 ± 0.04	0.16	0.15
Au-Au	32.0	14.0	37.1	162	0.14 ± 0.05	0.21	0.16

Experimental Results

The data for copper plotted in Fig. 2 curve c show both a slight asymmetry (about $V = 0$) and a slight positive shift in the signal. We attribute the asymmetry to a d.c. voltage bias due to the thermal voltage over the coaxial leads to the point contact at 1.2°K. This small voltage shift is about 0.5 mV. We interpret the slight positive shift as due to first harmonic leakage into the second harmonic channel as well as tunneling leakage in the contact itself [which is even (*8*) in the second derivative]. The continuous data were digitalized [$-D(\omega)$] on a grid of 0.5 mV. A new energy scale shifted by Δ was defined and the symmetric and antisymmetric parts in the shifted energy scale were found $\{D_A(\omega) = \tfrac{1}{2}[D(\omega - \Delta) \mp D(-\omega - \Delta)]\}$. The integral A of the antisymmetric part was defined as

$$A \int_0^{1.5\omega} D_A(\omega)d\omega \qquad (10)$$

The shift Δ was varied in steps of 0.1 mV until A_s was maximized. This Δ was the same for all noble metal point contacts. The resulting D_A's are shown in Fig. 3 together with literature values for the phonon density of states obtained by fitting Born-von Karman models to inelastic neutron scattering data (*14*). The close coincidence of the peaks in the second derivative and the transverse and longitudinal peaks of the phonon structure suggest that bulk phonons play a

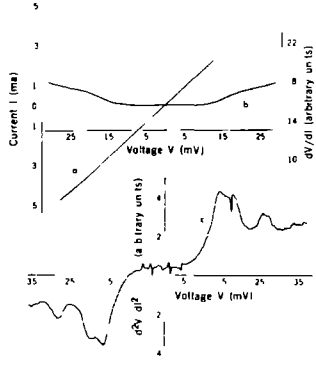

Fig. 2 (left). Photograph of the recorder sheet with (curve a) current I, (curve b) first derivative dV/dI, and (curve c) second derivative d^2V/dI^2 plotted against applied voltage. Fig. 3 (right). The measured voltage derivative of the resistance of point contacts as function of applied voltage for (a) Cu, (b) Ag, and (c) Au is plotted as solid lines (left hand scale). The right hand scale is the derived value for α^2F. The background functions are shown as short dashed curves and the phonon density of states as long dashed curves.

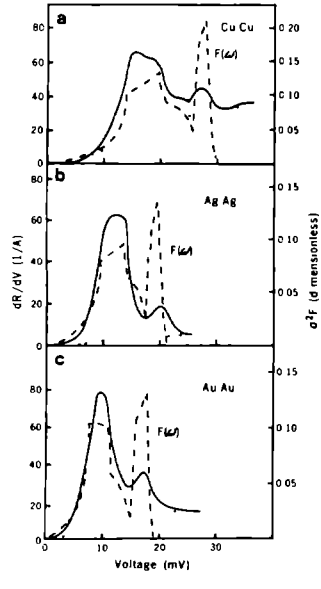

dominant role in the phenomena of point contacts As the resistance at zero bias R_0 is varied the ratio γ of the height of the first peak to that of the flat portion above the second peak varies inversely with $R_0^{1/2}$ Thus dR/dV contains two effects α^2F and the effect leading to the relatively flat dR $d\lambda$ above the phonon peaks By making point contacts of extremely high R_0 (> 100 ohms) Yanson (6) has shown that the flat portion can be made small relative to the phonon effect Because of its relative smallness at high R_0 we have called the flat portion the background (BG) effect Yanson only used data with high R_0 to find α^2F's we wished a more global treatment After some experimentation we found that the functional shape

$$BG(eV) = B \tanh^2(3\ eV/2k\theta_D) \quad (11)$$

where k is Boltzmann's constant given in appropriate units and θ_D is the Debye temperature worked well B is a constant fit at 30 mV This functional form yields the short-dashed curves in Fig 3 The difference between $dR/d\lambda$ and the background is the derived absolute α^2F from these experiments The right-hand scales of Fig 3 are found from the values listed in Table 1 and the derived relation between dR/dV and α^2F Apart from Yanson's values, we know of no other experimentally determined α^2F's for noble metals in the literature To check our results we integrated to find λ as

$$\lambda = 2\int_0^\infty \alpha^2F/\omega\ d\omega \quad (12)$$

These values are listed in Table 1 as λ_P and are in close (± 15 percent) agreement with the literature values λ_G (*15*) and λ_M (*16*) Using the fitted background function, we could derive similar values

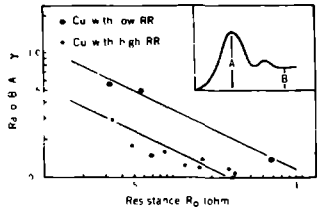

Fig 4 The ratio B/A (the background constant divided by peak height) as a function of the resistance R_0 for two different values of the residual resistivity ratio

of λ from dR/dV's for which R_0 ranged from 2 to 30 ohms

On the basis of the coincidence of the structure of our curves in Fig 3 with the structure of the phonon curves obtained from neutron scattering data and the good agreement of our λ's with those from the literature we conclude that the voltage derivative of the resistance of tiny point contacts (with background subtracted) provides a simple and convenient tool for measuring α^2F in normal metals

Background Effect

We now examine the background effect in greater detail In Fig 4 we have plotted the logarithm of γ the ratio of the background constant B to the peak height A of the derived α^2F, against the logarithm of R_0 for point contacts formed from copper having two different values of the residual resistivity ratio (RR) The large dots in Fig 4 are for material whose RR was 71 The small dots correspond to samples formed from spears of RR 71 and anvils of RR more than 4000, with a geometric mean of 500 Plotted in this way the data show that the background effect is related to the impurity concentration The constant B varies as RR$^{-1/2}$ With this separation by RR the data in Fig 4 are well fit by two lines of slope $-\frac{1}{2}$ that is γ varies as $R_0^{1/2}$

We believe that the high current densities within the tiny contacts are beneficial in that electromigration effects will be swift any impurity or defect will be rapidly swept away from the contact In this sense the contacts are self-cleaning

References and Notes

1 R S Sorbello *J Phys Chem Solids* **34** 937 (1973)
2 J C Maxwell *A Treatise on Electricity and Magnetism* (Clarendon Oxford 1904)
3 R H Holm *Electric Contacts* (Springer Verlag Berlin ed 4 1967)
4 A G M Jansen F M Mueller P Wyder in *Proceedings of the Second Rochester Conference on Superconductivity in d- and f-band Metals* D H Douglass Ed (Plenum New York 1976) p 601
5 — *Phys Rev B* **16** 1325 (1977)
6 I K Yanson *Zh Eksp Teor Fiz* **66** 1035 (1974) in *Proceedings of the International Conference on Low Temperature Physics LT14* (North Holland Amsterdam 1975) paper 1 131 and Yu N Shalov *Zh Eksp Teor Fiz* **71** 286 (1976)
7 T Huiben and K de Kort thesis University of Nijmegen (1973)
8 J M Rowell W L McMillan W L Feldman *Phys Rev* **180** 658 (1969)
9 F H Kennard *Kinetic Theory of Gases* (McGraw Hill New York 1938)
10 M Knudsen *Ann Phys* **28** 75 (1909)
11 Yu V Sharvin *Zh Eksp Teor Fiz* **48** 984 (1965)
12 M Born *Optik* (Springer Verlag Berlin 1933)
13 G Wexler *Proc Phys Soc London* **89** 927 (1966)
14 Copper R M Nicklow G Gilat H G Smith I J Raubenheimer M K Wilkinson *Phys Rev* **164** 922 (1967) silver W A Kamitaka hara and B M Brockhouse *Phys Lett A* **29** 639 (1969) gold J W Lynn H G Smith R M Nicklow *Phys Rev B* **8** 3493 (1973)
15 G Grimvall *Phys Scr* **14** 63 (1973)
16 R F Hoyt and A C Mota *Solid State Commun* **18** 139 (1976)

17 This work was performed as part of the research program of the Stichting voor Fundamenteel Onderzoek der Materie with financial support from the Nederlandse Organisatie voor Zuiver Wetenschappelijk Onderzoek

JOURNAL DE PHYSIQUE *Colloque C6, supplement au n° 8, Tome 39, août 1978, page* C6 602

STRUCTURE OF CURRENT VOLTAGE CHARACTERISTICS OF METAL POINT CONTACTS

A.P. Van Gelder, A.G.M. Jansen, S. Strassler[+] and P Wyder

Research Institute for Materials, University of Nijmegen, Toernooiveld, Nijmegen, The Netherlands

Résumé.- La structure observée dans le signal de fond de d^2J/dV^2 est caractéristique des contacts à pointe métalliques. Elle implique la présence d'un processus à deux phonons. On explique ainsi indirectement la forme du signal dc fond.

Abstract.- Structure has been observed in the background signal of d^2J/dV^2 characteristics of metal point contacts, implying double-phonon backflow-processes. An explanation of the background signal follows indirectly from this observation.

Point contacts between metals are useful to determine the parameter α^2F, the product of the electron-phonon interaction strength and the phonon density of states, from the structure of the d^2J/dV^2 characteristics (J = current, V = voltage)/1-4/. Yanson/1/ forms the metal-constriction as a short in a metal-oxyde-metal geometry, whereas our junctions are manufactured by carefully pressing a 'spear' upon an 'anvil' with a differential screw mechanism in combination with a piezo-electric translator. The spear consists of a metal wire with an electrolytically etched tip ($\sim$ 0.5 μ), the anvil is a chemically polished metal surface. Our method has permitted an extensive research of high purity materials, like Au/Au (with an RRR $\gtrsim$ 500). Phase sensitive detection techniques have for instance led to the d^2J/dV^2 characteristic of figure 1, which exhibits a small reproducible signal if $eV > \hbar\omega_D$, where ω_D is the Debye frequency of the metals.

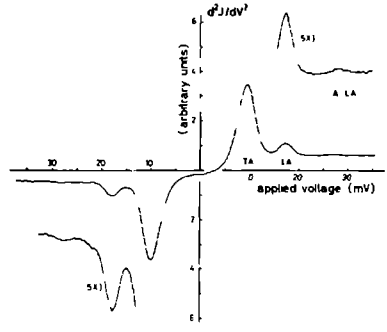

Fig. 1 : d^2J/dV^2 characteristic (recorder output) of an Au-Au point contact (resistance R = 2.2 Ω, temperature of heliumbath T = 1.2 K) showing the transverse (TA) and longitudinal (LA) phonon peaks at 10 mV and at 17.5 mV. The small signal at 27 5 mV (TA + LA) is believed to be due to double phonon scattering, followed by a backflow process.

In order to explain the observed structure of the current-voltage characteristics, it is important to note that the exact geometrical form of the orifice is not a priori known. For this reason, a number N of point contacts (assumed to be identical) is considered to represent the real junction, whereas in addition the tunneling probability for the electrons (T) may differ from unity. The point contacts are assumed to have a circular orifice with radius b. The current J through a point contact has been calculated by solving the semi-classical Boltzmann equation for electrons which interact with the lattice-vibrations and impurities/6/ The coupling between electrons and lattice is characterized by the parameter $\alpha^2F = g(\varepsilon)$, a function of the phonon-energy (ε) such that the energy-dependent electron mean free path $l(\varepsilon)$ is given by $l(\varepsilon)^{-1} = 2\pi(\hbar v_F)^{-1} \int_0^{\varepsilon} d\varepsilon_1\, g(\varepsilon-\varepsilon_1)$. For our calculations/6/ it is assumed that the temperature is sufficiently low that thermally excited phonons may be ignored ; this assumption is only reasonable for such values of the applied voltage V that eV is large compared with the temperature. If in addition the assumption is made that excited phonons may be ignored, the current through the orifice may be expressed as the sum of an (infinite) series of terms, which may be labelled according to the number (n) of collisions entering in it, and supplemented with a factor b^{n+2} in view of dimensional considerations. The leading term, proportional to b^2, represents the field-emission current through the contact, pro-

[+] Brown Boveri Research Centre, CH-5401 Baden, Switzerland.

portional to V and the area of the orifice. The next term, proportional to b^3, accounts for the backflow of electrons through the orifice. This backflow is possible only after the electron has interacted with the lattice and during the process spontaneously created a phonon. The following term, proportional to b^4, represents the backflow contribution after two collisions, with a net production of two phonons etc. The kinetic processes corresponding with these terms are shown in figure 2.

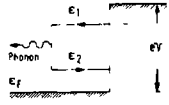

Fig. 2 : Backflow process, following a scattering event where a non-equilibrium phonon is spontaneously created.

For instance, the single-collision backflow term of the current is proportional to $b^3 \int_0^{eV} d\varepsilon_2 \int_{\varepsilon_2}^{eV} d\varepsilon_1$ $g(\varepsilon_1-\varepsilon_2)$ for the process of figure 2. The experimentally observed structure of d^2J/dV^2 is hence proportional to $b^3 g(eV)$, in agreement with reference/1/, but different by a numerical factor of 1.81. We find that $d^2J/dV^2 = -AT^2Nb^3.g(eV)$, with a constant $A = 4\pi n^o e^3 (Mv_F^2 m)^{-1}$, for this process if n^o, e and m are the density, charge and mass of the electrons. The double-collision term gives rise to a contribution to d^2J/dV^2 proportional to $T^2Nb^4 \int_0^{eV} d\varepsilon\ g(\varepsilon)$ $g(eV-\varepsilon)$. The small two-phonon contribution shown in figure 1 is in good agreement with this term, and of order b/l(eV) in comparison with the single-collision one. It may be concluded that the main background signal saturating to a constant value if $eV > \hbar\omega_D$ cannot be explained in terms of multiple-scattering backflow processes. The main background signal can be shown to result from stimulated phonon-emission processes, involving the created phonons, and is proportional to $T^2Nb^4 \int_0^{eV} d\varepsilon\ g(\varepsilon)/$ $\{\varepsilon\ \lambda(\varepsilon)\}$, where $\lambda(\varepsilon)$ is the phonon-mean free path. The relatively large magnitude of this term, compared with the double-phonon collision one, results from the smallness of the phonon-mean free path in comparison with $l(\varepsilon)$. An unambiguous identification of the terms proportional to b^3 and to b^4 (background) is possible, and hence of the function g(eV) by comparing the d^2J/dV^2-characteristics of different point contacts. Typical values for N of order $l \sim 5$ have been found for high-ohmic junctions, and tunneling parameters of roughly equal order of magnitude.

References

/1/ Yanson,I.K., Sov. Phys. JETP 44 (1976) 148 and references therein

/2/ Shalov,Yu.N. and Yanson,I.K., Sov. J. Low Temp. Phys. 3 (1977) 48

/3/ Jansen,A.G.M., Mueller,F.M. and Wyder,P., Proc. of the Second Rochester Conference on Superconductivity in d- and f- band Metals ; ed. D.H. Douglass (Plenum Press, New York, 1976)

/4/ Jansen,A.G.M., Mueller,F.M. and Wyder,P., Phys. Rev. B 16 (1977) 1325, and Science 199 (1978) 1037

/5/ Lynn,J.W., Smith,H.G. and Nicklow,R.M., Phys. Rev. B 8 (1969) 639

/6/ Van Gelder,A.P., Solid State Commun. (in press)

Reprint Workshop on Current Problems in Superconductivity. Gwatt (Thun), Switzerland, 25-27 october 1979.

A.G.M. Jansen, A.P. van Gelder, F.M. Mueller,
S. Strässler* and P. Wyder

Research Institute for Materials, University of Nijmegen,
Toernooiveld, Nijmegen, The Netherlands

*Brown Boveri Research Center, Baden, Switzerland

The behaviour of real superconductors can most clearly be described on the basis of the celebrated Eliashberg equations, where the detailed form of the electron-phonon interaction is explicitly taken into account (see Prof. M. Peter, Theory of Real Superconductors). One of the important ingredients of this description is the Eliashberg function $\alpha^2F(\omega)$; here, loosely speaking, α is some averaged electron-phonon interaction matrix element, and $F(\omega)$ is the density of states of phonons with energy $\hbar\omega$. It seems to be rather difficult to get reliable values for α^2F, essential for the analysis of superconducting properties of real materials, from theoretical bandstructure calculations. Therefore it is of considerable importance to be able to measure this function experimentally. In part, this can be done by inelastic neutron scattering or diffuse X-ray scattering, where $F(\omega)$ is determined, or with the Mössbauer effect (measuring the moment $\int \alpha^2F(\omega)\omega^n d\omega$, $n = \pm 1, \pm 2$) or with tunneling spectroscopy with superconducting tunnel junctions. As the same electron-phonon interaction is responsible for the resistivity, it should also be possible to get α^2F from a suitable analysis of the temperature dependence of the electrical resistance of metals.

It is the purpose of this note to discuss a new method (point contact spectroscopy) which in principle allows to measure α^2F in all reasonably pure normal metals with a not too short mean free path ℓ. Point contact spectroscopy has been discovered by Yanson[1,2], who measured the voltage dependence of the resistance between two evaporated normal metal films, separated by an oxide layer with a short circuit that formed the metallic contact. The same deviations from Ohm's law in simple metals can be seen by measuring the voltage dependence of the point contact resistance between an electrochemically sharpened whisker ("spear") (with a curvature radius at the "point" of some μm) pressed against a bulk piece of metal

("anvil"), single crystals or not[3,4]. Fig. 1 shows directly the recorder output of the current I and its first and second derivative with respect to the voltage as a function of the voltage V applied over the point contact, measured for such a "spear and anvil" arrangement in simple off-the-shelf copper. The structure in the second derivative appears at the typical phonon energies of Cu (one sees clearly two transverse and one longitudinal mode) and it is obvious that this signal is related to the electron-phonon interaction in Cu.

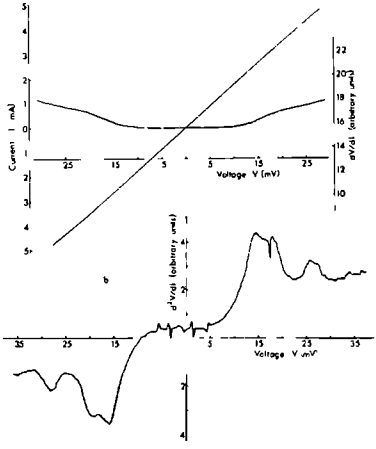

Fig. 1. Recorder sheet with (a) current I and first derivative dV/dI, and (b) second derivative d^2V/dI^2 plotted against applied voltage for a Cu-Cu point contact.

Although some exact theories of this effect do exist, based on the solution of the full non-linear Boltzmann equation, we will limit ourselves here to a more heuristic and pedagogical discussion.

The problem of the constriction resistance of a small contact between two metals has been studied for the first time by Maxwell quite some time ago[5]. He solved Poisson's equation for the electrical potential V as a function of the position $\underline{r}$, $\nabla^2 V(\underline{r})=0$, in oblate spherical coordinates. Contours of constant potential of a current flowing through a constricting circular orifice of radius a are given by $V(\underline{r}) = \pm \frac{V_o}{2}[1 - (2/\pi) \arctan (1/\xi)]$, where the oblate spherical coordinate ξ may be found from the more familiar spherical polar coordinates r and z by solving the implicit equation $r^2/a^2 = (1+\xi^2)(1-z^2/\xi^2a^2)$ (Fig. 2). The two signs refer to the two sides of the circular orifice. The resistance of such a contact may be found by dividing the total voltage drop (here V_o) by the total current flowing through any contour of constant voltage. For simplicity we choose the contour $V(\underline{r})=0$, that is the orifice itself ($\xi=0$). The total current is then given by $I = \int d\underline{O}\cdot\underline{j}$. Explicitly using Ohm's law in the form $j_z = \sigma E_z = (1/\rho)\cdot(\partial V/\partial Z)$, where $\sigma = 1/\rho$ is the conductivity of the bulk material, one gets for the Maxwellian resistance

$$R_M = (\rho/2a) \ . \qquad (1)$$

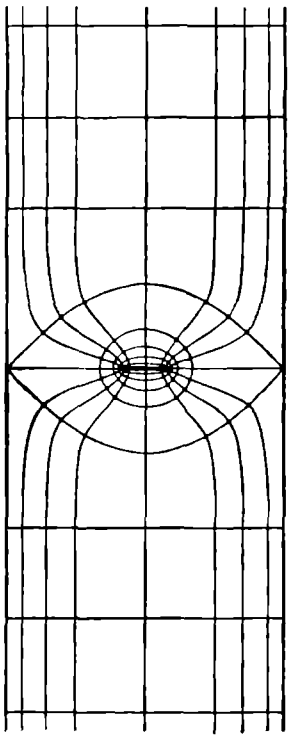

Fig. 2. Maxwell's solution for current- and equipotential-lines for the constriction resistance.

For finite K, a suitable interpolation between Eqs. (1) and (2) can be found by solving the linearized Boltzmann equation with the variational principle, and one gets[7]

$$R = (\rho/2a)\cdot\Gamma(K) + (4/3\pi)\cdot K\cdot(\rho/a) \quad . \qquad (3)$$

It is obvious that the validity of this calculation breaks down if the mean free path ℓ of the electrons becomes comparable to the size of the orifice a, i.e. if the Knudsen number $K = \ell/a$ is getting important (Fig. 3). The limiting case for large K has been discussed by Sharvin[6]. If there is a voltage drop V across the contact, the electrons passing through the orifice are getting a speed increment $\Delta v = eV/p_F$, where p_F is the Fermi momentum. The current due to this speed increment is then given by $I = \pi a^2 ne\Delta v = \pi a^2 (ne^2/p_F)V$, where n is the particle density. Using a Drude-like expression for the resistivity $\rho = p_F/(ne^2\ell)$ one gets for the resistance of a point contact in the high K regime $R_S = V/I = \rho\ell/(\pi a^2)$. An integration over all angles gives the numerical factor in front and leads to the Sharvin resistance

$$R_S = \frac{4}{3}\frac{\rho\ell}{\pi a^2} = \left(\frac{8}{3\pi}\right) K\cdot R_M \quad . \qquad (2)$$

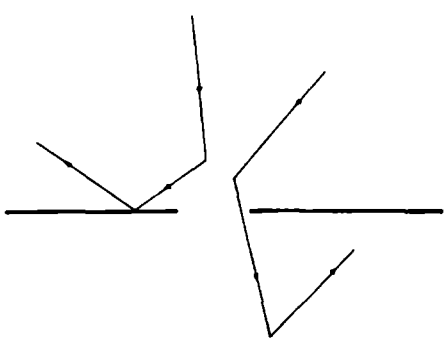

Fig. 3. Point contact in the Knudsen regime.

$\Gamma(K)$ is a slowly varying function of K with $\Gamma(K=0)=1$ and $\Gamma(K=\infty)=(9\pi^2/128)$. The first term in Eq. (3) is like the Maxwell resistance, the second like the Sharvin resistance.

If the mean free path ℓ is energy dependent, $\ell=\ell(E)$, one gets a voltage dependence of $R=R(V)$. As the combination of $\rho\cdot\ell$ in the Sharvin-like term in Eq. (3) is independent of the mean free path $\ell(\varepsilon)$, only the first term enters the partial derivative

$$\frac{\partial R}{\partial V} = \frac{\partial R_M}{\partial V} = \Gamma(K)\,\frac{\rho\ell}{2a}\,\frac{\partial}{\partial V}\left(\frac{1}{\ell(E=eV)}\right) . \qquad (4)$$

Note that the Sharvin-like term in Eq. (3) leads to no structures; however, the term is essential as he allows to set up an electric field over the point contact, otherwise impossible in a metal.

Assuming the validity of Matthiessen's rule, the total mean free path ℓ is given by $\ell^{-1} = \ell_{imp}^{-1} + \ell_{ep}^{-1}$, where ℓ_{imp} is the energy independent scattering length due to impurities. ℓ_{ep} is the mean free path due to the electron-phonon scattering, $\ell(E) = v_F\cdot\tau(E)$. The lifetime $\tau(E)$, due to the electron-phonon interaction of an electron with energy E above the Fermi level, is given by using the "golden rule" as

$$\frac{1}{\tau} = \frac{2\pi}{\hbar}\sum_k |g_q|^2 \left[\,\delta(\varepsilon_p-\varepsilon_k-\hbar\omega_q)(N_q+1-f_k)+\delta(\varepsilon_p+\hbar\omega_q-\varepsilon_k)(N_q+f_k)\,\right] . \qquad (5)$$

Here, g_q is the matrix-element for the electron-phonon interaction for a phonon of momentum q and energy $\hbar\omega_q$, ε_p and ε_k the energies of electrons with momenta p and k, N_q the Bose distribution function of the phonons and f_k the Fermi distribution function of the electrons. Replacing the k-summation in the usual way

$$\sum_k = N_o \int d\omega \int \frac{q\,dq}{(2k_F^2)} \qquad (6)$$

where N_o is the density of states at the Fermi level, and introducing the Eliashberg function

$$\alpha^2F(\omega) = N_o \int \left(\frac{q\,dq}{2k_F^2}\right) |g_q|^2\,\delta(\omega-\omega_q) , \qquad (7)$$

one gets

$$\frac{1}{\tau(E)} = \frac{2\pi}{\hbar}\int d\omega\;\alpha^2F(\omega)\,\left[\,2N(\omega)+1-f(E-\hbar\omega)+f(E+\hbar\omega)\,\right] . \qquad (8)$$

At T=0, this reduces to

$$\frac{1}{\tau(E,T=0)} = \frac{2\pi}{\hbar} \int d\omega\ \alpha^2F(\omega)\ \theta\ (\hbar\omega - E) \quad . \tag{9}$$

Therefore, one finally gets as the grand result for the voltage derivative of the point contact resistance

$$\frac{dR}{dV}(V) = \frac{\rho\ell}{2a}\ \Gamma(K)\ \frac{2\pi e}{\hbar v_F}\ \alpha^2F(eV) \quad . \tag{10}$$

Eq. (10) allows a direct determination of the energy dependence of the Eliashberg function $\alpha^2F(\omega)$.

Fig. 4 shows the point contact spectrum dR/dV of Au, together with $F(\omega)$ determined by inelastic neutron scattering. As expected, the van Hove singularities measured by the two different experiments coincide. Fig. 5 shows point contact spectra for all noble metals, again together with $F(\omega)$

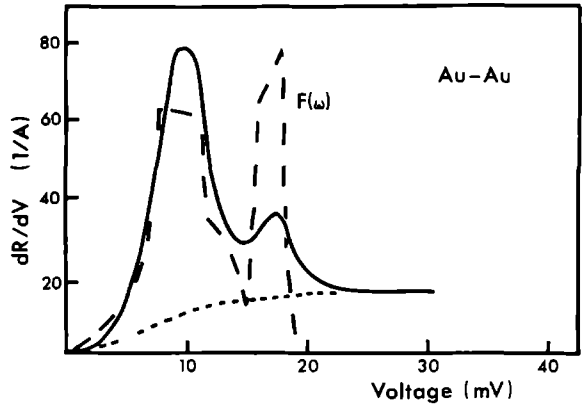

Fig. 4. Point contact spectrum of a Au-Au point contact. Long-dashed curve: Phonon density of states from inelastic neutron scatttering. Short-dashed curve: Background signal.

as determined by neutron scattering. As an interesting detail, Fig. 5d shows the point contact spectrum of a Au-spear with a Cu-anvil; the phonons of both metals, Au and Cu, can clearly be detected indicating that spear and anvil together are responsible for the signal. From the point of view of understanding the electron-phonon interaction in noble metals, it is very important to note that the ratio's of the α^2F to the related $F(\omega)$'s show a strong ω or energy dependence. Transverse phonons couple to the electron gas about four times more effectively

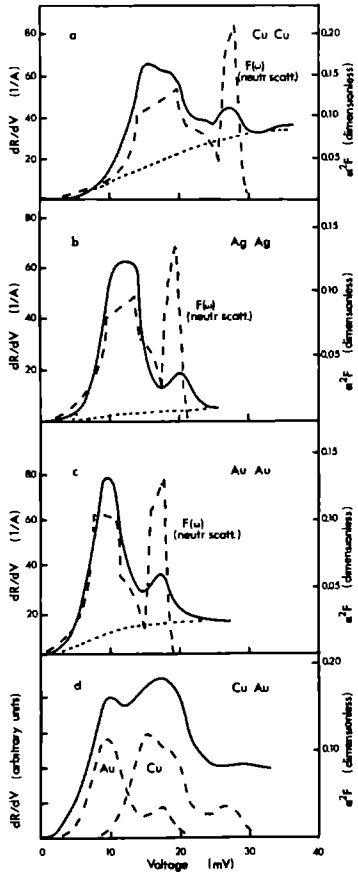

Fig. 5. Measured voltage derivative of the resistance of point contacts as a function of applied voltage of (a) Cu-Cu, (b) Ag-Ag, (c) Au-Au and (d) Cu-Au plotted as the solid lines. The right hand scale is the derived value for α^2F_{pc}. In (a), (b) and (c), the background functions are shown as short-dashed curves and the phonon density of states from neutron scattering as long-dashed curves.

than longitudinal phonons in noble metals. This is consistent with the results of bandstructure calculations showing that d-electrons are important and are strongly umklapp coupled to transverse phonons in noble metals.

It is interesting to compare α^2F as measured with point contact spectroscopy with theoretical bandstructure calculations of the electron-phonon interaction. The most detailed and reliable pseudopotential calculations have been carried out on the alkalis[8]. Figs. 6, 7 and 8 show point contact spectra for α^2F for Li, Na and K, together with theoretical calculations, and $F(\omega)$ determined from inelastic neutron scattering. The agreement is remarkable and confirms the pseudopotential calculations. Note that in Li, just as in the case of the noble metals, the electrons are more strongly coupled to the transverse phonons than to the longitudinal ones, while in the case of Na and K it is the other way around.

It is very clear and obvious that the theoretical discussion on the mechanism of point contact spectroscopy as sketched here is at most a guideline for experiments. The full nonlinear Boltzmann equation has to be solved in order to understand these highly nonlinear phenomena. This sort of solutions are now becoming available[9,10]. Most of them are based on the "back-scattering" concept of van Gelder[10]: The solutions of the Boltzmann equation are expanded in terms of the collision kernel. The zeroth approximation is a Sharvin-like field-emission term where electrons

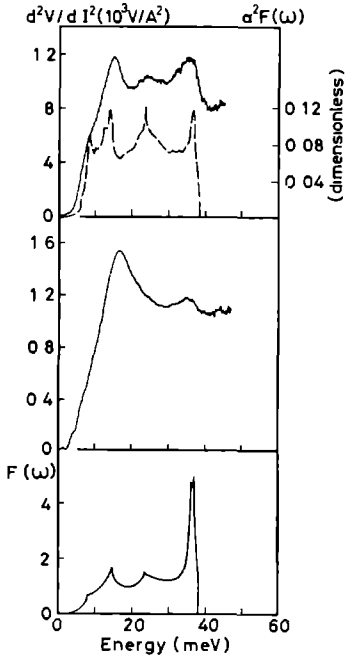

Fig. 6. Point contact spectroscopy of Li. The two solid curves (left hand scale) in the top part are measured point contact spectra for Li (junction resistances 25.4 Ω (uppermost curve) and 11.8 Ω). The dashed curve is the theoretically obtained function $\alpha^2F(\omega)$ (Hayman and Carbotte). The curve in the bottom part represents the phonon density of states $F(\omega)$ obtained from inelastic neutron scattering experiments.

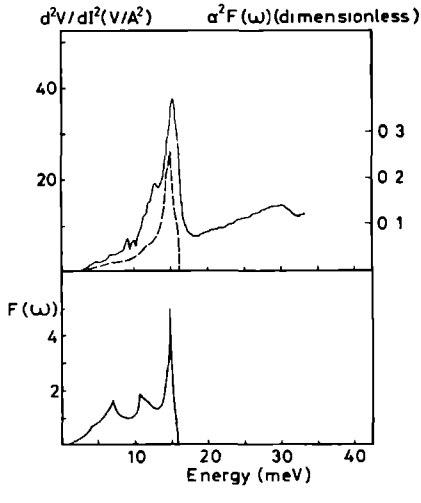

Fig. 7. Point contact spectroscopy of Na (junction resistance 2.9 Ω).

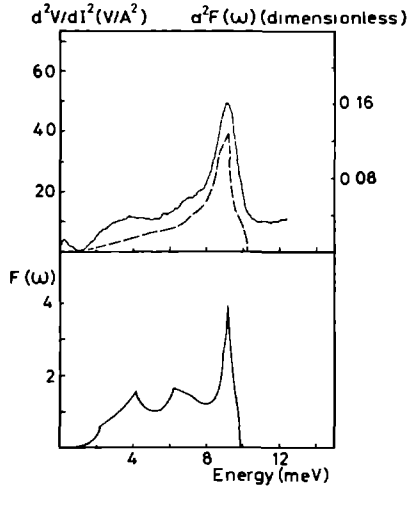

Fig. 8. Point contact spectroscopy of K (junction resistance 1.1 Ω).

The dashed curve (right hand scale) is the theoretically obtained function $\alpha^2F(\omega)$ (Carbotte and Dynes). The curve in the bottom part represents the phonon density of states $F(\omega)$ obtained from inelastic neutron scattering experiments.

are injected into the other metal, leading to the disturbed Fermi surfaces as sketched in Fig. 9. While this does not lead to a voltage dependent structure in the signal, the first order term is given by the back-streaming of the electrons through the orifice, after one scattering with a phonon. This term leads to a decrease in the total net-current and therefore to an increase in the resistance, an essential difference with the usual tunneling process through an oxide layer which should be pointed out clearly. The second order corrections[11] include collisions with two phonons before the electron is scattered back through the orifice; this leads to a signal at twice the characteristic phonon energy, and can clearly be seen in Fig. 7 at energies of around 30 meV, while the typical Debye energy is at 15 meV.

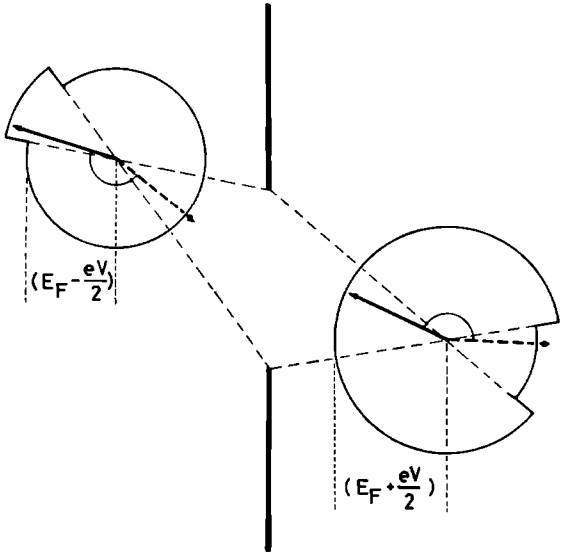

Fig. 9. Zeroth approximation electronic distribution function for the theoretical analysis of point contact spectroscopy.

In addition, due to the kinematics involved, the theory predicts an interesting efficiency factor. The measured signal is not quite α^2F, but

$$S(\omega) = N_o \int \left(\frac{qdq}{2k_F^2}\right) |g_q|^2 \delta(\omega-\omega_q)\eta(q) \qquad (11)$$

where the efficiency factor $\eta(q)$ is a function of the scattering angle $\theta=\theta(\underline{p},\underline{k})$. For instance in the expression for the simple dc-resistivity ρ,

η leads to the well known transport-relaxation time with the famous $\eta_{dc}(q) = \{1-\cos\theta(\underline{p},\underline{k})\}$, while in the case of point contacts one has

$$\eta_{pc} = \frac{1}{2}\{1-\theta/tq\theta\} \quad . \tag{12}$$

As follows from Eq. (12), η_{pc} is effective for low phonon energies. This can clearly be seen in Fig. 10 where α^2F_{pc} measurements from point contact spectroscopy in the normal state of Pb are compared with measurements of α^2F_t from strong coupling tunneling in the superconducting state using the Rowell-McMillan scheme.

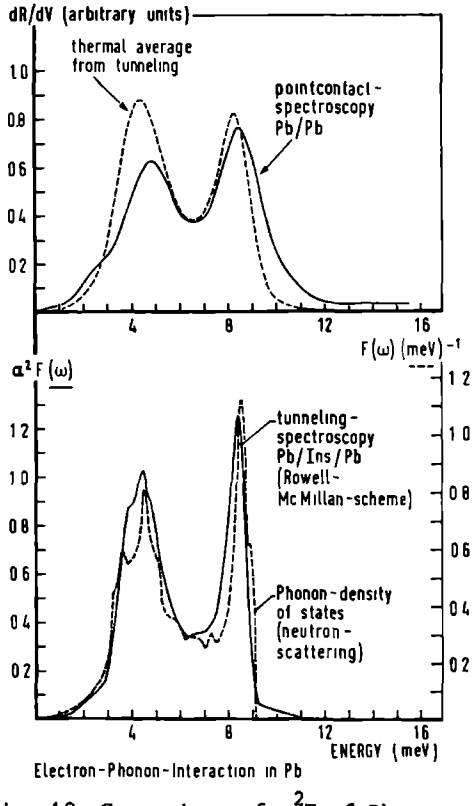

Fig. 10. Comparison of α^2F of Pb as measured by point contact spectroscopy in the normal state and superconducting tunneling in the superconducting state.

As there are no phonons present above the Debye cut-off frequency ω_D, i.e. $F(\omega > \omega_D)=0$, the point contact spectrum should vanish for energies $eV > \hbar\omega_D$. Nevertheless, as is indicated in Fig. 2 with the short-dashed curve, a "background signal" is present on top of the α^2F_{pc}-signal which levels off at a constant non-zero value for energies above ω_D. This can be understood by realizing that in these highly nonlinear processes the presence of phonons which are not in thermal equilibrium has to be taken explicitly into account. It is possible to show that this background signal (constant for energies above ω_D) is due to the stimulated emission of phonons during the back-flow process.

References

1. I.K. Yanson, Zh. Eksp. Teor. Fiz. 66, 1035 (1974) [Sov. Phys. - JETP 39, 506 (1974)].
2. I.K. Yanson and I.O. Kulik, J. Phys. (Paris) 39, C6-1564 (1978), and references therein.
3. A.G.M. Jansen, F.M. Mueller and P. Wyder, Phys. Rev. B16, 1325 (1977).
4. A.G.M. Jansen, F.M. Mueller and P. Wyder, Science 199, 1037 (1978).
5. J.C. Maxwell, A Treatise on Electricity and Magnetism (Clarendon, Oxford, 1904).
6. Yu.V. Sharvin, Zh. Eksp. Teor. Fiz. 48, 984 (1965) [Sov. Phys. - JETP 21, 655 (1965)].
7. G. Wexler, Proc. Phys. Soc. Lond. 89, 927 (1966).
8. B. Hayman and J.P. Carbotte, J. Phys. F: Metal Phys. 1, 828 (1971); J.P. Carbotte and R.C. Dynes, Phys. Rev. 172, 476 (1968).
9. I.O. Kulik, A.N. Omel'yanchuk and R.I. Shekheter, Fiz. Nizk. Temp. 3, 1543 (1977) [Sov. J. Low Temp. Phys. 3, 740 (1978)].
10. A.P. van Gelder, Solid State Commun. 25, 1097 (1978).
11. A.P. van Gelder, A.G.M. Jansen, S. Strässler and P. Wyder, J. Phys. (Paris) 39, C6-602 (1978).

Chapter VII : TEMPERATURE DEPENDENCE OF POINT-CONTACT SPECTROSCOPY IN COPPER.

ABSTRACT

The current-voltage characteristics of Cu point contacts have been studied experimentally between 5 and 300 K. The effect of the temperature on the measured d^2V/dI^2-curves is a broadening of the spectrum for the electron-phonon interaction in the metal. The measured resistance of a point contact is compared with the resistivity of bulk material as a function of the temperature. An analysis of the broadening of the spectra and the temperature dependence of the contact resistance is given. Differences between the temperature dependences of the resistance of a point contact and that of the bulk are ascribed to different transport efficiencies for the electron-phonon interaction in these two cases.

I. Introduction.

During the past few years a new spectroscopic method has been employed for studying the electron-phonon interaction in metals using point contacts between metals. The experimentally observed current (I) - voltage (V) characteristics of a metallic contact at liquid helium temperatures are non-linear and allow a direct determination of the well known Eliashberg function $\alpha^2F(\omega)$ by measuring the second derivative d^2V/dI^2 as a function of the applied voltage[1,2]. $\alpha^2F(\omega)$ is the product of the density of states of the phonons and the squared matrix element for the electron-phonon interaction, averaged over the Fermi surface. The great importance of this point-contact method lies in the fact that it is up to now the only existing method to obtain such detailed information about the electron-phonon interaction in normal metals. Recently also theoretical work[3,4] becomes available, which solves the Boltzmann equation for the point-contact problem in order to explain the observed phenomena in the experiments.

In this paper we present point-contact experiments, which for the first time have been performed within the entire temperature range between liquid helium and room temperature, in order to investigate the temperature dependence of the spectroscopic data. With increasing temperature the experiments show that the measured d^2V/dI^2-spectrum is broadened due to thermal averaging. A weight function given from a theoretical analysis of the point-contact problen describes the broadening very well. Furthermore, the theory predicts an analogous behaviour for the temperature dependence of the point-contact resistance and that of the bulk resistivity arising from the electron-phonon interaction. Our experiments show a strong similarity between the measured point-contact resistance and the

bulk resistivity as a function of temperature. Small differences between the point-contact resistance and the bulk resistivity may be ascribed to small differences of the efficiency of the electron-phonon scattering process. In the next section we will discuss theoretically the current through a metallic point contact as a function of the temperature and the applied voltage. From the expression for the current we obtain the voltage derivatives (first and second) of the current. The experiment will then be described, and the experimentally determined dV/dI- and d^2V/dI^2-curves for Cu point contacts are presented and analysed theoretically.

II. Current-voltage relations for a point contact.

The interesting behaviour of a point contact in the clean limit, i.e. if the linear dimension a of the metallic contact is smaller than the mean free path ℓ of the electrons, has been realized for the first time by Sharvin[5]. Due to the applied voltage over this type of junction, an electric field exists within the metal in the region of the contact, and the electrons are accelerated by the electric field near the orifice. Via inelastic scattering processes with elementary excitations (e.g. phonons) in the metal a relaxation of the accelerated electrons takes place, yielding a non-linear current-voltage characteristic as a result of the energy-dependent electron-phonon interaction. To calculate the current through the orifice one needs the distribution function of the electrons. The Boltzmann equation for the distribution of the electrons has been solved for this problem by iteration with respect to the collision term, taking into account the appropriate boundary conditions[3,4].

In zeroth order (where the collision term in the Boltzmann equation is zero) a distribution function is obtained for the electrons with an

energy difference for electrons which have or have not passed through the orifice, due to the potential drop eV over the contact. Using this disturbed distribution function, the Sharvin current[5] is obtained and is given for a circular orifice with radius a by

$$I_0 = \frac{3\pi a^2}{4e\rho\ell} \int_{-\infty}^{\infty} d\varepsilon [\, f(\varepsilon - eV) - f(\varepsilon) \,] = \frac{3\pi a^2}{4\rho\ell} V = \frac{V}{R_0} \,. \qquad (1)$$

The product $\rho\ell$ (ρ is the resistivity and ℓ the mean free path of the electrons) is a material constant and satisfies $\rho\ell = mv_F/n_o e^2$ (Drude formula), where m, e and v_F are the mass, the charge and the Fermi velocity of an electron and n_o the density of electrons in the metal. $f(\varepsilon)$ is the equilibrium Fermi distribution function for electrons with an energy ε with respect to the Fermi level. We have assumed that the electronic density of states is constant near the Fermi energy E_F for applied voltages with $eV << E_F$; self-energy effects are hence ignored.

In next order, single collisions involving phonons are taken into account. These inelastic collisions give a negative correction to the current, because the electrons can change their momentum and flow back through the orifice after a scattering process has occurred. In first order, considering only single collisions and ignoring departures from equilibrium of the phonon system, the correction to the current is given by

$$I_1 = -\frac{4\pi a^3}{\hbar e v_F \rho\ell} \int_{-\infty}^{\infty} d\varepsilon [\, f(\varepsilon - eV) - f(\varepsilon) \,]$$

$$\times \int_0^{\infty} d\omega \; \alpha^2 F_p(\omega) [\, 1 + 2\nu(\omega) + f(\varepsilon+\omega) - f(\varepsilon-\omega) \,] \,, \qquad (2)$$

where $\nu(\omega)$ is the Bose-Einstein distribution for the phonons. The factor $[f(\varepsilon-eV)-f(\varepsilon)]$ equals the density of injected electrons of energy ε, relative to the Fermi level of the low-voltage side of the contact. The energy levels $\varepsilon\pm\omega$ (with respect to the low voltage side) correspond with electrons, which flow back through the orifice after spontaneous or stimulated emission ($\varepsilon-\omega$), or stimulated absorption ($\varepsilon+\omega$) of a phonon with energy ω has taken place. In the expression above the electron-phonon interaction function α^2F has a subscript p to indicate that in the specific point-contact geometry α^2F_p differs from the usual α^2F of Eliashberg by an efficiency function $\eta(\theta) = \frac{1}{2}(1-\theta/\mathrm{tg}\theta)$, which depends on the scattering angle θ between the velocity directions of the electron before and after the collision event with a phonon[6]. In a similar way, one has defined in the DC-transport theory for the calculation of the electrical resistivity the function α^2F_{tr}[7], involving the well-known efficiency function $(1-\cos\theta)$. If the temperature T is zero, equation (2) reduces to[4]

$$I_1 = -\frac{4\pi a^3}{\hbar e v_F \rho \ell} \int_0^{eV} d\varepsilon_2 \int_0^{\varepsilon_1} d\varepsilon_1 \, \alpha^2F_p(\varepsilon_1) \ . \qquad (3)$$

It should be noted that I_1 is of first order in a/ℓ_{ep}, because $I_1 \sim I_0 \, a/\ell_{ep}$; here

$$1/\ell_{ep}(\varepsilon) = \frac{2\pi}{\hbar v_F} \int_0^{\infty} d\omega \, \alpha^2F(\omega)[1+2\nu(\omega)+f(\varepsilon+\omega)-f(\varepsilon-\omega)] \qquad (4)$$

is the inverse of the electron-phonon scattering length for an electron with energy ε above the Fermi level (Fermi's golden rule).

In point-contact spectroscopy, the derivatives of the current-voltage characteristics show interesting phenomena. Differentiating the current $I = I_0+I_1$ with respect to the applied voltage the temperature dependence of the resistance at zero voltage is given by:

$$R_0(T) = R_0 + R_0^2 \frac{4\pi a^3}{\hbar v_F \rho \ell} \int_0^\infty d\omega\ \alpha^2 F_p(\omega)\ \frac{\omega/2k_BT}{\sinh^2(\omega/2k_BT)} \tag{5}$$

for the case where $R_0(T) - R_0 < R_0$. A similar expression can be found for the temperature dependent resistivity in bulk material with the electron-phonon interaction function $\alpha^2 F_{tr}$ [7]:

$$\rho(T) = \frac{2\pi m}{\hbar n_o e^2} \int_0^\infty d\omega\ \frac{\omega/2k_BT}{\sinh^2(\omega/2k_BT)}\ \alpha^2 F_{tr}(\omega)\ . \tag{6}$$

The second derivative of the current $I = I_0 + I_1$ with respect to the voltage V is

$$\frac{d^2I}{dV^2} = -\frac{4\pi a^3 e}{\hbar v_F \rho \ell} \int_{-\infty}^\infty d\omega\ \alpha^2 F_p(\omega)\ \chi\left(\frac{\omega-eV}{k_BT}\right)\ . \tag{7}$$

$\chi(z)$ is a bell-shaped function with half-width 5.4 k_BT:

$$\chi(z) = \frac{1}{k_BT}\, e^z\, \frac{(z-2)e^z+z+2}{(e^z-1)^3}\ . \tag{8}$$

In inelastic tunneling spectroscopy for metal-oxide-metal structures with normal metal films a similar thermal broadening was found[8]. For T = 0 d^2I/dV^2 becomes proportional to $\alpha^2F_p(eV)$ and in point-contact experiments at liquid helium temperatures a direct determination of the electron-phonon interaction is possible. We have measured the spectra $d^2V/dI^2 (= -R^3\, d^2I/dV^2)$ for Cu point contacts between low temperatures and roomtemperature. Using the spectrum for the lowest measuring temperature (5 K), which is proportional to α^2F_p, it is possible to check the validity of equation (7). In addition, we have also investigated the temperature dependence of the point-contact resistance at zero voltage and compared this result with the measured electrical resistivity of bulk material.

III. Experiments and results.

The experiments were performed for copper point contacts. The point contacts consisted of a sharply etched needle, pressed against a flat surface of bulk material. The needle was fabricated by electro-chemically etching of a polycrystalline Cu wire, 50 μ in diameter. The other part of the contact was a single crystal of Cu with the (110)-plane parallel to the contact surface. The point contact was mounted in a holder, which was totally fabricated from copper except for the electrical isolation, to avoid the instability of the contacts upon cooling down because of different thermal expansion coefficients of the materials used in the sample holder. With a screw mechanism stable metallic contacts were adjusted at roomtemperature and mounted in a variable temperature cryostat to control the temperature between 300 and 5 K with an accuracy of 0.5 K. In this configuration it was possible to obtain stable point contacts, and reliable in the sense that the contact geometry remained unchanged during a run

between roomtemperature and heliumtemperature. The derivatives (dV/dI and d^2V/dI^2) of the current-voltage characteristics were measured using phase sensitive detection with modulation voltages in the range of 500 μV. Because the change in the contact resistance is only a few percent, we used a bridge circuit[9] to compensate the unchanging part of the resistance in order to achieve higher resolution.

In the Figs. 1 and 2 we have plotted the measured d^2V/dI^2-curves for Cu-Cu point contacts between 5 and 40 resp. 270 (K). The observed second derivative is an anti-symmetric function around zero voltage. For the lowest measuring temperature, the transverse (17 mV) and longitudinal (28 mV) phononpeaks are clearly visible. The measured structure in the Cu point-contact spectra is characteristic for point-contact spectroscopy and has been observed in pressure-type point-contact experiments in all the noble metals (Cu, Ag and Au) at liquid helium temperatures[2]. According to formula (7), the measured spectrum at low temperatures will be proportional to the electron-phonon interaction $\alpha^2F_p(eV)$. Sometimes we observed (see Fig. 2) structure at the sum-frequency of transverse and longitudinal phonons (45 mV). These signals at double phonon frequencies were recently observed in point-contact experiments[10] and can be explained by an extra iteration in the solution of the Boltzmann equation involving double collision processes[4]. For voltages higher than the Debye energy, the measured signal should vanish because the phonon density of states is zero. In the experiment however, a smooth background signal is observed which is nearly a constant above the Debye energy. It has been realized that the phonons are not in thermal equilibrium at the orifice[10]. The non-equilibrium phonons act as additional scattercenters for the electrons (stimulated emission and absorption processes), which yield an extra negative term to the current. By solving the transport equation for the

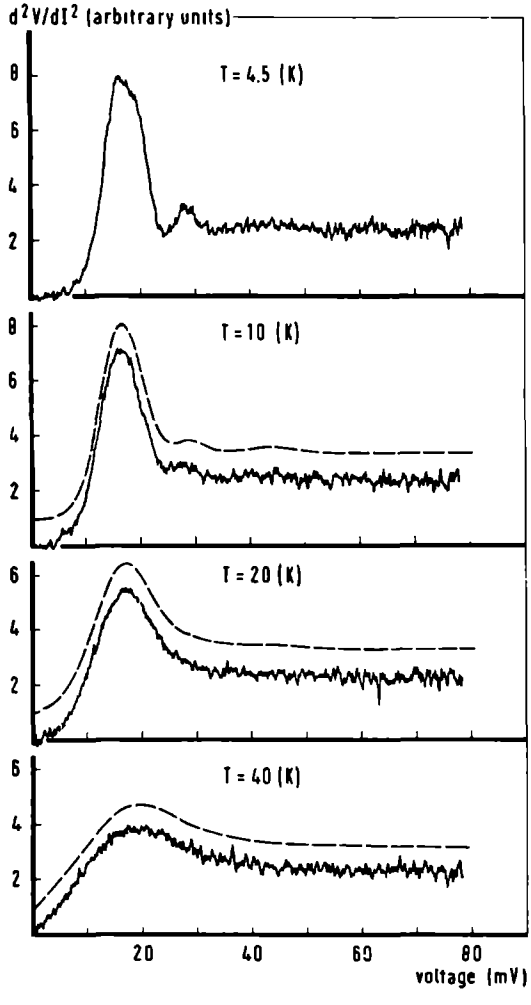

Fig. 1 : Point-contact spectra for Cu between 4.5 and 40 K. The dashed lines (shifted one division on the vertical scale) have been calculated by means of the theoretical given thermal average of the spectrum at 4.5 K. The point-contact resistance was 2.2 Ω at low temperatures.

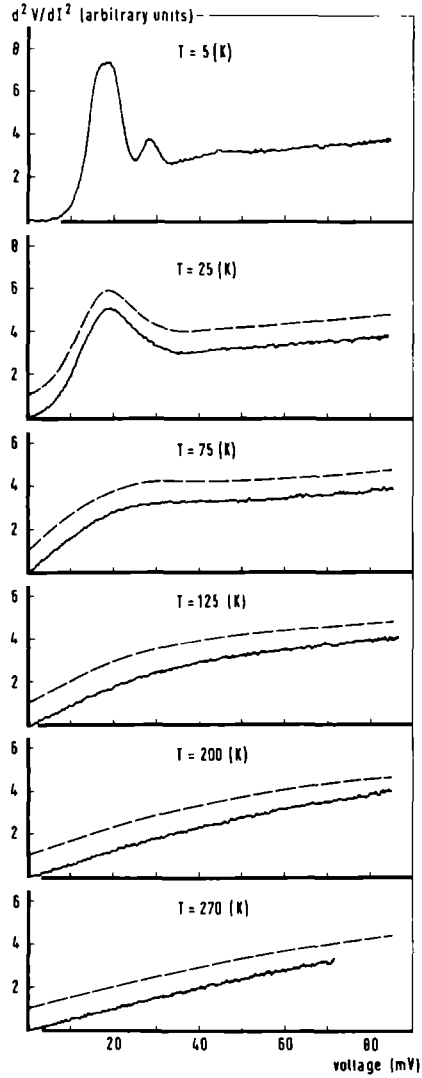

Fig. 2 : Point-contact spectra for Cu between 5 and 270 K. The dashed lines (shifted one division on the vertical scale) have been calculated by means of a theoratical given thermal average of the spectrum at 5 K. The point-contact resistance was 1.7 Ω at low temperatures.

phonons a signal in the point-contact spectrum has been found, which is constant at voltages above the Debye energy[10].

By increasing the temperature from heliumtemperature up to roomtemperature, the point-contact spectra were smeared out due to thermal averaging. Eq. (8) gives an expression for the thermal averaging function χ. Using the measured spectrum at $T_0 \sim 5$ K, we have calculated by a convolution product the spectra at higher temperatures T as follows:

$$\frac{d^2V}{dI^2}(eV)\Big|_T = \int_{-10\,k_BT}^{10\,k_BT} dE\, \frac{d^2V}{dI^2}(E)\Big|_{T_0}\, \chi\left(\frac{E-eV}{k_BT_{eff}}\right) . \qquad (9)$$

In the argument of the function χ, we have taken an effective temperature $T_{eff} = \sqrt{T^2-T_0^2}$ instead of T, as we are interested in the spectral averaging due to the temperature difference between T and T_0. We have subtracted the temperature T from T_0 quadratically in analogy to the quadratical addition of the standard deviations, or equivalently the linewidths for the superposition of Gaussian distributions. The introduction of this effective temperature will only have an effect on the analysis of the spectra at the lowest measuring temperatures. For the signal values at voltages beyond the measured voltage range, a linear interpolation of the spectrum at the lowest measuring temperature was used. The calculated results, indicated by the dashed lines in the Figs. 1 and 2, show that the thermal averaging is very well described by the function χ. In section II we haven't discussed the influence of the temperature on the background function, on which the electron-phonon interaction function α^2F_p is superimposed. Because the background function will be a smooth function of the applied voltage, the averaging will hardly influence the

background for temperatures T < 100 K. For temperatures T > 100 K the experiments show that the broadening of the background is equally well described by the function χ.

A great part of the temperature dependence of the resistivity in a metal is determined by the electron-phonon interaction. Eqs. (5) and (6) show that the behaviour as a function of temperature is similar for the resistance of a point contact and the resistivity of a bulk metal, except for differences in the efficiency of the collisions. To look into this problem, we have also measured in detail the resistance of a point contact at zero voltage as a function of temperature. First we will look at the qualitative difference in the contact resistance between roomtemperature and liquid heliumtemperature. It is not unreasonable that the weighted integrals over α^2F_p and α^2F_{tr} in Eqs. (5) and (6) are roughly equal, because in the high temperature limit the weighted integrals reduce to the expression for the mass-enhancement parameter $\lambda = 2 \int \alpha^2F(\omega)/\omega \, d\omega$ for the electron-phonon interaction, which can be shown to be equal for α^2F_p and α^2F_{tr} due to a sum-rule argument[6]. With the equality for the weighted integrals we obtain for the temperature dependent part of the resistance of a metallic contact, using Eqs. (1), (5), (6) and the Drude formula $\rho\ell = mv_F/n_oe^2$:

$$R(T) - R_0 = 0.360 \frac{\rho(T)}{a} . \qquad (10)$$

This expression resembles the Maxwellian constriction-resistance[11] ($R_M = \rho/2a$) for a circular contact in the dirty limit, i.e. the electronic mean free path is small compared to the linear dimension of the contact, where Ohm's law is valid. Using formula (10) and the resistivity $\rho(T)$ at

roomtemperature we can estimate from the experimentally measured variation in resistance between helium- and roomtemperature the linear dimension a of the orifice. The radius of the orifice can also be determined from the Sharvin resistance measured at low temperatures (Eq. (1)). Using Eqs. (1) and (10) we established the values of the radius of the contact for all measured point contacts, which agreed within 10% for the two determinations. From this we can conclude that the assumption of a single circular orifice gives a realistic description of the point-contact geometry.

In Fig. 3 we have plotted the measured temperature dependence of a Cu point-contact resistance. In the same figure we have also given as a dashed line the resistance of a piece of bulk wire from which the sharp needle of the point contact was fabricated. For a relative comparison, the scaling of the two curves in Fig. 3 has been done in such a way that the curves fall together at low temperatures and have the same slope at higher temperatures. The overall dependence on temperature is similar for the point-contact resistance and the bulk resistance, but the observed difference is characteristic for our experiments on point contacts and bulk material. An explanation for this difference in the temperature dependence of the resistance could lie in the fact, that the two parts of the point contact have not been fabricated from the same starting material. The deviations in the temperature dependent resisitivity, due to different purities of samples are known as Deviations of Mathiessen's Rule (DMR), which are smaller than the residual resistivity at low temperatures[12]. In our case the difference in the two curves at higher temperatures is approximately two times the residual resistance of the bulk wire and cannot likely be described in terms of DMR. One part of the Cu point contact is a single crystal which might yield a different spectrum for $\alpha^2 F_p$ compared with a polycrystalline sample. However, in pressure-type point-contact

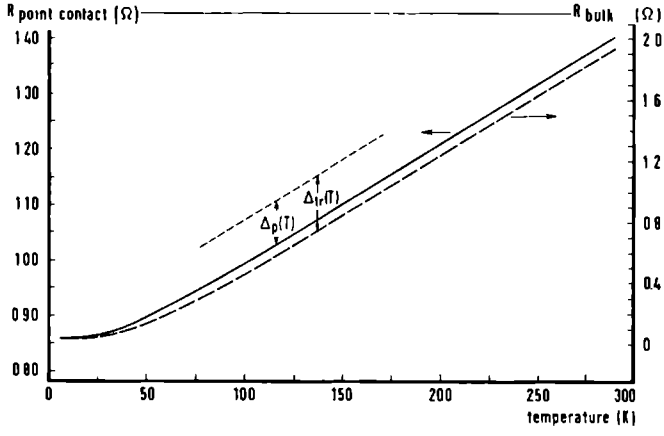

Fig. 3 : Point-contact resistance as a function of the temperature. For comparison the dashed line represents the resistance of a bulk-wire (spear-part of the point contact). The values $\Delta_p(T)$ and $\Delta_{tr}(T)$ correspond to the difference between the measured resistance and the straight line through R(T=0) parallel to the high temperature limit of the resistance.

experiments on Cu no strong dependence was observed in the measured spectra for different crystalline orientations of the point contact[2,13]. We therefore conclude that the difference as shown in Fig. 3 might be due to the efficiency functions for the electron-phonon interaction in the bulk resistivity and the point-contact resistance.

To show the influence of the efficiency function more clearly we will analyse Eqs. (5) and (6) for the resistance of a point contact and a bulk sample. We define a function $\Delta(T) = T+[R(0)-R(T)]/[dR/dT]$, denoted as $\Delta_p(T)$ if R is the resistance of the point contact, and as $\Delta_{tr}(T)$ if R is the resistance of the bulk material. The function $\Delta(T)$ corresponds with the difference between the measured resistance and the straight line $(R(T) = T(\frac{dR}{dT})_{T=\infty})$ parallel to the resistance at high temperatures. The experimental results in Fig. 3 indicate that $\delta\{\Delta(T)\} = \Delta_p(T)-\Delta_{tr}(T)<0$. It follows from Eqs. (5) and (6), that $\Delta(T) = T-T[P(T)-Q(T)]/[P(T)+Q(T)]$ or, approximately

$$\Delta(T) \approx 2T\ Q(T)/P(T) \tag{11}$$

for the case $(Q/P) << 1$, where

$$Q(T) = \int d\omega\ \alpha^2F(\omega)\ q(\omega/k_BT)\ ;\quad q(x) = \frac{x^2chx-xshx}{sh^3x}$$
$$P(T) = \int d\omega\ \alpha^2F(\omega)\ p(\omega/k_BT)\ ;\quad p(x) = \frac{x^2chx}{sh^3x}\ . \tag{12}$$

For the function α^2F in the definitions of Q(T) and P(T) we take α^2F_p for the function $\Delta_p(T)$ and α^2F_{tr} for the function $\Delta_{tr}(T)$. The ratio (Q/P)

decreases roughly like (1/T) and appears to be quite small compared to unity. Eq. (11) is useful for comparing the differences between the transport efficiencies for point-contact and bulk resistances. For this purpose the difference $\delta\{\Delta(T)\} = \Delta_p(T) - \Delta_{tr}(T)$ can be related to the difference $\delta\{\alpha^2F(\omega)\} = \alpha^2F_p(\omega) - \alpha^2F_{tr}(\omega)$ in the electron-phonon interaction functions

$$\frac{\delta\{\Delta(T)\}}{\Delta(T)} = \frac{\delta Q}{Q} - \frac{\delta P}{P} = \int d\omega\ \delta\{\alpha^2F(\omega)\}\ \left[\frac{q(\omega/kT)}{Q(T)} - \frac{p(\omega/kT)}{P(T)}\right] . \qquad (13)$$

The right hand side of Eq. (13) vanishes if one substitutes $\delta\{\alpha^2F\} \to$ const. α^2F, by virtue of the defining equations (12). Consequently, the factor of the integrand between brackets on the right hand side of Eq. (13) must have at least one zero at ω_o ($0 < \omega_o < \omega_D$) because $\alpha^2F \geq 0$. A number of conclusions may be drawn from the experimental fact that $\delta\{\Delta(T)\} < 0$. For instance, it is not possible that the function α^2F_p is shifted to higher frequencies compared with α^2F_{tr}, such that $\alpha^2F_p < \alpha^2F_{tr}$ at $\omega < \omega_o$ and $\alpha^2F_p > \alpha^2F_{tr}$ at $\omega > \omega_o$. Because of the normalisation $\int d\omega\ \alpha^2F_p(\omega)/\omega = \int d\omega\ \alpha^2F_{tr}(\omega)/\omega$ it is not allowed that the difference between α^2F_p and α^2F_{tr} will be positive or negative for all frequencies. We hence conclude that the function α^2F_p is shifted to lower frequencies compared with α^2F_{tr}, such that $\alpha^2F_p > \alpha^2F_{tr}$ at $\omega < \omega_o$ and $\alpha^2F_p < \alpha^2F_{tr}$ at $\omega > \omega_o$. We want to compare this result for the electron-phonon interaction functions α^2F_p and α^2F_{tr} with the behaviour of the efficiency functions of the scattering mechanism at small phonon frequencies. For normal processes the efficiency functions $\eta(\theta)$ and $(1-\cos\theta)$ behave both like ω^2 for small angle scattering at low frequencies, and therefore no difference is expected between α^2F_p and α^2F_{tr}. Umklapp scattering however is much more dominant in the noble metals and particularly important in the point-contact case because of the

singularity in the function $\eta(0)$ at $\theta = \pi$. Considering umklapp scattering as the main contribution to the electron-phonon interaction function, we find that $(1-\cos\theta) \propto$ const. and $\eta(\theta) \propto \omega^{-\frac{1}{2}}$. According to these arguments the ω-power will be smaller for α^2F_p than for α^2F_{tr}, which yield a stronger signal of α^2F_p at low energies. This is in agreement with the result, deduced from the experimentally measured temperature dependence of a point-contact resistance and that of bulk material resistivity.

IV. Conclusions.

Point-contact experiments were performed between 5 and 300 K. The measured d^2V/dI^2-curves of Cu point contacts showed thermal broadening of the structure, caused by the electron-phonon interaction, upon increasing the temperature. A thermal weight function, obtained from a theoretical analysis, fits the experimental result very well. The measured resistance of Cu point contacts revealed interesting behaviour as a function of the temperature, which resembled the resistivity of bulk material. In a relative comparison one observes that the resistance of a point contact increases more rapidly than the resistance of bulk material. We concluded that the relative difference could be reduced to differences in the electron-phonon interaction α^2F for a point contact geometry (α^2F_p) and bulk material (α^2F_{tr}). On the basis of simple arguments, which include that umklapp processes are dominant over normal processes in noble metals, the α^2F_p-signal will be stronger at low frequencies than the α^2F_{tr}-signal. As the weight function in Eqs. (5) and (6) dominates at low frequencies, the difference in the α^2F-signals is in agreement with experimental observation. Note however that a more detailed analysis is needed to support this conclusion, for instance because of the non-sphericity of the Fermi-

sphere in copper. These problems are similar to the calculation of the temperature dependent resistivity. It is of interest to determine the power law of the temperature dependence of the point-contact resistance at low temperatures to study the relevant scattering processes in a point-contact geometry, in analogy to experimental work on the temperature dependence of the resistivity in bulk material.

Acknowledgement.

Part of this work has been supported by the "Stichting voor Fundamenteel Onderzoek der Materie" (FOM) with financial support of the "Nederlandse Organisatie voor Zuiver Wetenschappelijk Onderzoek" (ZWO).

References.

1. I.K. Yanson, Zh. Eksp. Teor. Fiz. 66, 1035 (1974) [Sov. Phys. - JETP 39, 506 (1974)]; I.K. Yanson and I.O. Kulik, J. Phys. (Paris) 39, C6-1564 (1978), and references therein.
2. A.G.M. Jansen, F.M. Mueller and P. Wyder, Phys. Rev. B16, 1325 (1977) and Science 199, 1037 (1978).
3. I.O. Kulik, A.N. Omel'yanchuk and R.I. Shekhter, Fiz. Nizk. Temp. 3, 1543 (1977) [Sov. J. Low Temp. Phys. 3, 740 (1978)].
4. A.P. van Gelder, Solid State Commun. 25, 1097 (1978).
5. Yu.V. Sharvin, Zh. Eksp. Teor. Fiz. 48, 984 (1965) [Sov. Phys. - JETP 21, 655 (1965)].
6. A.P. van Gelder, to be published.
7. B. Hayman and J.P. Carbotte, J. Phys. F 2, 915 (1972).
8. J. Lambe and R.C. Jaklevic, Phys. Rev. 165, 821 (1968).
9. J.G. Adler and J.E. Jackson, Rev. Sci. Instr. 37, 1049 (1966).
10. A.P. van Gelder, A.G.M. Jansen, S. Strässler and P. Wyder, J. Phys. (Paris) 39, C6-602 (1978).
11. J.C. Maxwell, A Treatise on Electricity and Magnetism, 1891 (Dover, New York, 1954).
12. J. Bass, Adv. Phys. 21, 431 (1972).
13. I.K. Yanson and G. Batrak, Zh. Eksp. Teor. Fiz. Pis'ma Red. 27, 212 (1978) [JETP Lett. 27, 197 (1978)].

Chapter VIII : APPLICATION OF POINT-CONTACT SPECTROSCOPY IN METALS TO THE KONDO PROBLEM.

ABSTRACT

A general relationship between the characteristic structure in the electrical resistance of a point contact between two metals and the dynamics of the scatterers is used to discuss new experimental results on Kondo systems. The method allows to measure directly the energy dependence of the relaxation time of the conduction electrons.

The problem of point contact spectroscopy with respect to the electron-phonon interaction has recently been discussed in several papers[1]. Here we want to show that the method can be generalized to obtain information on the dynamics of arbitrary scatterers. In particular we have applied the method of point contact spectroscopy for the first time to Kondo systems.

The expression for a current I flowing through a point contact is given by $I = \iint dx\, dy\, j_z(x,y,0)$, where the integral is taken over the surface of the orifice. The current density j is given by (unit volume) $\underline{j}(\underline{r}) = 2e \sum_{\underline{k}} \underline{v}_{\underline{k}}\, f_{\underline{k}}(\underline{r})$. Here, $\underline{v}_{\underline{k}}$ is the band velocity with wave vector $\underline{k}$ and the electron distribution $f_{\underline{k}}(\underline{r})$ satisfies the Boltzmann equation

$$(\underline{v}_{\underline{k}} \cdot \nabla_{\underline{r}} + \frac{e}{\hbar}\, \underline{E} \cdot \nabla_{\underline{k}}) f_{\underline{k}} = \left.\frac{\partial f}{\partial t}\right|_{coll} . \tag{1}$$

The electric field E must be determined from Poissons equation

$$-\Delta\phi = e\underline{\nabla} \cdot \underline{E} = -\frac{2e}{\varepsilon_o} \sum_{\underline{k}} f_{\underline{k}}(\underline{r}) . \tag{2}$$

The following boundary conditions must be satisfied:

$$f_{\underline{k}}(z \to \pm\, \infty) = f_T(\varepsilon(\underline{k})),\ \phi(z \to \pm\, \infty) = \pm\, eV/2 \tag{3}$$

f_T is the equilibrium Fermi function and V the applied voltage over the point contact. $\varepsilon(\underline{k})$ is the electronic energy measured relative to the chemical potential μ. The collision term in Fq. (1) for scattering of the electron from an arbitrary target (phonons, spins, etc.) is

$$-\left.\frac{\partial f}{\partial t}\right|_{coll} = \sum_{\underline{k}'} \Gamma(\underline{k},\underline{k}')f_{\underline{k}}(1-f_{\underline{k}'})-\Gamma(\underline{k}',\underline{k})f_{\underline{k}'}(1-f_{\underline{k}}) \qquad (4)$$

where

$$\Gamma(\underline{k},\underline{k}') = \frac{2\pi}{\hbar}\sum_{if} p_i\,\delta(\varepsilon_f-\varepsilon_i-(\varepsilon_{\underline{k}}-\varepsilon_{\underline{k}'}))\;|\langle \underline{k}'\, f|U|\underline{k}\, i\rangle|^2 \,. \qquad (5)$$

Here p_i is the probability for the target to be in the state i and ε_i and ε_f are the initial and final energies of the target. U describes the interaction between scattering electrons and target.

Of particular interest is the voltage dependence of the point contact resistance $R(V) = dV/dI$ because it contains information about the scatterer and the interaction. This information can be obtained easily only in the limit where the mean free path is comparable or larger than the diameter d of the orifice. Therefore it is appropriate to solve Eqs. (1) and (2) by iteration with respect to the collision terms. In zeroth order one obtains[1] $I^{(o)} = eD_o\langle|v_{\underline{k}z}|\rangle_o V$, where D_o is the area of the orifice and $\langle\cdots\rangle_\omega = \sum_{\underline{k}} \cdots\, \delta(\varepsilon_{\underline{k}}-\omega)$. In first order the result is $I^{(1)} = I^{(o)} + \Delta I^{(1)}$, where

$$\Delta I^{(1)} = -2e\int_o^{eV} d\omega \int_o^{\omega} d\omega' \,\langle\langle\Gamma(\underline{k},\underline{k}')K(\underline{k},\underline{k}')\rangle_{\omega'}\rangle_{\omega} \,. \qquad (6)$$

The weight factor $K(\underline{k},\underline{k}')$ in Eq. (6) is the common volume defined by the two cylinders constructed with the boundary line of the orifice and whose walls are // to $\underline{v}_{\underline{k}}$ or $\underline{v}_{\underline{k}'}$, respectively. In the case of independent localized isotropic scatterers the change in the resistance is given by $R = R_o + \Delta R$, where $R_o = V/I^{(o)}$ and

$$\Delta R = C \int_0^{eV} d\omega' \; \Gamma(eV,\omega')N(eV)N(\omega') \; . \qquad (7)$$

Here $C = R_o^2 \, 2e^2 \, \langle\langle K(\underline{k},\underline{k}')\rangle_o\rangle_o$, and $N(\omega) = \langle 1\rangle_\omega / \langle 1\rangle_o$ is the normalized density of states. The relaxation time τ for an electronic state with energy eV above the Fermi surface is

$$\tau^{-1}(eV) = \sum_{\underline{k}'} \Gamma(\underline{k},\underline{k}') \equiv \langle 1\rangle_o \int_0^{eV} \Gamma(eV,\omega')N(\omega')d\omega' \; . \qquad (8)$$

For a dilute system the resistance change linear in the target concentration is simply related to the relaxation time by ($N(\omega) = 1$)

$$\Delta R = \frac{C}{\langle 1\rangle_o} \tau^{-1}(eV) \; . \qquad (9)$$

It follows from Eq. (9) that it is possible to measure directly the energy dependence of the relaxation time $\tau(\omega)$ by measuring the voltage dependence of the point contact resistance R(V). We have applied this finding to Kondo systems.

For Kondo systems, the relaxation time has been evaluated theoretically in several Refs.[2]. In particular, Hamann[2] gives for $eV > k_B T$:

$$\tau^{-1}(eV) = \frac{c}{\pi\langle 1\rangle_o} \left\{ 1 - \ln\left(\frac{eV}{k_B T_K}\right)\left[\ln^2\left(\frac{eV}{k_B T_K}\right) + S(S+1)\pi^2 \right]^{-\frac{1}{2}} \right\} \qquad (10)$$

where T_K is the characteristic Kondo temperature of the dilute alloy and c the concentration of magnetic impurities with spin S.

We have investigated the current-voltage characteristics of point contacts of two systems with a Kondo temperature above and below the measuring temperature of the helium bath (T = 1.5 K): CuFe and AuMn, with T_K resp. ∿ 30 K and ∿ 0 K and with nominal magnetic impurity concentrations between 0.03 and 1.0 at.%[3]. The point contacts were of the pressure type and could be adjusted by pressing a sharply etched wire against a flat surface, both parts fabricated from the same starting material. The derivatives dV/dI of the contacts were measured using phase sensitive detection. The modulation voltage was in the range of 100-300 μV and didn't exceed the expected thermal broadening of a few k_BT. With a superconducting coil a magnetic field up to 30 kG could be applied perpendicular to the contact surface.

In all point contacts of the investigated alloy systems the measured second derivative d^2V/dI^2 showed structures at voltages corresponding to the phonon frequencies, as explained for the pure metal case in terms of the electron-phonon interaction[1] (see the inserts in the figures 1 and 2). At voltages lower than the phonon frequencies we observed maxima in the resistance dV/dI, which were practically symmetric around zero voltage. Because of the observed phonon structure in the point contact spectra our observations in the metal-metal contacts are essentially different from the spectroscopy with metal-oxide-metal tunneljunctions, where the exchange coupling between the electrons and the magnetic impurities in the oxide layer results in a minimum (as compared with the maximum in the point contact case) in the resistance around zero voltage, as firstly recognized experimentally by Wyatt[4].

In Fig. 1 the measured resistance of a AuMn point contact is shown as function of the applied voltage. Because of the small Kondo temperature of the AuMn system ($|\ln T_K| >> 1$) Eq. (10) leads to $\tau^{-1}(eV) \propto$

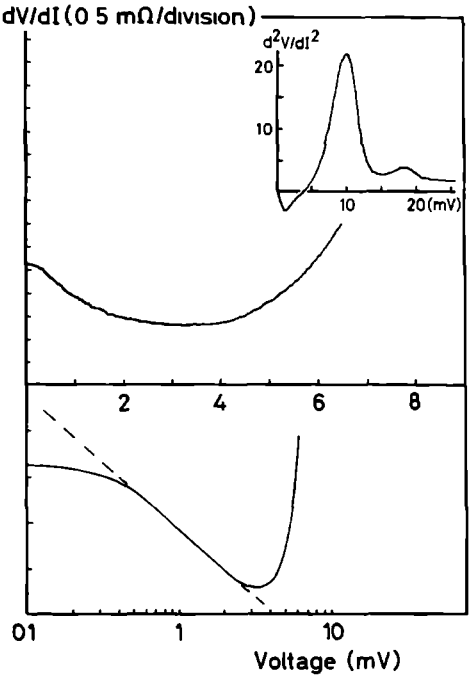

Fig. 1 : Differential resistance dV/dI of a Au-0.03 at.% Mn point contact as a function of the applied voltage on a linear and a logarithmic scale (R=2.1Ω; T = 1.5 K). The dashed line gives the theoretically expected logarithmic behaviour. The inserted d^2V/dI^2-curve indicates the well known typical point contact behaviour with the phonon peaks for Au at 10 and 18 mV.

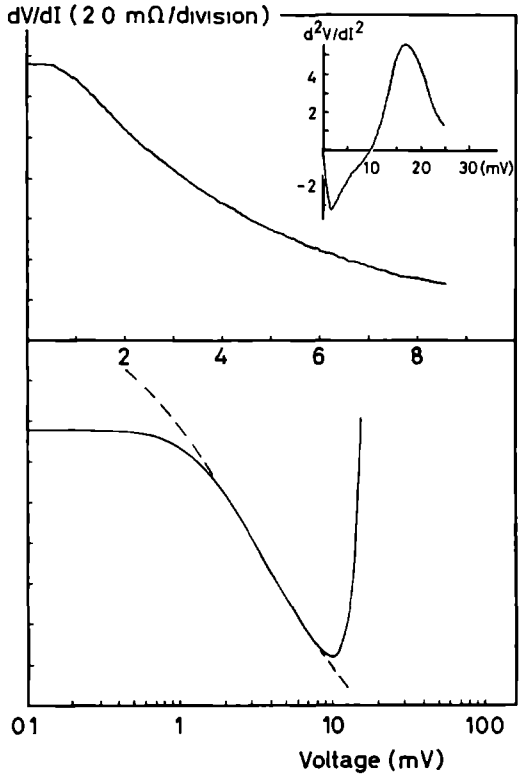

Fig. 2 : Differential resistance dV/dI of a Cu-0.1 at.% Fe point contact as function of the applied voltage on a linear and a logarithmic scale (R = 1.2 Ω; T = 1.5 K). The dashed curve is the fitted Hamann-function with $k_B T_K$ = 3.5 mV and S = 0.5. The inserted d^2V/dI^2-curve indicates the well known typical point contact behaviour with the phonon peak for Cu at 17 mV.

$[1-2\ln(eV)/\ln(k_BT_K)]$. As shown in Fig. 1 on a log-scale the resistance behaves over a limited range of V like logV around 1 mV. At higher voltages the resistance increases due to the electron-phonon interaction. At lower voltages the deviation is probably due to thermal averaging around zero voltage and ordering effects. Note that ordering effects have also been observed in measurements of the temperature dependence of the electrical resistivity in bulk Au samples with Mn concentrations $\geq$ 0.02 at.%[5]. In Fig. 2 the measured voltage dependence of a CuFe point contact resistance is given on a linear scale and a log-scale. Between 2 and 7 mV a logV behaviour is seen for the CuFe system as expected according to formula (10) at voltages corresponding to the Kondo temperature (30 K $\sim$ 2.6 mV). For smaller voltages the contact resistance becomes nearly constant and a fit to the Hamann-function isn't successful. Note that using the Hamann-formula the obtained temperature dependence of the electrical resistivity is similar to the energy dependence of the scattering rate[2]. Below the Kondo temperature the same deviation has been measured in the electrical resistivity of the bulk material (see Fig. 18 in Ref. 6). The point contact resistance becomes a constant at applied voltages which are roughly twice the corresponding temperatures in the electrical resistivity measurements.

By applying a magnetic field the resistance maximum at zero voltage splits up in two maxima for the case of AuMn, as shown in Fig. 3. For the CuFe case the magnetic fields up to 30 kG lead only to a rounding off of the flat resistance maximum, without significantly influencing the amplitude of the change in resistance. Assuming that the "Kondo field" $H_K = k_BT_K/\mu_B$ acts in a similar way as the temperature, the quantitative difference for the two systems can be understood. A similar magnetic field dependence has been observed in bulk resistivity measurements as

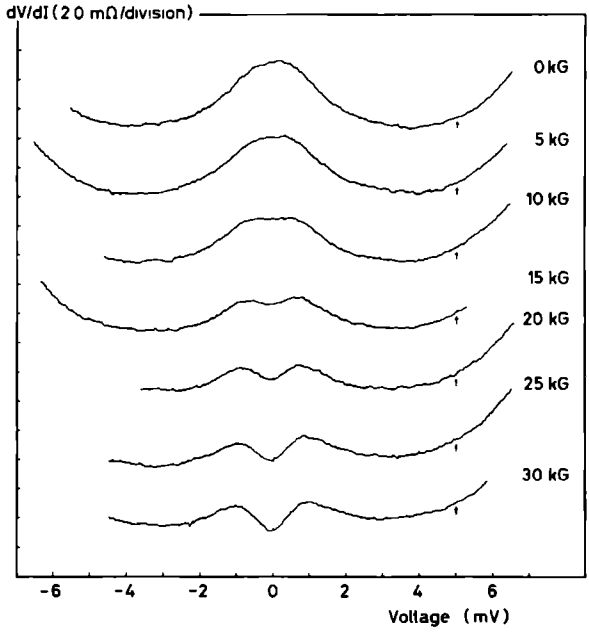

Fig. 3 : Magnetic field dependence of the differential resistance dV/dI of a Au-0.1 at.% Mn point contact as function of the applied voltage (R = 2.5 Ω; T = 1.5 K). The curves are shifted with respect to the reference point indicated by (↑) .

function of temperature for dilute alloys with a low and a high Kondo temperature[7]. With increasing Mn concentration in the Au samples the curves of the point contact resistances as function of voltage resembled the pattern plotted in Fig. 3 upon increasing the magnetic field, probably due to ordering or, equivalently, internal fields. This has also been seen experimentally in bulk resistivity measurements[5].

In the case of CuFe point contacts we also observed minima in the resistance around zero voltage in some cases. It should be noted however that zero bias anomalies (resistance minima and maxima and no structure at all) have also been observed in the pure metal point contacts in an irreproducible way. It is of interest to establish experimentally whether these anomalies in the pure metal case are due to magnetic impurities. Furthermore, it is not unlikely for the used nominal concentrations of Fe in Cu, that the impurities are not distributed homogeneously over the sample.

We conclude from our observations on the voltage and magnetic field dependence of the resistance of point contacts in Kondo systems to have extended the usefulness of the point contact spectroscopy to obtain the energy dependence of the scattering rate of the conduction electrons in a Kondo system.

We are most thankful to Dr. B. Knook from the Kamerlingh Onnes Laboratorium in Leiden for preparing the Kondo samples and very grateful to Prof. J. Bass for his stimulating interest in a early stage of this study. Part of this work has been supported by the Stichting FOM.

References

1. I.K. Yanson, Zh. Eksp. Teor. Fiz. 66, 1035 (1974) [Sov. Phys. - JETP 39, 506 (1974)]; A.G.M. Jansen, F.M. Mueller and P. Wyder, Phys. Rev. B 16, 1325 (1977); A.G.M. Jansen, F.M. Mueller and P. Wyder, Science 199, 1037 (1978); I.K. Yanson and I.O. Kulik, J. Phys. (Paris) 39, C6-1564 (1978) and references therein.

2. Magnetisn, vol. V, edited by H. Suhl (Academic Press, New York, 1973); D.R. Hamann, Phys. Rev. 158, 570 (1967).

3. The samples were prepared by Dr. B. Knook at the Kamerlingh Onnes Laboratorium in Leiden and are registrated under KOL 78131-132 and KOL 78134-137.

4. A.F.G. Wyatt, Phys. Rev. Lett. 13, 40 (1964).

5. J.W. Loram, T.E. Whall and P.J. Ford, Phys. Rev. B 3, 953 (1971).

6. J.W. Loram, T.E. Whall and P.J. Ford, Phys. Rev. B 2, 857 (1970).

7. P. Monod, Phys. Rev. Lett. 19, 1113 (1967).

This thesis deals with an experimental investigation of interesting deviations from Ohm's law which have been observed at low temperatures in metallic point contacts, if the linear dimension of the contact becomes comparable to the mean free path of the electrons. This geometry allows to have an electric field within a metal in the region of the contact due to an applied voltage. The conduction electrons are accelerated in this electric field and come back in equilibrium via collisions with elementary excitations (i.e. phonons) in the metal. Because these inelastic scattering processes depend strongly on the energy of the accelerated electrons, the current-voltage characteristic of a point contact is non-linear. The observed non-linearity allows an energy resolved spectral analysis of the inelastic collisions of the electrons in a metal using point contacts. The measured second derivative d^2V/dI^2 of metallic point contacts reveal structures at applied voltages which are in agreement with the phonon frequencies of the metal and allow a direct measurement of the energy dependence of Eliashbergs electron-phonon interaction parameter α^2F.

After a general introduction to the spectroscopic method, chapter II gives a survey on the theoretical and experimental work done in point-contact spectroscopy up to now. The full non-linear Boltzmann equation for the current through a metallic constriction is solved, using an iterative procedure with respect to the inelastic collision term in the transport equation. It is found that the measured resistance of a point contact as a function of the applied voltage, is proportional to the inverse of the energy-dependent scattering time of the electrons in a metal, forming the contact. For the electron-phonon interaction, this means that the second derivative signal is proportional to the α^2F-spectrum, taking into account a transport efficiency function due to the specific geometry. The experimental techniques used for point-contact spectroscopy are discussed. The data for various metals give detailed and novel results on the energy dependence of the electron-phonon interaction, especially for the normal (i.e. non-superconducting) metals.

The following chapters contain experiments dealing with certain aspects of point-contact spectroscopy. Experiments with pressure-type point contacts of the noble metals (chapter III and IV) give a remarkable inte-

resting α^2F-spectrum which shows that the coupling of the electrons is stronger with transverse phonons than with longitudinal phonons. It is shown that the observed background signal, on which the α^2F-spectrum is thought to be superimposed, can not be explained by double phonon processes only, and non-equilibrium phonons have to be involved (chapter V). In chapter VII experiments on the temperature dependence of the spectroscopic method are described, and one finds an analogy between the temperature dependence of the contact resistance at zero voltage and that of the bulk resistivity, except for small differences arising from the different geometrical transport efficiencies in the two cases. In chapter VIII, experimental evidence is given for the detection of the energy dependent exchange interaction between electrons and paramagnetic impurities in point-contact experiments with magnetically dilute alloys (Kondo systems).

Dit proefschrift behandelt een experimenteel onderzoek van interessante afwijkingen van de wet van Ohm, die bij lage temperaturen zijn waargenomen in puntkontakten tussen metalen, waarvan de afmetingen vergelijkbaar zijn met de vrije weglengte van de elektronen. Door het aanleggen van een spanning over het puntkontakt ontstaat bij het kontakt een elektrisch veld in het metaal. De geleidingselektronen worden versneld in dit elektrische veld en kunnen weer in evenwicht komen door middel van botsingen met elementaire excitaties (b.v. fononen) in het metaal. Omdat deze inelastische verstrooiingsprocessen sterk afhangen van de energie van de versnelde elektronen, is het verband tussen stroom en spanning in een puntkontakt niet lineair. De waargenomen afwijking van de wet van Ohm maakt het mogelijk de inelastische botsingen van de elektronen in een metaal als funktie van de energie van de elektronen spektraal te analyseren met behulp van puntkontakten. In de tweede afgeleide d^2V/dI^2, gemeten aan een puntkontakt tussen metalen, is een struktuur te zien bij aangelegde spanningen, die overeenkomen met de frequenties van de fononen in het metaal en de Eliashberg functie α^2F voor de elektron-fonon interaktie valt hieruit direkt te bepalen.

Na een algemene inleiding op de methode, geeft hoofdstuk II een overzicht van het theoretische en experimentele werk, dat tot op heden aan puntkontaktspektroskopie gedaan is. De Boltzmann vergelijking voor het transport van elektronen door een puntkontakt wordt opgelost door gebruik te maken van een iteratieve methode ten opzichte van de inelastische verstrooiingsterm in de transportvergelijking. Men komt tot de conclusie dat de weerstand van een puntkontakt, die als funktie van de aangelegde spanning wordt gemeten, omgekeerd evenredig is met de verstrooiingstijd van de elektronen in het metaal, die van de energie van de elektronen afhangt. Dit heeft voor de elektron-fonon interaktie tot gevolg dat het signaal van de tweede afgeleide evenredig is met het α^2F-spektrum, daarbij moet rekening worden gehouden met de effectiviteit van het transport van elektronen in de specifieke geometrie van een puntkontakt. De experimentele technieken, die gebruikt worden voor puntkontakten, worden besproken. De experimentele resultaten voor de verschillende metalen laten gedetailleerd zien hoe de elektron-fonon interaktie van de energie afhangt; met name voor de normale (d.w.z. niet-supergeleidende) metalen kan deze af-

hankelijkheid voor het eerst experimenteel bepaald worden.

De volgende hoofdstukken bevatten experimenten die bepaalde aspecten van puntkontaktspektroskopie behandelen. Experimenten met puntkontakten van de edele metalen, (hoofdstuk III en IV) geven een opmerkelijk α^2F-spektrum te zien, waarvoor geldt dat de koppeling van de elektronen sterker is met transversale fononen dan met longitudinale fononen. De waargenomen achtergrond in het gemeten signaal kan niet alleen verklaard worden door processen, waarbij de elektronen aan twee fononen verstrooid worden; in een analyse van dit achtergrondsignaal moet rekening worden gehouden met het feit dat de elektronen niet in evenwicht zijn (hoofdstuk V).

In hoofdstuk VII worden puntkontakten als funktie van de temperatuur bestudeerd, en wat betreft de afhankelijkheid van de temperatuur ziet men een analoog gedrag voor de puntkontaktweerstand en voor de weerstand van bulk materiaal, behoudens kleine verschillen in de effectiviteit van de verstrooiing van de elektronen.

In hoofdstuk VIII laten experimenten aan puntkontakten met Kondo-systemen zien dat ook de wisselwerking tussen elektronen en paramagnetische verontreinigingen in een metaal met deze methoden bestudeerd kunnen worden.

CURRICULUM VITAE

A.G.M. Jansen

Geboren : 3 februari 1952 te Breda.

1964 - 1970 : Middelbare schoolopleiding aan het Onze Lieve Vrouwe Lyceum te Breda; afgesloten met het eindexamen Gymnasium β.

1970 - 1977 : Universitaire studie natuurkunde aan de Faculteit der Wiskunde en Natuurwetenschappen van de Katholieke Universiteit Nijmegen; afgesloten met het doctoraal-examen natuurkunde met als hoofdvak experimentele natuurkunde.

1977 - 1980 : Promotieonderzoek op de afdeling Experimentele Natuurkunde 4, Faculteit der Wiskunde en Natuurwetenschappen, Katholieke Universiteit Nijmegen, in het kader van een FOM-beleidsruimte projekt onder leiding van Prof. P. Wyder.

STELLINGEN

I

Met behulp van foto-thermische ionisatie-spektroskopie kunnen donoren en acceptoren in halfgeleiders afzonderlijk worden waargenomen. Uit het teken van de bijdrage van de minderheidsonzuiverheden aan de electrische geleiding kunnen conclusies worden getrokken over de relevante recombinatie processen.

H.W.H.M. Jongbloets, Proefschrift, Nijmegen 1980.

II

Bij de interpretatie van de resultaten van magnetische metingen aan een koper(I)-koper(II) complex is de door Schugar en medewerkers geïntroduceerde antiferromagnetische wisselwerking voor een groot deel toe te schrijven aan verzadigingseffecten ten gevolge van de grootte van het aangelegde veld. De temperatuurafhankelijkheid van hun metingen bij lage temperaturen wordt beter beschreven door deze hypothetische antiferromagnetische wisselwerking nul te kiezen, waarbij echter wel de schaalfactor moet worden aangepast.

H.J. Schugar et al., Inorg. Chem. 19, 543 (1980).

III

De levensduur van geëxciteerde electronen bij cyclotron resonantie in halfgeleiders kan worden bepaald uit een gecombineerde meting van de absorptie van straling ten gevolge van cyclotron resonantie en van de corresponderende verandering van het electrische geleidingsvermogen voor halfgeleiders met parabolische banden en als functie van het ingestraalde vermogen.

J.C. Maan, Proefschrift, Nijmegen 1979.

IV

Door de gelijkrichtende werking van puntkontakten tussen metalen te bestuderen als functie van de ingestraalde frekwentie (> THz) kunnen de relaxatietijden van de electron-fonon wisselwerking in een metaal bepaald worden.

V

Indien de waargenomen verhoging van de kritische stroom en temperatuur voor een supergeleider onder invloed van microgolf straling toe te schrijven is aan een verhoging van de orderparameter van de supergeleider kan dit nader worden onderzocht door een bepaling van het kritische veld.

T.M. Klapwijk, Proefschrift, Delft 1977.

VI

Verschillen tussen de met behulp van puntkontakten gemeten spektra van de functie $\alpha^2 F$, die worden toegeschreven aan anisotropie effecten ten gevolge van de verschillende kristalorientaties in de buurt van het kontakt, kunnen worden geanalyseerd door de spektra opgebouwd te denken uit 3 functies voor de verschillende kristalrichtingen.

VII

De uitgever verhoogt de service aan de lezers van zijn boeken door, zoals in het verleden gebruikelijk, bij zijn boeken weer een antwoordkaart of soortgelijke bladwijzer te voegen.

VIII

Het kraken van woningen werkt de maatschappelijke integratie van de politie tegen.

IX

Uit het feit dat in de identiteitsbewijzen van de gehuwde vrouw het bijvoegsel "echtgenote van" staat en niet in die van de gehuwde man, blijkt dat de formele gelijkstelling van man en vrouw bij de betreffende overheidsinstanties nog niet ten volle is doorgedrongen.

A.G.M. Jansen

Nijmegen, 27 maart, 1980.